OPEN

IC3D Classification of Corneal Dystrophies—Edition 3

Jayne S. Weiss, MD, Christopher J. Rapuano, MD,† Berthold Seitz, MD,‡ Massimo Busin, MD,§¶ Tero T. Kivelä, MD, FEBO,‖ Nacim Bouheraoua, MD, PhD,** Cecilie Bredrup, MD, PhD,†† Ken K. Nischal, MD, FAAP, FRCOphth,‡‡ Harshvardhan Chawla, MD,§§ Vincent Borderie, MD, PhD,** Kenneth R. Kenyon, MD,¶¶ Eung Kweon Kim, MD, PhD,‖‖*** Hans Ulrik Møller, MD, PhD (Emeritus),††† Francis L. Munier, MD,‡‡‡ Tim Berger, MD,‡ and Walter Lisch, MD§§§*

Purpose: The International Committee for the Classification of Corneal Dystrophies (IC3D) was created in 2005 to develop a new classification system integrating current information on phenotype, histopathology, and genetic analysis. This update is the third edition of the IC3D nomenclature.

Methods: Peer-reviewed publications from 2014 to 2023 were evaluated. The new information was used to update the anatomic classification and each of the 22 standardized templates including the level of evidence for being a corneal dystrophy [from category 1 (most evidence) to category 4 (least evidence)].

Results: Epithelial recurrent erosion dystrophies now include epithelial recurrent erosion dystrophy, category 1 (*COL17A1* mutations, chromosome 10). Signs and symptoms are similar to Franceschetti corneal dystrophy, dystrophia Smolandiensis, and dystrophia Helsinglandica, category 4. Lisch epithelial corneal dystrophy, previously reported as X-linked, has been discovered to be autosomal dominant (*MCOLN1* mutations, chromosome 19). Classic lattice corneal dystrophy (LCD) results from *TGFBI* R124C mutation. The LCD variant group has over 80 dystrophies with non-R124C *TGFBI* mutations, amyloid deposition, and often similar phenotypes to classic LCD. We propose a new nomenclature for specific LCD pathogenic variants by appending the mutation using 1-letter amino acid abbreviations to LCD. Pre-Descemet corneal dystrophies include category 1, autosomal dominant, punctiform and polychromatic pre-Descemet corneal dystrophy (PPPCD) (*PRDX3* mutations, chromosome 10). Typically asymptomatic, it can be distinguished phenotypically from pre-Descemet corneal dystrophy, category 4. We include a corneal dystrophy management table.

Conclusions: The IC3D third edition provides a current summary of corneal dystrophy information. The article is available online at https://corneasociety.org/publications/ic3d.

Key Words: corneal dystrophy, inherited corneal diseases, cornea, cornea pathology, genetic disease

(*Cornea* 2024;43:466–527)

Received for publication August 3, 2023; revision received September 8, 2023; accepted September 24, 2023. Published online ahead of print February 12, 2024.

From the *Departments of Ophthalmology, Pathology and Pharmacology, Louisiana State University Eye Center of Excellence, Louisiana State University Health Sciences Center, New Orleans, LA; †Cornea Service, Wills Eye Hospital, Sidney Kimmel Medical College at Thomas Jefferson University, Philadelphia, PA; ‡Department of Ophthalmology, Saarland University Medical Center, Homburg/Saar, Germany; §Department of Translational Medicine, University of Ferrara, Ferrara, Italy; ¶Istituto Internazionale per la Ricerca e Formazione in Oftalmologia, Forlì, Italy; ‖Department of Ophthalmology, University of Helsinki and Helsinki University Hospital, Helsinki, Finland; **Department of Ophthalmology, Quinze-Vingts National Ophthalmology Hospital and Sorbonne Université, Paris, France; ††Department of Clinical Medicine, University of Bergen, Bergen, Norway; ‡‡Division of Pediatric Ophthalmology, Strabismus and Adult Motility, University of Pittsburgh Medical Center Children's Hospital of Pittsburgh, Pittsburgh, PA; §§Department of Ophthalmology, Louisiana State University Health Sciences Center, New Orleans, LA; ¶¶Department of Ophthalmology, Tufts University School of Medicine and Harvard Medical School, Schepens Eye Research Institute and New England Eye Center, Boston, MA; ‖‖Corneal Dystrophy Research Institute, Yonsei University College of Medicine, Seoul, Korea; ***Saevit Eye Hospital, Goyang, Korea; †††Department of Pediatric Ophthalmology, Aarhus University Hospital, Aarhus, Denmark; ‡‡‡Retinoblastoma and Oculogenetic Units, Jules-Gonin Eye Hospital and Fondation Asile des Aveugle, University of Lausanne, Lausanne, Switzerland; and §§§Department of Ophthalmology, Johannes Gutenberg University Mainz, Mainz, Germany.

J. S. Weiss MD: project support from Louisiana Lions Eye Foundation. C. J. Rapuano MD: consulting fees from Avellino Lab USA, Bio-Tissue, Inc. E. K. Kim MD, PhD: payments and/or honoraria from Avellino Lab USA, participation on the medical advisory board of Avellino Lab USA, and stock and/or stock options held by relatives in Avellino Lab USA.

The other authors have no funding or conflicts of interest to disclose.

Correspondence: Jayne S. Weiss MD, Department of Ophthalmology, LSU School of Medicine, 533 Bolivar St, Room 459, New Orleans, LA 70112 (e-mail: jweiss@lsuhsc.edu).

WHAT IS THE IC3D?

IC3D First Edition History

The International Committee for the Classification of Corneal Dystrophies (IC3D) was created in 2005 to address the difficulties presented by the antiquated nomenclature for corneal dystrophies and to correct errors embedded in the literature.[1] The goal was to create a new classification system that would retain some aspects of traditional corneal dystrophy nomenclature while incorporating new genetic, clinical, and pathologic information.

It had been well recognized that incorrect nomenclature increased the difficulty of correct diagnosis. Over a decade

earlier, 1 author (J.S.W.) suggested changing the name of Schnyder crystalline corneal dystrophy to Schnyder corneal dystrophy (SCD) precisely because misdiagnosis was caused by the deceptive nomenclature.[2] Because only 50% of patients with SCD actually had corneal crystals, the 50% of patients without crystals were repeatedly misdiagnosed. Owing to the name, many ophthalmologists and ophthalmic pathologists assumed that the presence of corneal crystals was an integral requirement for diagnosis. Consequently, patients with both clinical and/or histopathologic findings of SCD often escaped correct clinical diagnosis because they lacked the corneal crystals described in the original dystrophy name.[3] This was only 1 of many examples of challenges presented by the antiquated dystrophy nomenclature.

The underlying problem was that the original nomenclature began in 1890, before the invention of the slit lamp and more than a century before genetic mapping became available.[4,5] Although our knowledge base had markedly expanded, the nomenclature system remained static. An update of the outdated nomenclature was long overdue.

The initial and subsequent IC3D committees comprised clinicians, pathologists, and geneticists with first-hand knowledge of the corneal dystrophies. One-page summary "templates" for each dystrophy were written containing a "brief summary of the current genetic, clinical and pathologic information about the disease and representative images."[1] At the same time, the IC3D committee also corrected errors that had been perpetuated in the literature. One of the goals of the initial nomenclature revision was not only to devise a new nomenclature that was both accurate but also "flexible enough to facilitate the expansion of knowledge from other sources including genotyping."[1] The new nomenclature published in 2008 was well received. At the time of the writing of this article, it had been cited 245 times according to the Clarivate Analytics Web of Science. By 2015, continued expansion of the corneal dystrophy knowledge base mandated the publication of the IC3D second edition.[6]

Corneal Dystrophy—Problems With the Historic Definition

In the first edition of the IC3D, we explained that "the term 'corneal dystrophy' has been used to refer to a group of inherited corneal diseases that are typically bilateral, symmetric, slowly progressive and without relationship to environmental or systemic factors."[1] However, we also acknowledged that there were exceptions to each part of the definition. Some patients with posterior polymorphous corneal dystrophy (PPCD) only had unilateral changes, so PPCD could be asymmetric. Fleck corneal dystrophy (FCD) was an example of a corneal dystrophy that was nonprogressive. Immunophenotypes of macular corneal dystrophy (MCD) were classified by the level of antigenic serum keratan sulfate, which suggested a systemic factor was associated. Both epithelial basement membrane dystrophy (EBMD) and central cloudy dystrophy of François (CCDF) did not seem to have hereditary patterns. Consequently, it was likely these 2 conditions were not corneal dystrophies and instead were corneal degenerations. We concluded that "the separation of entities into the category called corneal dystrophies may have more historical than practical meaning. There remains no consensus as to the precise definition of corneal dystrophy, but according to custom, we have chosen to primarily deal with the entities formerly called corneal dystrophies."[1] Although we conclude that EBMD and CCDF are likely corneal degenerations rather than inherited corneal diseases, it would be exceptionally challenging to change decades of teaching and publications by excluding these from the list of corneal dystrophies. As we observed in the first edition of the IC3D, "once established in textbooks, it is exceedingly difficult to purge incorrect information."[1] We have decided that the more practical approach, currently, is to continue to include these entities in the list of corneal dystrophies, while at the same time indicating that the lack of heredity suggests these are degenerations.

IC3D Corneal Dystrophy Categories

A category system was suggested by Professor Gordon K. Klintworth MD, PhD, to indicate the level of evidence supporting the existence of a given corneal dystrophy depending on how substantive was the knowledge of its clinical, pathologic, and genetic basis.[1] He proposed that the existence of a new corneal dystrophy must begin with identification of a clinical phenotype and should progress to characterization of the causative gene mutation(s).

"An example of a monogenic category 1 dystrophy is SCD which is caused by mutations in 1 gene, *UBIAD1*. Another category 1 dystrophy, posterior amorphous corneal dystrophy (PACD) is caused by deletion of multiple genes, keratocan (*KERA*), lumican (*LUM*), decorin (*DCN*), and epiphycan (*EPYC*). The genetic basis of other dystrophies, such as some types of Fuchs endothelial corneal dystrophy (FECD), seems to be complex and involves multiple genes."[6]

These categories were specified as follows:

- "Category 1: A well-defined corneal dystrophy in which the gene has been mapped and identified and the specific mutations are known."
- "Category 2: A well-defined corneal dystrophy that has been mapped to one or more specific chromosomal loci, but the gene(s) remain to be identified."
- "Category 3: A well-defined corneal dystrophy in which the disorder has not yet been mapped to a chromosomal locus."
- "Category 4: This category is reserved for a suspected, new, or previously documented corneal dystrophy, although the evidence for it, being a distinct entity is not yet convincing."[1]

It was postulated that as our knowledge about a dystrophy increased, the category should progress over time from 4 to 3 to 2 to 1. Conversely, "Suspected dystrophies that remain category 4 because no further information ever becomes available may be eventually removed from the nomenclature.

The group did not further specify specific criteria for removal of category 4 dystrophy."[1]

IC3D Second Edition

The second edition of the IC3D was published in 2015 because of the continued increase in the knowledge base of corneal dystrophies.[6] In addition to clinical photographs included in the first edition, pathology images were now also included.[6] Congenital hereditary endothelial dystrophy (CHED) was reclassified. Literature review had revealed that many and possibly all 5 families previously described to have autosomal dominant CHED (CHED1) most likely had PPCD.[7–9] Consequently, CHED1 was removed from the nomenclature and autosomal recessive CHED, previously called CHED2, was renamed CHED. Another change was the introduction of a new anatomic subcategory, the epithelial-stromal *TGFBI* dystrophies.

TABLE 1. The IC3D Classification

	Category (C)
Epithelial and subepithelial dystrophies	
1. Epithelial basement membrane dystrophy (EBMD)	C3
2. Epithelial recurrent erosion dystrophies (EREDs)	
Epithelial recurrent erosion dystrophy (ERED)	C1
Franceschetti corneal dystrophy (FRCD)	C4
Dystrophia Smolandiensis (DS)	C4
Dystrophia Helsinglandica (DH)	C4
3. Subepithelial mucinous corneal dystrophy (SMCD)	C4
4. Meesmann corneal dystrophy (MECD)	C1
5. Lisch epithelial corneal dystrophy (LECD)	C1
6. Gelatinous drop-like corneal dystrophy (GDLD)	C1
Epithelial-stromal *TGFBI* dystrophies	
1. Reis–Bücklers corneal dystrophy (RBCD)	C1
2. Thiel–Behnke corneal dystrophy (TBCD)	C1
3. Lattice corneal dystrophies (LCDs)	
Classic LCD	C1
LCD variants	C1
4. Granular corneal dystrophy, type 1 (GCD1)	C1
5. Granular corneal dystrophy, type 2 (GCD2)	C1
Stromal dystrophies	
1. Macular corneal dystrophy (MCD)	C1
2. Schnyder corneal dystrophy (SCD)	C1
3. Congenital stromal corneal dystrophy (CSCD)	C1
4. Fleck corneal dystrophy (FCD)	C1
5. Posterior amorphous corneal dystrophy (PACD)	C1
6. Central cloudy dystrophy of François (CCDF)	C4
7. Pre-Descemet corneal dystrophies (PDCDs)	
Pre-Descemet corneal dystrophy (PDCD)	C4
Punctiform and polychromatic pre-Descemet corneal dystrophy (PPPCD)	C1
Endothelial dystrophies	
1. Fuchs endothelial corneal dystrophy (FECD)	C1, C2, or C3
2. Posterior polymorphous corneal dystrophy (PPCD)	C1
3. Congenital hereditary endothelial dystrophy (CHED)	C1 or C3
4. X-linked endothelial corneal dystrophy (XECD)	C2
Removed dystrophies	
1. Grayson-Wilbrandt corneal dystrophy (GWCD)	C4

For the first time, corneal dystrophy nomenclature would be guided by genetics. All corneal dystrophies known to map to the *TGFBI* gene would be included in 1 category instead of the former approach of separating these into either Bowman layer or stromal dystrophies. The new epithelial-stromal *TGFBI* anatomic category facilitated explanation of why the dystrophies in this group had some overlap of the clinical signs, symptoms, and histopathologic changes.

Another change was the removal of the category 4, Grayson-Wilbrandt corneal dystrophy, from the IC3D classification. The category system allowed for a removal of a category 4 corneal dystrophy "in which no further information to prove or disprove its existence is forthcoming."[1] IC3D considered this an equivalent of "corneal dystrophy purgatory." Grayson-Wilbrandt dystrophy was described in only 1 publication in 1966, supported by an artist rendition of the changes. There were no photographs or genotyping, and there were no subsequent articles over the following 5 decades. Consequently, Grayson-Wilbrandt corneal dystrophy was consigned to a category entitled "Removed Dystrophies" (Table 1).[10] If a future publication substantiates its existence, the reference publication is easily retrievable, and it can be "resurrected from purgatory."

IC3D Third Edition

The continued rapid expansion of corneal dystrophy knowledge suggested it was time for yet another update, reflected in this current third edition of IC3D. The revision includes new category 1 corneal dystrophies such as epithelial recurrent erosion dystrophy (ERED) and likely an entirely new category 1 corneal dystrophy, punctiform and polychromatic pre-Descemet corneal dystrophy (PPPCD), including its mutated gene (Table 1).

EPITHELIAL RECURRENT EROSION DYSTROPHIES: THE IMPORTANCE OF GENOTYPE

Most clinicians diagnose a specific corneal dystrophy solely on the basis of history and phenotype, and they do not or cannot obtain genetic analysis. As such, the IC3D corneal dystrophy nomenclature system is still primarily based on phenotype. Unfortunately, the lack of objective genotypic confirmation of the ophthalmologist's clinical impression has the disadvantage of not knowing whether the clinician's phenotypic assessment is correct or incorrect.

Epithelial recurrent erosion dystrophy (ERED) provides such an example. ERED was introduced in the first edition of IC3D as a new template to encompass Franceschetti corneal dystrophy (FRCD) and dystrophia Smolandiensis (DS), believed to be a variant of the former.[1] FRCD was category 4, and DS was category 3, both primarily characterized by recurrent corneal erosions without other corneal findings beginning in the first decade of life. The second edition of IC3D introduced an updated template called the epithelial recurrent erosion dystrophies (EREDs) after introduction of a further entity, dystrophia Helsinglandica (DH).[6] Each of these 3 autosomal dominant dystrophies had been characterized by recurrent erosions in childhood with no corneal findings between attacks. By

adulthood, corneal opacification with decreased vision could occur while erosion frequency diminished and possibly ceased. Although there was no gene or gene locus identified for any of the described EREDs, it was noted that "The difference in severity of corneal opacification in FRCD, DS, and DH could be explained by the presence of polymorphism and difference in expressivity of a common gene."[6]

Subsequent to the publication of the IC3D second edition, another corneal dystrophy, with similar symptoms and signs as FRCD, DH, and DS, was described by Jonsson et al who identified the associated abnormal gene as *COL17A1*. They classified this corneal dystrophy as epithelial recurrent erosion dystrophy (ERED).[11]

In 1997, almost a decade prior, Yee et al[12] had diagnosed a Bowman layer dystrophy mapping to 10q23-24 as Thiel–Behnke corneal dystrophy (TBCD). This observation was controversial because although there was possibly some phenotypic similarity, TBCD was previously known to only be associated with mutations on the *TGFBI* gene on chromosome 5. The IC3D group was skeptical, and in the second edition, the group wrote "we believe that there is insufficient evidence to consider this a variant of TBCD. Is it a distinct dystrophy?" Our observation proved to be prescient. Subsequently, Jonsson et al provided evidence that the abnormal gene in this dystrophy was also *COL17A1*.[11] Consequently, this corneal dystrophy, initially believed to be TBCD, was actually ERED.[13] Genotyping provided the necessary information to correct the misdiagnosis based on phenotype alone. Subsequently, ERED, resulting from mutations in *COL17A1*, has been reported in several countries.

The ERED story is an example of the importance of genotype. Only genotype can assist in confirming or refuting the phenotypic diagnosis. The TBCD/ERED saga also demonstrates the necessity of requiring a high level of evidence before deciding that there is a distinct genetic causation for a previously known corneal dystrophy. This evidence ideally includes examination of the cornea through a dilated pupil and examination of multiple generations of a family.[14–16]

The Evolution of the EREDs Template

After the discovery of ERED in 2015 from mutations in the *COL17A1* gene, the logical question was whether FRCD, DS, and DH mapped to this same gene. Unfortunately, there are no publications regarding this information. Personal communication from Dr. Irina Golovleva (Umeå, Sweden) suggests that DH maps to *COL17A1*, implying that DH and ERED may be the same dystrophy. While we suspect that FRCD and DS may also map to *COL17A1*, until published confirmation is attained, the EREDs template includes the category 1 corneal dystrophy ERED and corneal dystrophies of FRCD, DH, and DS demoted to category 4. If future studies demonstrate that *COL17A1* is the responsible gene for these dystrophies, we may have substantiation for concluding these are different names for the same entity, called ERED.

EPITHELIAL-STROMAL *TGFBI* CORNEAL DYSTROPHIES

Initially, corneal dystrophies were named on the basis of inheritance, phenotype, and when available, histopathology.[17,18] The addition of the epithelial-stromal *TGFBI* dystrophies anatomic category in the second edition of IC3D facilitated the opportunity to think about these corneal dystrophies genotypically rather than just phenotypically. For example, although Reis–Bücklers corneal dystrophy (RBCD) and granular corneal dystrophy type 1 (GCD1) have distinct mutations on *TGFBI*, both dystrophies are autosomal dominant, can develop recurrent erosions, show bright red deposits with Masson trichrome, and demonstrate rods on transmission electron microscopy. Although the phenotypes of RBCD and GCD1 are very different, the overlap in symptoms, signs, and histopathology is easily explained because both corneal dystrophies map to the same gene.

The Lattice Corneal Dystrophy Variants Compared with Classic Lattice Corneal Dystrophy

Since the introduction of the epithelial-stromal *TGFBI* category, this category has continued to grow in importance because of the ongoing discovery of dystrophies with distinct *TGFBI* mutations. These often have similar, though not identical, phenotypes to the *TGFBI* dystrophies that had already been described before discovery of their shared genetic background. For example, while classic lattice corneal dystrophy (classic LCD) is associated with the R124C mutation in the *TGFBI* gene, the expanding group called LCD variants in the IC3D nomenclature results from other distinct *TGFBI* mutations with clinical findings often similar though not identical to classic LCD. Although their phenotypes are typically reminiscent of classic LCD, some LCD variants lack distinct lattice lines, causing difficulty in making the clinical diagnosis. By histopathology, all LCD variants demonstrate corneal amyloid deposition as their primary diagnostic feature, although some may have minor deposits of keratohyalin. When compared with classic LCD, which is geographically widely spread and reported in 5 continents, known LCD variants are currently relatively geographically restricted. While classic LCD is caused by the R124C pathogenic variant in the first FAS1 domain of the TGFBI protein (earlier known as keratoepithelin), LCD variants are caused by several dozen distinct heterozygous amyloidogenic *TGFBI* variants that, with rare exceptions, localize to the fourth FAS1 domain of *TGFBI*. Over 80 LCD variants have already been published (Table 2).

Lattice Variant Nomenclature

We propose a nomenclature system for this expanding category of LCD variants. For the first time, actual names of dystrophies will be primarily assigned based on genotype rather than phenotype. Consequently, for both consistency of reporting and to facilitate literature searches, we recommend referring to the specific pathogenic variant, when known, by

TABLE 2. Lattice Corneal Dystrophy Variants

DNA Change	Protein	Exon	FAS1	Earliest Onset (Decade)	Erosions	Depth	Lines	Reported as	Clinical Description	Countries/ Ethnicity	Clinical Publications (Listed by PMID)	Experimental Publications (Listed by PMID)
c.370C>T	p.R124C	4	1	Early 1st	Yes	All eventually	Thin	LCDI	See LCD template (classic LCD)	Australia; Bangladesh; Brazil; Bulgaria; Canada; China; France; Greece; Germany; Hungary; India; Japan; Mexico; Singapore (Malay descent); Spain; Switzerland; Turkey; Ukraine; the United Kingdom; the United States	9054935, 9463327, 9497262, 9559741, 9592740, 9886734, 10798644, 10832717, 10844062, 11024425, 11095060, 11262611, 11146721, 11297504, 11413412, 11741113, 11923233, 11927442, 12138697, 12072720, 12225829, 12586172, 12770961, 15013897, 15017378, 15564760, 15623763, 16008913, 16118514, 16329070, 16380889, 16809844, 16710170, 16331487, 17063427, 16440005, 17768377, 17846354, 17982422, 18470323, 18615206, 19001012, 19062536, 19350511, 20161820, 20360992, 20664689, 20680100, 20806046, 21921985, 21462384, 21887843, 21835759, 22355247, 22773977, 22876129, 24801599, 25055147, 25876897, 25785536, 25932442, 26949635, 26748743, 27348782, 27737463, 27829782, 28393022, 28358433, 29085627, 30098247, 30805211, 31555324, 33513810, 34937214, 35484844, 35985662	21948648, 22080335, 23861389, 25557343, 26207300, 30387319

TABLE 2. (*Continued*) Lattice Corneal Dystrophy Variants

DNA Change	Protein	Exon	FAS1	Earliest Onset (Decade)	Erosions	Depth	Lines	Reported as	Clinical Description	Countries/ Ethnicity	Clinical Publications (Listed by PMID)	Experimental Publications (Listed by PMID)
c.1486C>T	p.R496W	11	3	Late 9th	No	Mainly deep	Minor	LCDIV	Corneal haze with many isolated or fused refractile opacities, mostly dots, some lattice lines, mainly in deep stroma	Japan	20974628	
c.1501C>A	p.P501T	11	None	Late 7th	Yes	Mainly anterior	Thick	LCDIIIA Japanese	*Asymmetric*; late-developing thick ropy lattice lines; linear thick branching rod-like opacities from limbus to limbus and discrete nodular deposits; thick ropy lattice lines	China; Japan; South Korea	9497262, 10218700, 10832717, 11004271, 11024425, 11501939, 12400061, 16809844, 21462384, 23884333, 26748743	
c.1504A>G	p.M502V	11	4	Late N/A	N/A	Unclassifiable	N/A	LCD atypical	Unclassifiable phenotype because of extensive corneal opacifications, 32-year-old daughter with small round, refractive deposits predominately in the anterior stroma	Mexico	19303004	
c.1514T>A	p.V505D	11	4	Early 1st	Yes	Mainly anterior	Thin	LCDI	Symmetrical opacities more prominent in the central cornea, in younger patients a few thin lattice lines anteriorly and axially with light central stromal clouding, with increasing age opacities spread posteriorly and centrifugally, 1–2 mm clear peripheral zone	China	15838722	
c.1526T>C	p.L509P	11	4	Early 2nd	Yes	Mainly anterior	Thin	LCDI; LCDIIIA; RBCD	Cloudy and geographic primarily subepithelial opacities, small granules in anterior stroma; confluent irregular and coarse geographic subepithelial and anterior stromal opacities; diffuse subepithelial opacities in direct illumination, paracentral stromal lattice lines in retroillumination; a network of thick lattice lines and dots; diffuse grayish-white subepithelial deposits, distinct refractile lattice lines spreading to the periphery; geographic opacities at Bowman layer level, lattice lines in deeper layers	France; Germany; South Korea	19001012, 21617751, 25055147, 26748743, 35683443	
c.1526T>G	p.L509R	11	4	Early 2nd	Yes	Mainly anterior	Thin	LCD atypical; EBMD	Irregularly shaped maps, faint gray–white patches 1 to several millimeters in size, map-dot-fingerprint changes; bilateral subepithelial geographic map-like opacities, lattice lines; geographic opacities at Bowman layer level, lattice lines in deeper stroma	France	16652336, 21617751	
c.1553T>C	p.L518P	12	4	Early 2nd	Yes	Mainly anterior	Thin	LCDI; LCDI Atypical	Dense superficial opacity, fine lattice lines in superficial stroma and midstroma, age 17 years fine lattice lines in superficial stroma and midstroma; age 15 round subepithelial central opacities, later extend into peripheral and deep stroma	Japan	10482106, 10837380, 11095060, 12138697, 21948648	
c.1553T>G	p.L518R	12	4	N/A	N/A	N/A	N/A	LCD//IIIA	Advanced subepithelial and stromal amyloid deposits	Switzerland (Swiss, Italian, or French descent)	11923233	
c.1565T>A	p.I522N	12	4	Early 2nd	Yes	Mainly anterior	Thin	LCDI	Distinct lattice lines and diffuse opacification in subepithelial and anterior stroma, thick lattice lines, and diffuse grayish-white clouding that partly hides central lattice lines	China; Mexico	19956413	

(*Continued*)

TABLE 2. (*Continued*) Lattice Corneal Dystrophy Variants

DNA Change	Protein	Exon	FAS1	Earliest Onset (Decade)	Erosions	Depth	Lines	Reported as	Clinical Description	Countries/ Ethnicity	Clinical Publications (Listed by PMID)	Experimental Publications (Listed by PMID)
c.1580T>G	p.L527R	12	4	Late 7th	No	Mainly deep	Thick in some eyes	LCDIII; LCDIV; LCD deep	*Asymmetric*; large nodular gray–white deposits from deep stroma to pre-Descemet in pupillary zone or large filiform and lattice line opacities in various parts of stroma; deep stromal nodular deposits and thick lattice lines; distinct lattice lines; lattice-shaped granular deposits in asymmetric patterns, nodulolinear deposits mainly in anterior stroma, less linear and macular opacities; bifurcating thick lattice lines in superficial stroma in midperiphery, extending to central stroma, no nodular deposits; discrete and nodular opacities in deep central stroma, no visible lattice lines; haze composed of isolated or fused refractile opacities, most dot-like, some lattice-like; several bifurcating thick lattice lines in superficial to midstroma; discrete nodular opacities in deep stroma	Japan; South Korea	9799082, 10832717, 11024425, 11095060, 11501939, 11413411, 12138697, 15022435, 15770959, 15923518, 16453189, 17846354, 20357204, 21191728, 21835759, 22876129, 24505203, 26748743	21948648
c.1612A>C	p.T538P	12	4	Early 1st	Yes	Mainly anterior	Thin	LCDI	Lattice lines in central stroma; numerous fine lattice lines and dots in anterior central stroma	Australia; China	16809844, 21462384, 35985662	22605926
c.1613C>G	p.T538R	12	4	Early 1st	Yes	Mainly anterior	N/A	LCDI/IIIA	LCDI-like	Switzerland (American descent); Ukraine	11923233, 19062536	
c.1616T>A	p.V539D	12	4	Late 6th	N/A	Mainly anterior	N/A	N/A	Lattice lines in anterior stroma; anterior and midstromal lattice lines	India	15623763	
c.1617T>A	p.F540S	12	4	Late 5th	No	Mainly deep	Thick	N/A	Thick ropy lattice lines	Germany; China	15790870	25557343
c.1625C>G	p.P542R	12	4	Late 5th	Yes	Anterior to deep	Thick	LCD atypical	Distinct lattice lines; relatively thick lattice lines from the limbus in superficial and deep stromal layers, stromal haze in 1 eye	South Korea	22876129, 26748743	
c.1631A>G	p.N544S	12	4	Late 7th	No	Mainly deep	Thin	LCDIV atypical	Distinct lattice lines; dots and lattice lines in midstroma to deep stroma; tiny nodular deposits and thin lattice lines in midstroma	Japan; South Korea	11024425, 15559315, 15770959, 26748743	
c.1636G>A	p.A546T	12	4	Intermediate 4th	Yes	Anterior to deep	Thick	LCDIIIA French	Age 55 years predominantly central thick ropy lattice lines, some small nodular opacities, diffuse haze between the lines, age 35 years superficial lattice lines	Brazil; China; France	10682981, 11297504, 11927442, 16440005, 21462384	25910219, 34097874
c.1637C>A	p.A546D	12	4	Intermediate 3rd	No	Deep to anterior	Minor to thin	LCDIIIA; PCA; GCD1/2	Multiple polymorphic, polygonal, refractile chipped ice-like gray and white opacities, occasional deep filamentous lines without distinct lattice pattern but producing a small focal network; polymorphic chipped ice-like opacities in posterior stroma, occasional filamentous lines without distinct lattice pattern; polymorphic stromal opacities, distinct branching filamentous lattice opacities, small granular opacities in peripheral cornea; atypical GCD1-like; five predominantly GCD2-like phenotype, one GCD1-like, one LCD-like phenotype; typical IIIA phenotype with focal central and distinct relatively thick lattice lines; polymorphic opacities predominantly in central cornea; short lineal	China; Germany; Mexico; Taiwan; the United States	15177960, 17063427, 17893671, 19001012, 19303004, 21462384, 22355247, 28393022, 35470743, 35484844	23592924

TABLE 2. (*Continued*) Lattice Corneal Dystrophy Variants

DNA Change	Protein	Exon	FAS1	Earliest Onset (Decade)	Erosions	Depth	Lines	Reported as	Clinical Description	Countries/ Ethnicity	Clinical Publications (Listed by PMID)	Experimental Publications (Listed by PMID)
									deposits, without a clear lattice pattern; polymorphic opacities in central stroma, conspicuous interdigitating branching filamentous opacities and multiple lattice lines in peripheral stroma, also small granular opacities in peripheral cornea			
c.1640T>C	p.F547S	12	4	Intermediate 4th	N/A	Deep to anterior	Minor	PCA	Snowflake-like central deposits, fine linear and chipped-ice deposits, more abundant in central cornea, extending throughout stroma, numerous pre-Descemet deposits	Hungary	17982422	
c.1643G>C	p.R548P	12	4	Late 7th	N/A	Deep to anterior	Minor	LCD variant; RBCD	Diffuse central corneal haze with edema without visible lattice lines	South Korea	26748743	
c.1649T>C	p.L550P	12	4	N/A	N/A	Deep to anterior	Thin	GCD2	Deposits typical of GCD2 with bilateral symmetrical discrete lattice lines in peripheral cornea; fine peripheral lattice lines with powdery central lesions, another patient with lattice and granular stromal deposits	Mexico; South Korea	19303004, 33513810	
c.1673T>C	p.L558P	12	4	Intermediate 3rd	N/A	Deep to anterior	Thin	LCDIV; PCA	Initially scarce central punctiform 50–100 μm stromal deposits, later confluent, white–gray under direct illumination, typical branched filamentous opacities 0.5–3.0 μm length with no haze in some patients, in 1 patient with granular opacities arranged in irregular round shape in lower cornea; polymorphic corneal amyloidosis with deep stromal opacities	Spain; Ukraine	19062536, 31056827	
c.1673T>G	p.L558R	12	4	Late 6th	No	Deep to anterior	Minor	LCD	Fine translucent gray–white branching stromal lattice lines and dots at all depths	Czech Republic	27028151	
c.1694T>A	p.L565H	13	4	Late 5th	N/A	N/A	Minor to thin	LCDIIIA; LCD atypical	Haze and diffuse opacities in central stroma, lack of typical lattice lines, oval-shaped or short comma-shaped spots with indistinct margins within deep stroma; diffused opacities in central stroma, fine lattice lines in paracentral and peripheral stroma; small diffused translucent punctate opacities and a few chipped ice-like lattice lines; uniformly diffused punctate opacities in central stroma, fine lattice lines mostly in paracentral stroma	China	31555324, 35484844	
c.1694T>C	p.L565P	13	4	Late 6th	Yes	Deep to anterior	Minor	LCD atypical	Round, oval, and short comma-shaped opacities with indistinct margins, no visible lattice lines	Poland	24473223	
c.1706T>A	p.L569Q	13	4	Late 6th	Yes	N/A	Thick	LCDI	Large lattice lines; typical lattice lines	South Korea	25932442, 26748743	
c.1706T>G	p.L569R	13	4	Early 1st	Yes	Mainly anterior	Thin	LCDI	Diffuse subepithelial and anterior stromal clouding, typical fine branching lattice lines in midperipheral anterior stroma; age 7 years numerous fine refractile lattice lines and dots in central cornea; typical fine branching lattice lines, area of central opacification	The United States (Swiss, Italian, and Irish descent)	14597039	

(*Continued*)

TABLE 2. (*Continued*) Lattice Corneal Dystrophy Variants

DNA Change	Protein	Exon	FAS1	Earliest Onset (Decade)	Erosions	Depth	Lines	Reported as	Clinical Description	Countries/ Ethnicity	Clinical Publications (Listed by PMID)	Experimental Publications (Listed by PMID)
c.1715A>G	p.H572R	13	4	Intermediate 3rd	Yes	Anterior to deep	Thin to thick	LCDI	*Asymmetric*; elevated subepithelial opacities, diffuse haze, thin to thick lattice lines, diffuse haze; elevated subepithelial opacities, thick lattice lines, diffuse haze; subepithelial and stromal white dots, thin linear irregular branching refractile lines; mild cases resemble LCDI with refractile lattice lines from central stroma to periphery with limbal sparing, in advanced cases lattice lines usually obscured by diffuse stromal opacity, difficult to distinguish from leukoma, corneal surface eventually becomes irregular because of elevated thick lattice lines; lattice lines thicker and less crowded than in LCDI, in anterior stroma yellowish discoloration	Thailand; Chile; China	17013691, 20161820, 20806046, 31270466, 33513810	32637173
c.1772C>T	p.S591F	13	4	Intermediate 4th	Yes	Deep to anterior	Thick	LCD asymmetric	*Asymmetric*; translucent subepithelial irregularity, relatively short and thick, branching central lattice lines, extending midperipherally; discrete relatively short and thin branching lattice lines in anterior and midstroma in central stroma	Finland; the United States (Spanish descent)	33645289, 35315300	
c.1781G>T	p.G594V	13	4	Late 6th	N/A	Deep	Thick	LCD atypical	Thick lattice lines in deep stroma, extending to limbus	India	15623763	
c.1828T>G	p.V613G	14	4	Late 9th	N/A	N/A	N/A	LCD	Corneal opacities, child with small dots and a star-shaped opacity	Algeria	21617751	
c.1856T>A	p.M619K	14	4	Late 5th	No	Anterior to deep	Thick	GLCD	In younger individuals, central subepithelial needle-like deposits; in older individuals, polymorphic semiconfluent anterior stromal opacities, combined granular lattice; axially distributed linear branching anterior and midstromal deposits, gray–white on direct illumination and translucent on retroillumination, additionally discrete semiconfluent anterior and midstromal polymorphic deposits; peripheral cornea with linear branching opacities similar to LCDI; dense confluent gray–white anterior and midstromal deposits in central stroma, a few linear extensions of central opacity	The United States (Hispanic)	18332318	28381645
c.1858G>C	p.A620P	14	4	Intermediate 4th	Yes	Mainly anterior	Thin	LCDIIIA granular	Distinct lattice lines; diffuse superficial haze and extensive lattice lines; focal superficial opacity, thick lattice lines	China; South Korea	25321938	
c.1859C>A	p.A620D	14	4	Intermediate 3rd	Yes	Mainly anterior	Thin	LCD variant	Subepithelial and anterior stromal scarring, radially oriented linear opacities in central anterior to midstroma	China; South Korea	21835759, 26949635, 26748743, 33513810	
c.1861A>C	p.T621P	14	4	Late 5th	Yes	Mainly anterior	Thick	LCDIIIA	*Asymmetric*; thick branching ropy lattice lines; thick ropy lattice lines extending to limbus with intervening opacities in central stroma	South Korea	25932442, 27163623, 35484844	
c.1864A>C	p.N622H	14	4	Late 5th	No	Anterior to deep	Thick	LCDIIIA; LCD late	*Asymmetric*; thick central ropy lattice lines	Australia; the United Kingdom	10328397, 35985662	28381645
c.1866T>G/A	p.N622K	14	4	Intermediate 4th	Yes	N/A	Thick	LCDIIIA	Large, ropy lattice lines in anterior stroma	Switzerland (Italian, South American descent)	11923233	

TABLE 2. (*Continued*) Lattice Corneal Dystrophy Variants

DNA Change	Protein	Exon	FAS1	Earliest Onset (Decade)	Erosions	Depth	Lines	Reported as	Clinical Description	Countries/ Ethnicity	Clinical Publications (Listed by PMID)	Experimental Publications (Listed by PMID)
c.1867G>C	p.G623R	14	4	Intermediate 3rd	Yes	Mainly anterior	Minor to thin	LCD	In a young patient, single subtle greyish lattice line; in an older patient, subepithelial map-like opacities in central and midperipheral stroma, 2 branching lattice lines in anterior stroma, delicate thin anterior to midstromal lines in midperipheral cornea	Germany	19001012	28381645
c.1868G>A	p.G623D	14	4	Intermediate 3rd	Yes	Anterior	Minor to thin	LCDI/IIIA; RBCD; TBCD; EBMD	Tiny discrete linear subepithelial deposits in anterior stroma, middle, and posterior stroma free; patchy subepithelial central stromal haze, a single refractile lattice-like line; several foci of subepithelial haze, a single branching refractile anterior stromal lattice line-like deposit in 1 eye; scattered central patches of subepithelial haze without lattice lines, delicate thin anterior and midstromal lattice lines most dense axially and absent from peripheral 2 mm, a horseshoe-shaped opacification at Bowman layer level in 1 eye; central subepithelial haze, a prominent central subepithelial opacity, very fine branching lattice lines in central anterior stroma, other eye with scattered gray–white subepithelial opacities forming an arrowhead pattern, no lattice lines; subepithelial deposits resembling RBCD; diffuse or geographic superficial stromal opacity, small refractile granules or lines, diffuse axial anterior stromal haze with small lattice lines; geographic pattern of subepithelial haze and tiny granular structures; diffuse subepithelial haze and small refractile structures; subepithelial nodular opacification in a geographic pattern	Switzerland (Swiss, Italian, or French descent); the United Kingdom; the United States	11923233, 15885785	
c.1870G>A	p.V624M	14	4	Late 5th	No	Deep to anterior	Thick	LCD	*Asymmetric*; thick ropy linear opacities in deep stroma, fellow eye with small deep short rod-shaped stromal opacities	The United States	18385782	22155582, 25557343
c.1874T>A	p.V625D	14	4	Early 2nd	Yes	Anterior	Thin	LCD	Ridgy round pattern of opacities with uneven surface and thin lattice lines; diffuse anterior stromal haze, small granular focal opacities, lattice lines not visible	China	17765440, 27737463	
c.1877A>C	p.H626P	14	4	Early 1st	Yes	Anterior	N/A	LCDI/IIIA; early-onset superficial keratopathy	Dense haze, lattice lines; confluent subepithelial opacities; irregular corneal surface, discrete subepithelial gray–white polymorphic opacities project from Bowman layer level into epithelium, with longer duration increasing scarring, neovascularization and calcification with no visible lattice lines	Switzerland (Swiss, Italian, or French descent); Czech; New Zealand	11923233, 18259096, 18728790	
c.1877A>G	p.H626R	14	4	Intermediate 3rd	Some	Anterior to deep	Thick	LCDI/IIIA LCDIIIA LCDIIIB; LCDi; LCD asymmetric	*Asymmetric*; broad lattice lines; broad lattice lines, dense central scarring, initially lower cornea, initially thin lines in fellow eye; subepithelial clumps of translucent material; initial asymmetric stellate deposits in the lower central cornea; thick lattice lines in the	Canada; China; Finland; France; India; Mexico; Switzerland; Ukraine; Vietnam; the United	10328397, 10798644, 11146721, 11297504, 11923233, 11927442, 12072720, 12770961, 15623763,	28381645, 28689406, 30387319

(*Continued*)

TABLE 2. (*Continued*) Lattice Corneal Dystrophy Variants

DNA Change	Protein	Exon	FAS1	Earliest Onset (Decade)	Erosions	Depth	Lines	Reported as	Clinical Description	Countries/ Ethnicity	Clinical Publications (Listed by PMID)	Experimental Publications (Listed by PMID)
									whole stromal layer; a band-shaped deposition of amyloid close to Descemet membrane; initially subepithelial stellate deposits in lower central cornea; lattice lines and central patchy deposits; fewer but thicker and deeper lattice lines, extending more to the periphery than those of LCD1; anterior-to-midstromal lattice lines; fine GCD1-like opacities mainly in the central cornea; lattice lines in family, PCA in a sporadic patient; bilateral symmetrical fine translucent lattice lines in the superficial and middle stromal layers; thick lattice lines in peripheral and central cornea with small contralateral stellate or snowflake-like deposits; lattice lines and recurrent diffuse stromal haze; thick lattice lines in deep stroma; thick lattice lines extending toward periphery; delicate fragile rare lattice lines located centrally; thick, distinct lattice lines extending from limbus to limbus accompanied by stromal haze; radially oriented curvilinear opacities; gray–white thick lattice lines extending across the cornea; asymmetric, branching, translucent lattice lines, focally with stromal haze, a single patch peripherally in fellow eye; coarse, branching, lattice lines, with prominent stromal haze, a single patch peripherally in fellow eye; translucent focally delicate and branching, focally coarse deposits associated with stromal haze; GCD2 phenotype; numerous translucent, thick lattice lines in superficial and midstroma in central and peripheral cornea; minor lattice lines predominantly below the visual axis; lattice lines predominantly below the visual axis; gray–white thick lattice lines in deep stroma; thick, ropy lattice lines extending to periphery, superficial scar from recurrent erosions	Kingdom; the United States	16008913, 16888689, 18728790, 19001012, 19350511, 19303004, 20664689, 21921985, 21835759, 24579556, 24589966, 24801599, 25876897, 26949635, 27348782, 27737463, 28358433, 30851800, 33513810	
c.1892T>A	p.V631D	14	4	N/A	N/A	Deep to anterior	N/A	LCD deep	Initially stellate pre-Descemet deposits with round Descemet indentations, later radial lattice lines in midstroma, anterior third of stroma mostly intact; opacities typically in central stroma	Switzerland (Italian descent)	11923233, 23455751	

EBMD, epithelial basement membrane dystrophy; GCD, granular corneal dystrophy; GLCD, granular-lattice corneal dystrophy; LCD, lattice corneal dystrophy; LCDI, previously called lattice corneal dystrophy, type 1 and now renamed classic lattice corneal dystrophy; LCDi, lattice corneal dystrophy intermediate; PCA, polymorphic corneal amyloidosis; RBCD, Reis-Bücklers corneal dystrophy; TBCD, Thiel-Behnke corneal dystrophy.

appending the protein change using 1-letter amino acid abbreviations. For example, the LCD variant named LCD-H626R results from the His626Arg missense mutation. Identification of the variant by genetic mutation may be helpful in the future, should gene-targeted therapies be developed.

The Wide Variety of Lattice Variant Phenotypes

While lattice lines are typically evident within the many variants, the spectrum of their phenotypes may vary wildly with some variants having remote or no clear resemblance to classic LCD. The age of onset and the

depth of the deposits differ between variants, and some variants include opacities that have been described as polymorphic, polygonal, refractile chipped ice-like, gray to white, snowflake or geographic, rather than linear.[15] These LCD variants may initially be misdiagnosed as other corneal dystrophies like epithelial basement membrane dystrophy (EBMD), RBCD, TBCD, or GCD1 (Table 2) until genotyping reveals the true diagnosis.

There are at least 5 recurring major phenotypes which are distinguished by the onset of clinical signs in addition to the shape and depth of the opacities. There is often histopathologic confirmation regarding the depth and distribution of amyloid deposits. Similar to classic LCD, phenotypic variation can be found between both eyes and among individual patients with the same mutation. Some advanced cases may have severe anterior stromal scarring that obscures other phenotypic features. In these instances we do not know the earlier phenotype, when these patients were younger, that preceded the severe corneal scarring.

The 5 major phenotypes of LCD variants include (Table 2) the following:

1. Early-onset LCD variants.

   Similar features and age of onset to classic LCD
   (eg, LCD-V505D, LCD-L518P, LCD-T538P, and LCD-P569R).

2. Typically intermediate and sometimes late-onset LCD variants.

   Thicker, often ropy, more prominent lattice lines than classic LCD.
   (eg, LCD-P501T, LCD-A546T, LCD-S519F, LCD-T621P, and LCD-H626R which is the second most common and widespread LCD).[19]

3. Late-onset LCD variants.

   Lattice lines can range from inconspicuous/infrequent to distinct. Amyloid deposits mostly in deep stroma close to Descemet membrane.
   (eg, LCD-R496W, LCD-G594V, and LCD-V631D).

4. Early or intermediate-onset LCD variants with superficial geographic opacification from Bowman layer deposits.

   Infrequent and/or indistinct lattice lines. Easily misdiagnosed as RBCD or TBCD or even EBMD.
   (eg, LCD-L509R, LCD-G623D, and LCD-H626P).

5. Intermediate, sometimes late-onset LCD variants with polymorphic deposits.

   Distinct or inconspicuous/infrequent lattice lines which may resemble chipped ice. The deposits vary in form and depth and are mostly dot-shaped and comma-shaped. Later in the disease course, with further dystrophy progression, some corneas demonstrate more prominent central opacification
   (eg, LCD-L527R, LCD-A546D, LCD-A547S, LCD-L558P, and LCD-L565P).

PRE-DESCEMET CORNEAL DYSTROPHY (PDCD)

In the second edition of the IC3D, we reported that isolated pre-Descemet corneal dystrophy (PDCD) was not well defined because it was neither clearly hereditary nor degenerative. In the IC3D third edition, we have expanded the PDCD template to a template entitled PDCDs, which also includes the degeneration, cornea farinata, as well as punctiform and polychromatic pre-Descemet corneal dystrophy (PPPCD). In 2020, PPPCD was mapped to the *PRDX3* gene on chromosome 10.[20] The pre-Descemet opacities in PPPCD are polychromatic, larger, and more punctate than those in the degeneration, cornea farinata. We have chosen to include PPPCD within the PDCDs template so that clinicians can easily compare the findings of PPPCD, with which they may be unfamiliar, with the more common degenerative condition of cornea farinata. The goal is that the clinician presented with this additional knowledge has an opportunity to revise their diagnosis accordingly. In addition, a single patient with PPPCD was found to also have polychromatic crystals beneath their lens capsule, introducing the question of whether PPPCD is actually a corneal dystrophy or a manifestation of a systemic disease.[20]

SHOULD GENETIC TESTING BE PERFORMED WHEN SUSPECTING A CORNEAL DYSTROPHY?

How can an ophthalmologist confirm that their phenotypic diagnosis is correct when genotypic information is not available? If the dystrophy requires surgical intervention to improve vision, excision of corneal tissue may be submitted for pathology to further substantiate the clinical diagnosis. However, most patients with corneal dystrophies do not need surgical intervention. It has also been found that if the pathologist is unsure of what they seek, they may erroneously confirm an ophthalmologist's postulated though erroneous diagnosis.[3]

How critical is the accuracy of a specific corneal dystrophy diagnosis? Patients are interested in their prognosis, and different dystrophies have distinct clinical courses. Among the *TGFBI* corneal dystrophies which are typically distinguished on corneal examination and history, GCD1 usually results in more frequent corneal erosions and earlier visual loss than granular corneal dystrophy type 2 (GCD2). GCD2 will progress more rapidly after corneal injury, including surgery, while this does not occur with classic LCD. This type of information is of importance to an affected patient. While the clinical examination will often be sufficient to provide a specific corneal dystrophy diagnosis, this also depends on the experience and expertise of the examiner. Genetic testing is an easy way to confirm or refute the phenotypic diagnosis. The LCD variants are an excellent example in which a dystrophy may have a phenotype similar to classic LCD but a different mutation. In addition, some LCD variants do not resemble any widely recognized corneal dystrophy, and thus, genotyping may be necessary to even establish a corneal dystrophy diagnosis. Genotyping is infrequently performed because of inconvenience and cost. If genetic testing were performed more frequently, we might

discover that our phenotypic diagnoses are less accurate than we imagine. Genotyping might also reveal more genetic variants with distinct mutations, as has occurred with the LCD variants, a category that continues to grow. In addition, genotyping may prove important if gene-targeted therapy is developed.

THE SPORADIC CORNEAL DYSTROPHY

When should the diagnosis of a sporadic corneal dystrophy be considered? When the diagnosis of a typically autosomal dominant corneal dystrophy is considered in an individual with a negative family history, the clinician should try to examine both parents and possibly other family members to determine whether some other family members could manifest the dystrophy but remain asymptomatic. In addition, other conditions such as paraproteinemic keratopathy (PPK) associated with monoclonal gammopathy of undetermined significance (MGUS), smoldering plasma cell myeloma or Waldenström macroglobulinemia should be excluded.[21] PPK can mimic various corneal dystrophies including SCD, LCDs, or GCD1. The index of suspicion for PPK can increase if there is late and possibly unilateral onset with a negative family history. Serum protein immunoelectrophoresis can reveal the presence of a monoclonal gammopathy.[22]

If after careful history and examination, the clinical phenotype still suggests a sporadic corneal dystrophy, for example, GCD1 or RBCD, the possibility of a *de novo* mutation must be considered. This term describes a change in the DNA sequence of a gene (for GCD1 and RBCD, this would be *TGFBI*) that is seen for the first time in a person and has not appeared in previous generations. A *de novo* mutation explains how a patient can have a corneal dystrophy that did not occur in his or her parents or siblings. Therefore, to make the molecular diagnosis of a *de novo* autosomal dominant mutation, testing of both parents must be negative for the mutation detected in the index patient. True sporadic or *de novo* cases can only be confirmed by molecular testing of the affected patient, the parents, and if necessary, their siblings.

It is important to recognize that in the same pedigree, different affected individuals can show variable phenotypes from mild to severe because of variable expressivity. It is also possible that a molecularly affected individual may not show any signs of the disease because of reduced penetrance of the gene mutation. This is why when making the argument for a *de novo* mutation in an autosomal dominant corneal dystrophy, it is mandatory that molecular genetic testing, not simply clinical examination, be performed for the proband and also clinically unaffected parents and siblings.

THE FOUNDER EFFECT

The founder effect is the introduction of a new mutation that becomes more frequent over generations resulting in the loss of genetic variation in this subset of the larger population. The most common scenario is offspring of an individual who first developed a *de novo* genetic mutation and for geographical reasons (eg, living in a remote area or on an island), the genetic diversity is reduced. Over time, there is likely to be a higher rate of this gene mutation compared with an ethnically and racially similar population. As migration occurs and affected individuals move away from the original area or population, by comparing haplotypes between affected individuals, a founder effect can still be detected. A founder effect need not only be seen in autosomal dominant conditions.[23–25]

PRINCIPLES OF MANAGEMENT

The management of corneal dystrophies is essentially functional to improve visual acuity and/or symptomatic to relieve ocular discomfort or pain.

Abnormalities in the ocular surface result from corneal dystrophies affecting the epithelium and/or anterior stroma. Corneal surface irregularity may be associated with foreign body sensation or painful corneal erosive episodes resulting from poor epithelial adhesion. If corneal epithelial irregularity involves the visual axis, then irregular astigmatism reduces quality and/or visual acuity. Such corneal epithelial abnormalities can be managed conservatively with lubricants, hyperosmotic agents, patching, bandage contact lenses, or, when recalcitrant, minor surgical interventions such as manual epithelial debridement, superficial keratectomy (SK) of subepithelial debris and deposits, anterior stromal puncture, superficial diamond burr polishing, or excimer laser phototherapeutic keratectomy (PTK).

Deposition of opaque substances in epithelial, subepithelial, epithelial-stromal *TGFBI* or stromal corneal dystrophies may also result in vision reduction. Visual loss may also occur in endothelial corneal dystrophies because of corneal epithelial or stromal edema consequent to endothelial dysfunction. Stromal scarring can also result from multiple epithelial erosions and chronic stromal edema.

The ophthalmologist and patient must decide if and when intervention is required to improve comfort and vision, understanding that dystrophies can recur although the frequency of recurrence depends on the specific corneal dystrophy. For the more superficial epithelial basement membrane dystrophies or degenerations, such as EBMD, SK alone is remarkably effective in improving acuity and decreasing erosions, and these benefits are often sustained for years, if not indefinitely, without recurrence. For opacities involving only the subepithelial and/or superficial stromal layers, SK and PTK are currently preferred for their technical ease, although both can be associated with high rates of recurrence within a few years. Mitomycin C (MMC) application has been used in conjunction with PTK for some corneal dystrophies in an attempt to decrease the risk of recurrence without definitive evidence for efficacy. MMC does seem to reduce postoperative scarring/haze when deeper stromal ablations are required to remove the bulk of the corneal opacity.

For more diffuse and deep stromal deposits, stromal replacement surgery such as deep anterior lamellar keratoplasty (DALK) or penetrating keratoplasty (PK) can be performed with DALK having an advantage of retaining

unaffected endothelium, thereby eliminating endothelial immune rejection risk. PK may be reserved for failed DALK attempts. Mushroom-shaped PK can be alternatively used to allow maximal removal of the diseased stroma with minimal endothelial replacement. Compared with PTK and SK, latency of recurrence is longer for DALK and may be even longer for PK. In epithelial-stromal *TGFBI* dystrophies, recurrent deposits have been observed within the epithelium, superficial stroma, graft–host interface, or along suture tracks (refer to GCD1 template).

For dystrophies solely associated with endothelial dysfunction, endothelial keratoplasty, either by Descemet stripping automated endothelial keratoplasty (DSAEK) or Descemet membrane endothelial keratoplasty (DMEK), has become favored in comparison with PK because the former offers more rapid visual recovery, improved visual outcome, reduced immune rejection rates and lower risk of traumatic surgical wound dehiscence.

It is important to realize that not all corneal dystrophy patients require treatment. The ophthalmologist may be surprised by a patient's excellent visual acuity despite significant corneal opacification. Patients with SCD in their twenties, especially those without corneal crystals, often have no complaints. Early FECD with only corneal guttae and only mild stromal edema can retain excellent visual acuity and may be potentially benefited without surgical intervention, from regenerative medical therapies such as topical rho kinase inhibitors.[26,27] The progression of corneal dystrophies is often variable such that the diagnosis of a particular corneal issue does not necessarily predict its course or therapy requirement. Consequently, the ophthalmologist must understand both the patient's symptoms and their severity before determining whether and what interventions should be considered. The exact etiology of a patient's complaint must be verified by a complete eye examination. If bothersome ocular irritation, recurrent erosion, and/or decreased vision are present, it is imperative to ascertain whether such complaints are consequent to stromal opacity and/or irregular surface astigmatism, as well as to assess the potential contributions of other ocular disorders such as amblyopia, cataract, glaucoma, or retinal issues. The choice of treatment becomes critically dependent on such exact etiologic diagnosis of the patient's complaint.

Table 3 outlines the management strategies for various corneal dystrophies.[28–51] Several corneal dystrophies including FCD, PACD, CCDF, and PDCD are typically asymptomatic and do not require treatment. The table provides a broad overview of general treatment approaches rather than an exhaustive description of all possible treatments. More detailed sources should be consulted when contemplating treatment for a specific corneal dystrophy.

THE IC3D FUTURE

The first and second editions of the IC3D were directed toward the clinician and the pathologist to facilitate diagnosis of the patient with corneal dystrophy, and this third edition continues that goal. The IC3D first, second, and third editions are available at https://corneasociety.org/publications/ic3d. The examining ophthalmologist has ready online access to the dystrophy templates without charge while examining a patient, as a guide for their diagnosis. While the IC3D has continued to publish nomenclature updates every 7 to 8 years, our infrequent journal publications are not an optimal approach to keep pace with the rapid changes in the corneal dystrophy knowledge base. The Cornea Society has secured the website domain www.ic3dcornealdystrophy.org so that going forward, the IC3D will have the potential to make more frequent changes online as the corneal dystrophy knowledge base advances.

EPITHELIAL AND SUBEPITHELIAL DYSTROPHIES

Epithelial Basement Membrane Dystrophy (EBMD)

Mendelian inheritance in man (MIM) #121820.

Former Alternative Names and Eponyms

Anterior basement membrane dystrophy.
Map-dot-fingerprint dystrophy.
Cogan microcystic epithelial dystrophy.

Inheritance

Most cases have no inheritance documented. Consequently, EBMD is usually considered to be degenerative or secondary to trauma.

Genetic Locus

None.

Gene

None (see note below).

Onset

Commonly presents in adult life. Rarely described in children.

Signs

Maps

Irregular islands of thickened, gray, hazy epithelium with scalloped, circumscribed borders, particularly affecting the central or paracentral cornea. Isolated or combined with other signs (Fig. 1A).

Dots (Cogan)

Irregular round, oval, or comma-shaped nonstaining, putty-gray intraepithelial opacities, clustered like an archipelago in the central or paracentral cornea (Fig. 1B). Typically combined with other signs, especially with maps.

TABLE 3. Management of Corneal Dystrophies

Corneal Dystrophies	Management
Epithelial and subepithelial dystrophies	
Epithelial basement membrane dystrophy (EBMD)	Asymptomatic patients do not require treatment.
	For recurrent erosions, treatment may include lubricant drops, gels, or hyperosmotic agents during the day and/or ointments at bedtime. Patching or bandage contact lenses may also be necessary for acute attacks.[28] Oral tetracyclines with topical steroids may be considered for recalcitrant erosions.[29,30] SK to remove devitalized epithelium plus subepithelial pannus or deposits can improve epithelial–stromal adhesion and reduce irregular astigmatism. For persistent erosions outside the visual axis, anterior stromal micropuncture is recommended.[31] When severe erosions are in the visual axis, mechanical debridement of loosened epithelium with or without diamond burr-assisted polishing is preferable to micropuncture.[32]
	Excimer laser PTK is an alternative treatment, particularly if irregular astigmatism involves the visual axis or if there is underlying anterior corneal haze/scarring.[33] Consider avoiding LASIK in EBMD because of the increased risk of epithelial sloughing and epithelial ingrowth.[34]
Epithelial recurrent erosion dystrophies (EREDs)	For recurrent erosions, refer to section on EBMD management. For anterior stromal opacification, refer to section on RBCD/TBCD.
Subepithelial mucinous corneal dystrophy (SMCD)	For recurrent erosions, refer to section on EBMD management. For anterior stromal opacification, refer to section on RBCD/TBCD.
Meesmann corneal dystrophy (MECD)	Ocular discomfort due to epithelial microcysts and erosions can be managed with lubricants and occasionally bandage contact lenses. Epithelial debridement is rarely required.[35]
Lisch epithelial corneal dystrophy (LECD)	Refer to section on EBMD management. Surgical intervention is rarely required.[36]
Gelatinous drop-like corneal dystrophy (GDLD)	Lubricant eye drops and bandage contact lens provide symptomatic relief. Surgical interventions including superficial keratectomy, anterior lamellar keratoplasty (ALK), penetrating keratoplasty (PK), and as a final option, keratoprosthesis.[37]
Epithelial–stromal *TGFBI* dystrophies	
Reis–Bücklers corneal dystrophy (RBCD)	For recurrent erosions, refer to section on EBMD management.[37]
	For visually significant opacities, SK, PTK, and superficial anterior lamellar keratoplasty (SALK) may be performed.[38,39] Recurrence in the graft is common and may necessitate repeat interventions or possibly DALK.[40]
Thiel–Behnke corneal dystrophy (TBCD)	Refer to section on RBCD management.[41]
	Recurrence in the graft is common.
Lattice corneal dystrophies (LCDs)	For recurrent erosions, refer to section on EBMD management.
	For visually significant opacities, PTK, SALK, ALK (microkeratome-assisted), DALK, PK may be performed depending on the depth of stromal involvement.[42–44] DALK is advantageous in sparing the unaffected corneal endothelium. Failed DALK attempt may require conversion to PK. Beware of the risk of neurotrophic keratopathy in Meretoja syndrome.[45]
	Recurrence in the graft is common and may occur at variable intervals and patterns.[42]
Granular corneal dystrophy, type 1 (GCD1) and Granular corneal dystrophy, type 2 (GCD2)	For recurrent erosions, refer to section on EBMD management.
	For visually significant opacities, refer to the section on LCDs management.
	Recurrence in the graft is both more common and occurs earlier than in classic LCD (Figs. 12F, G).[42,46]
	In GCD2, injury to the cornea such as LASIK results in accelerated deposition of corneal opacities and is contraindicated (Fig. 13H).[47]
Stromal dystrophies	
Macular corneal dystrophy (MCD)	For recurrent erosions, refer to section on EBMD management.
	For visually significant opacities, refer to the section on LCDs management. Macular dystrophy does involve the corneal endothelium unlike LCD, so PK may be a better option than DALK.
	Recurrence after corneal grafting is less common compared with GCD1 and classic LCD.[48]
Schnyder corneal dystrophy (SCD)	PTK can be performed if crystals in the visual axis are symptomatic. Visual acuity may be limited by underlying panstromal lipid deposits, thereby requiring DALK or PK. Some patients with decreased vision from cataracts require DALK or PK to facilitate visualization if severe corneal opacification is present.
Congenital stromal corneal dystrophy (CSCD)	For visually significant opacities, refer to section on LCDs management.
Endothelial dystrophies	
Fuchs endothelial corneal dystrophy (FECD)	Asymptomatic patients should be observed. For minimal corneal decompensation, hypertonic saline drops and bandage contact lens may provide temporary symptomatic relief.[49]
	Endothelial keratoplasty including DSAEK and DMEK is the standard definitive treatment. Advanced cases with severe end-stage corneal edema and deep stromal scarring may require PK.[50]

TABLE 3. (*Continued*) Management of Corneal Dystrophies

Corneal Dystrophies	Management
	Alternative approaches such as Descemet stripping only (DSO), use of topical rho kinase inhibitors and intracameral injections of donor endothelial cells are under investigation.
Posterior polymorphous corneal dystrophy (PPCD)	Refer to section on FECD management.
	Intraocular pressure should be monitored, and if glaucoma is present, then managed.
	Amblyopia therapy is required in young children with high or asymmetric refractive error.
Congenital hereditary endothelial dystrophy (CHED)	Refer to section on PPCD management.
X-linked endothelial corneal dystrophy (XECD)	Refer to section on FECD management.
	Amblyopia therapy required in young children with high or asymmetric refractive error.[51]

Fingerprint Lines

Parallel, curvilinear lines, usually paracentral, best visualized with retroillumination (Fig. 1C). Isolated or combined with other signs, especially maps.

Bleb Pattern (Bron)

Subepithelial pattern like pebbled glass, best seen by retroillumination (Fig. 1D). Isolated or combined with other signs. Much less common than other signs.

EBMD can be seen in direct illumination but is often highlighted using retroillumination off the retina or iris. The lesions frequently cause the epithelial layer to be slightly elevated; this elevation can often be best appreciated by placing fluorescein dye on the cornea and looking for "negative staining" with the cobalt blue light.

Poor adhesion of basal epithelial cells to abnormal basal laminar material is believed to predispose to recurrent erosions.

Symptoms

EBMD can be asymptomatic, associated with mild to severely painful erosive episodes and/or may cause decreased vision by inducing mild irregular astigmatism (monocular diplopia or triplopia, "ghost" or "shadow" images).

Course

Location and degree of pathology can fluctuate with time.

Light Microscopy

Maps

Sheets of intraepithelial, multilamellar, basal laminar material (Fig. 1E).

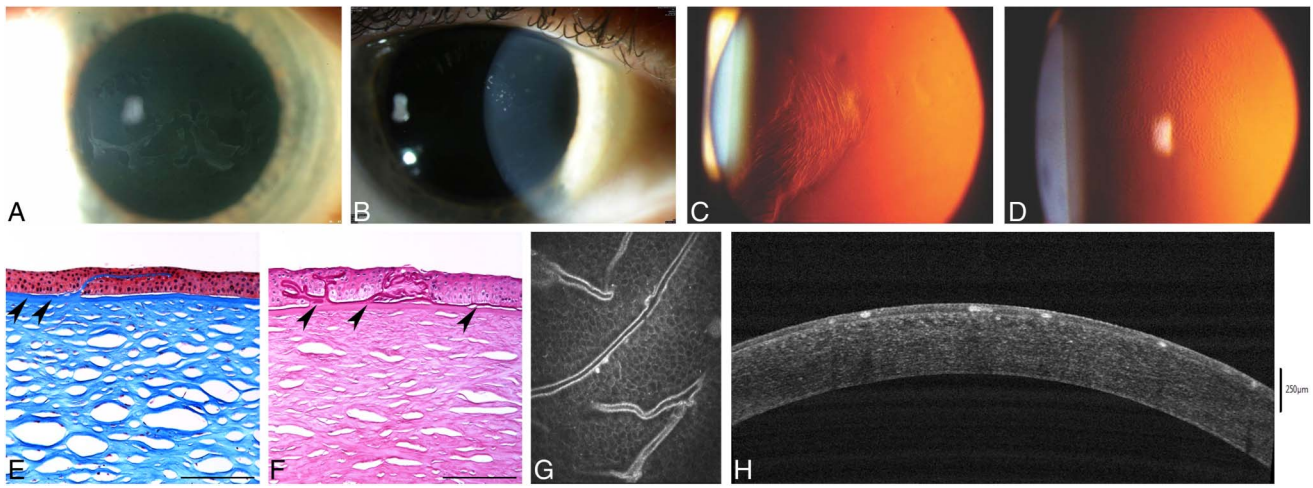

FIGURE 1. Epithelial basement membrane dystrophy (EBMD). A, Map-like changes. B, Intraepithelial dot opacities (Cogan cysts) underlying map-like figures. C, Fingerprint lines, best visualized with retroillumination. D, Multiple crowded blebs (Bron), only visible in retroillumination. E and F, Light microscopy shows excessive basement membrane material (arrowheads) between the distorted epithelium and the intact Bowman layer to form sheets corresponding to maps (E) and redundant folds corresponding to fingerprint lines (F) (E, Masson trichrome; F, Periodic acid–Schiff, bar = 200 μm). G, In vivo confocal microscopy demonstrates abnormal hyperreflective intraepithelial basement membrane material within suprabasal and basal epithelial cell layers (400 × 400 μm). H, Spectral domain OCT scan shows presence of hyperreflective dots (intraepithelial pseudocysts) within the epithelial layer. Figures 1A, B, C, D, E, F, and G from Figures 1A, B, C, D, E, F, and G in Weiss JS, Møller HU, Aldave AJ, et al. IC3D Classification of Corneal Dystrophies—Edition 2. *Cornea*. 2015;34:117–159.

Dots

Intraepithelial pseudocysts containing cytoplasmic debris.

Fingerprint Lines

Rib-like intraepithelial extensions of basal laminar material (Fig. 1F).

Bleb Pattern

Irregular, subepithelial accumulation of a fibrillogranular material.

In contrast to some other superficial dystrophies, the Bowman layer is normal.

Transmission Electron Microscopy

Maps

Thick, multilamellar sheets (2–6 nm thick) of epithelial basement membrane that extend into the epithelium.

Dots

Intraepithelial pseudocysts contain degenerating cells with pyknotic nuclei and cytoplasmic debris.

Fingerprint Lines

Fine fibrillar (17 nm diameter) and granular (8 nm) substance in addition to undulating waves of the basement membrane.

Bleb Pattern

Discrete noncystic mounds of abnormal granular material deposited between the epithelium and the Bowman layer that indents the overlying basal epithelial cells. May mimic cysts clinically, but no cysts are present on histology.

Confocal Microscopy

Maps

Highly reflective tissue in various configurations corresponds to abnormal basement membrane extending into the intermediate and basal epithelial cell layers. Adjacent basal epithelial cells appear distorted. No abnormalities in superficial epithelial cells or stroma.

Dots

Hyperreflective structures with sharp borders within the intermediate cell layers.

Fingerprint Lines

Linear hyperreflective structures corresponding to abnormal basement membrane projecting into the corneal epithelium (Fig. 1G).

Bleb Pattern

Circular or oval hyporeflective or hyperreflective areas at the level of the basal epithelium and the Bowman layer. Some areas contain hyperreflective spots.

Optical Coherence Tomography

Maps

Presence of an irregular and thickened epithelial basement membrane with duplication and/or insinuation into the corneal epithelium layer.

Dots

Hyperreflective dots (intraepithelial pseudocysts) within the epithelial layer (Fig. 1H).

Fingerprint Lines

Expansions and folds of the pathological basement membrane.

Bleb Pattern

Hyporeflective spaces between the corneal epithelial layer and the Bowman layer.

Category

Category 3. Most likely degenerative and not hereditary.

Note: Only 1 publication exists which reports 2 families with EBMD with *TGFBI* changes (L509R and R666S), with few family members with positive clinical findings and genetic testing and no histopathology. Although other familial cases of EBMD have been reported in the literature, the evidence of it being a dystrophy is inconclusive because of lack of genotyping and histopathology or presence of changes suggestive of other *TGFBI*-related corneal dystrophies (L509R has alternatively been reported as a LCD variant with superficial geographic opacification and lattice lines, see Table 2), or the change is not confirmed to the pathogenic (R666S remains a variant of undetermined significance [VUS]).

BIBLIOGRAPHY

- Boutboul S, Black GC, Moore JE, et al. A subset of patients with epithelial basement membrane corneal dystrophy have mutations in TGFBI/BIGH3. *Hum Mutat*. 2006;27:553–557.
- Bron AJ, Brown NA. Some superficial corneal disorders. *Trans Ophthalmol Soc U K*. 1971;91:13–29.
- Bron AJ, Tripathi RC. Cystic disorders of the corneal epithelium II. Pathogenesis. *Br J Ophthalmol*. 1973;57:361–375.
- Cogan DG, Donaldson DD, Kuwabara T, et al. Microcystic dystrophy of the corneal epithelium. *Trans Am Ophthalmol Soc*. 1964;62:213–225.
- Guerry D. Fingerprint-like lines in the cornea. *Am J Ophthalmol*. 1950;33:724–726.
- Hau SC, Tuft SJ. In vivo confocal microscopy of bleb-like disorder in epithelial basement membrane dystrophy. *Cornea*. 2011;30:1478–1480.

- Labbé A, De Nicola R, Dupas B, et al. Epithelial basement membrane dystrophy: Evaluation with the HRT II Rostock Cornea Module, *Ophthalmology*. 2006;113:1301–1308.
- Laibson PR, Krachmer JH. Familial occurrence of dot (microcystic), map, fingerprint dystrophy of the cornea. *Invest Ophthalmol Vis Sci*. 1975;14:397–399.
- Laibson PR. Microcystic corneal dystrophy. Trans Am Ophthalmol Soc. 1976;74:488–531.
- Lisch W, Lisch C. Die epitheliale Hornhautbasalmembrandystrophie. *Klin Monbl Augenheilkd*. 1983;183:251–255.
- Munier FL, Korvatska E, Djemaï A, et al. Kerato-epithelin mutations in four 5q31-linked corneal dystrophies. *Nat Genet*. 1997;15:247–251.
- Rodrigues MM, Fine BS, Laibson PR, et al. Disorders of the corneal epithelium. A clinicopathologic study of dot, geographic, and fingerprint patterns. *Arch Ophthalmol*. 1974;92:475–482.
- Vogt A. Lehrbuch und Atlas der Spaltlampenmikroskopie des lebenden Auges (1. Teil). Berlin, Germany: Springer; 1930:119–121.

Epithelial Recurrent Erosion Dystrophies (EREDs)

MIM #122400.

Former Alternative Names and Eponyms

Franceschetti corneal dystrophy (FRCD).
Dystrophia Smolandiensis (DS).
Dystrophia Helsinglandica (DH).

Note: EREDs includes ERED, FRCD, DS, and DH. Only ERED has a published genetic locus and gene.

Inheritance

Autosomal dominant.

Genetic Locus

10q25.1 (ERED).

Gene

Collagen, type XVII, alpha-1—*COL17A1* (ERED).

Onset

Early childhood.

Signs

Recurrent epithelial corneal erosions, presenting in the first decade of life, last 1 to 7 days. During pain-free intervals, no biomicroscopically visible corneal changes are initially present (Fig. 2A). By middle age, recurrent attacks may gradually lead to focal or diffuse, central, or paracentral subepithelial opacities (Fig. 2B) or elevated keloid-like scars, resulting from subepithelial fibrosis.

Symptoms

Painful epithelial erosive attacks commence in the first decade and may recur throughout life. The attacks often start at night. Erosive attacks decrease in frequency and severity by the late thirties and may stop. Visual impairment from central corneal opacification may occur in up to 50% of patients by the late thirties.

Course

ERED, FRCD, DS, and DH all have frequent erosions in childhood with absence of corneal changes during pain-free episodes in childhood. Corneal erosions become less frequent with age. ERED shows individual phenotypic variation in the age of onset, frequency, and severity of erosions. Corneal erosions become less frequent with age. In DS, erosions are reported to begin in the first year, decrease in the late thirties, and then can stop entirely. By the late thirties, visual acuity is markedly decreased with 50% reporting having had penetrating keratoplasty. In DH, erosions are reported to begin at age 4 to 7 years, decreasing in frequency and intensity by the late twenties and developing subepithelial fibrosis by the late thirties although visual acuity is not usually affected. FRCD demonstrates midlife subepithelial fibrosis.

Light Microscopy

ERED

Uneven epithelial thickness with intracellular vacuoles. Discontinuous basement membrane is often separated from basal epithelial cells by collagenous scar tissue, and the Bowman layer is absent (destroyed) (Fig. 2C). These specimens represent late stages of the dystrophy.

FRCD

Irregular basal epithelium with enlarged intercellular spaces. Alcian blue-positive deposits are present both intracellularly and intercellularly. Partial or complete destruction of the Bowman layer with intervening avascular fibrous pannus between the basal epithelium and the Bowman layer (Fig. 2D). Negative Congo red staining.

DS

Keloid-like structure stains positive with Congo red, indicating secondary amyloidosis.

Transmission Electron Microscopy

FRCD

Irregularity in size and shape of the basal epithelial cells and enlarged intercellular clefts corresponding to Alcian blue-positive deposits. Presumably "dystrophic" mitochondria in between basal epithelial cells. Pannus contains numerous fibroblasts (Fig. 2E).

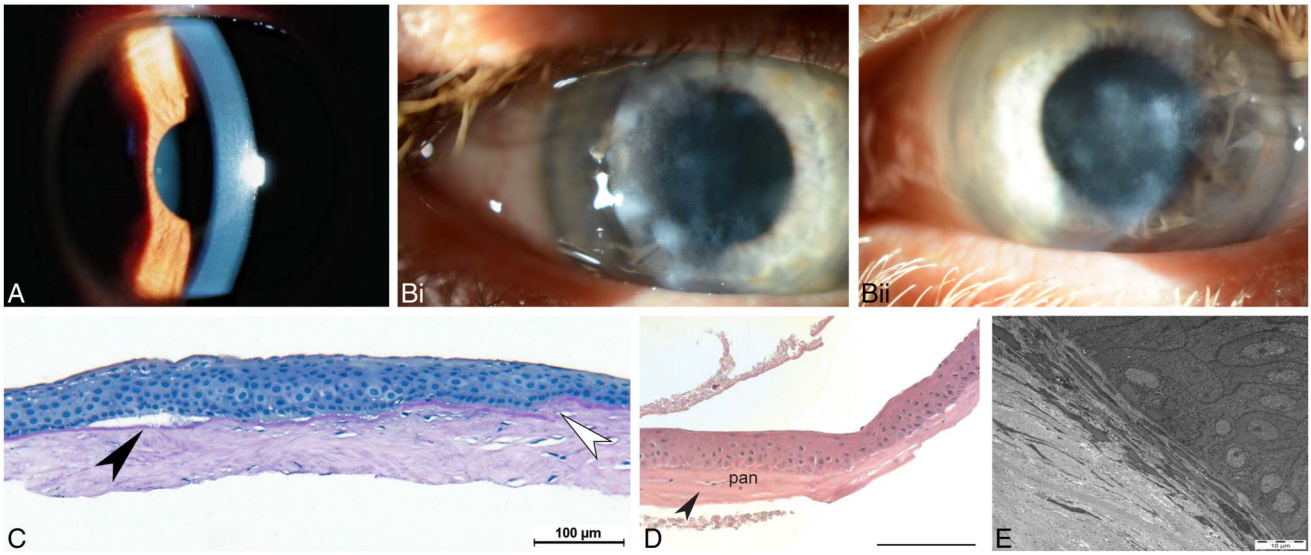

FIGURE 2. Epithelial recurrent erosion dystrophies (EREDs). A, In the first decades of life, the cornea appears normal without any dystrophy-specific signs after recurrent epithelial erosion. B, Bilateral central and paracentral opacities in the right (i) and left (ii) corneas of a 67-year-old with ERED and *COL17A1* mutation. C, Light microscopy of the 67-year-old in (B) with keloid pannus visible between the basal epithelium and the locally destroyed (therefore absent) Bowman layer. PAS, bar = 100 µm. In several places, the epithelium is loosely attached (black arrowhead) to the basement membrane which also demonstrates breaks (white arrowhead) (Gly1052 *COL17A1* mutation). D, Light microscopy: In advanced age, the Bowman layer (arrowhead) is partially destroyed and pannus (pan) is found between the basal epithelium and the Bowman layer (PAS, × 200 µm). E, Electron microscopy of pannus with numerous fibroblasts. Figures 2A and D from Figures 2A and C in Weiss JS, Møller HU, Aldave AJ, et al. IC3D Classification of Corneal Dystrophies—Edition 2. *Cornea*. 2015;34:117–159. Figure 2E from Figure 2 in Lisch W, Bron AJ, Munier FL, et al. Franceschetti hereditary recurrent corneal erosion. *Am J Ophthalmol*. 2012;153:1073–81.e4.

Immunohistochemistry

ERED

Corneal keratocytes in the subepithelial scar can demonstrate immunopositivity for syndecan (CD138), which is typical for activated fibroblasts, and smooth muscle actin, which is typical of myofibroblasts.

FRCD

Segmental reduced expression of the tight junction proteins claudin and E-cadherin, both of which are desmosome components. Decorin expression appears to be enhanced in the basal epithelial layer compared with normal postmortem cornea.

DS

Abundant fibronectin is present in areas of subepithelial fibrosis.

Confocal Microscopy

DS

Abnormal thinning of the corneal epithelium, absence of the Bowman layer with accumulation of abnormal material at the level of the Bowman layer. Subepithelial corneal nerves are sparse and tortuous.

Category

1. ERED
4. FRCD, DS, and DH

Note: Clinical, histopathologic, and electron microscopic descriptions of FRCD, DS, and DH are consistent with ERED, although neither linkage to the 10q25.1 locus nor *COL17A1* mutation screening has been published. The difference in severity of corneal opacification in FRCD, DS, and DH could be explained by the presence of polymorphism and differential expressivity of a common gene. Future DNA analysis will reveal more information about FRCD, DS, and DH which could facilitate differential diagnosis. A synonymous mutation in *COL17A1* can result in abnormal splicing and cause ERED, and 1 family that carries this variant was initially incorrectly diagnosed as a variant of Thiel–Behnke dystrophy linked to 10q23-q24. It is not clear whether subepithelial mucinous corneal dystrophy (SMCD) actually represents a unique dystrophy or could also fall under the EREDs group. The term "familial recurrent corneal erosions" should not be used to refer to EREDs because the former is a descriptive rather than diagnostic term as recurrent erosions also frequently occur in several other corneal dystrophies.

BIBLIOGRAPHY

- Franceschetti A. Hereditäre rezidivierende Erosion der Hornhaut. *Z Augenheilk*. 1928;66:309–316.

- Hammar B, Björck E, Lagerstedt K, et al. A new corneal disease with recurrent erosive episodes and autosomal-dominant inheritance. *Acta Ophthalmol*. 2008;86:758–763.
- Hammar B, Björck E, Lind H, et al. Dystrophia Helsinglandica: a new type of hereditary corneal recurrent erosions with late subepithelial fibrosis. *Acta Ophthalmol*. 2009;87:659–665.
- Hammar B, Lagali N, Ek S, et al. Dystrophia Smolandiensis: a novel morphological picture of recurrent corneal erosions. *Acta Ophthalmol*. 2010;88:394–400.
- Jonsson F, Byström B, Davidson AE, et al. Mutations in collagen, type XVII, alpha 1 *(COL17A1)* cause epithelial recurrent erosion dystrophy (ERED). *Hum Mutat*. 2015;36:463–473.
- Legrand J. Dystrophie épithéliale cornéenne récidivante familiale. *Bull Soc Ophtalmol*. 1963;5:384–387.
- Lin BR, Le DJ, Chen Y, et al. Whole exome sequencing and segregation analysis confirms that a mutation in *COL17A1* is the cause of epithelial recurrent erosion dystrophy in a large dominant pedigree previously mapped to chromosome 10q23-q24. *PLoS One*. 2016;11:e0157418.
- Lisch W, Bron AJ, Munier FL, et al. Franceschetti hereditary recurrent corneal erosion. *Am J Ophthalmol*. 2012;153:1073–1081.
- Oliver VF, van-Bysterveldt KA, Cadzow M, et al. A *COL17A1* splice-altering mutation is prevalent in inherited recurrent corneal erosions. *Ophthalmology*. 2016;123:709–722.
- Remler O. Beitrag zur hereditären rezidivierenden Hornhauterosion. *Klin Monbl Augenheilkd*. 1983;183:59.
- Shindo S. Familial recurrent corneal erosion. *Nippon Ganka Gakkai Zasshi*. 1968;72:998–1004.
- Turunen JA, Tuisku IS, Repo P, et al. Epithelial recurrent erosion dystrophy (ERED) from the common splice site altering *COL17A1* variant in families of Finnish-Swedish ancestry. *Acta Ophthalmol*. [online ahead of print June 8, 2023] DOI:10.1111/aos.15716.
- Valle O. Hereditary recurring corneal erosions. A familial study with special reference to Fuchs' dystrophy. *Acta Ophthalmol (Copenh)*. 1967;45:829–836.
- Wales HJ. A family history of corneal erosions. *Trans Ophthalmol Soc NZ*. 1955;8:77–78.

Subepithelial Mucinous Corneal Dystrophy (SMCD)

MIM #612867.

Former Alternative Names and Eponyms

None.

Inheritance

Autosomal dominant inheritance most likely, X-linked inheritance not excluded.

Genetic Locus

Unknown.

Gene

Unknown.

Onset

First decade of life.

Signs

Diffuse bilateral subepithelial opacities and haze, most dense centrally (Fig. 3A).

Symptoms

Painful episodes of recurrent corneal erosions, which decrease during adolescence (only 1 publication of a single family).

Course

Progressive loss of vision in adolescence.

Light Microscopy

Subepithelial band of eosinophilic, periodic acid–Schiff (PAS)-positive, Alcian blue-positive, hyaluronidase-sensitive material is present anterior to the Bowman layer (Fig. 3B).

Transmission Electron Microscopy

Subepithelial deposits of fine fibrillar material.

Immunohistochemistry

Subepithelial deposits are reactive for chondroitin-4-sulfate and dermatan sulfate.

Confocal Microscopy

Not reported.

Category

4.

Note: The clinical findings in SMCD resemble those of ERED. However, histopathology in SMCD has not demonstrated the subepithelial collagenous keloid pannus which can be seen in EREDs, and Alcian blue-positive material anterior to the Bowman layer has not been described in EREDs. The 1 reported family affected with SMCD declined genetic testing to determine whether they carried a mutation in the ERED gene, collagen, type XVII, alpha 1 *(COL17A1)* on chromosome 10 (personal communication R. Feder). Consequently, we are presently not able to confirm whether SMCD is a unique dystrophy distinct from ERED.

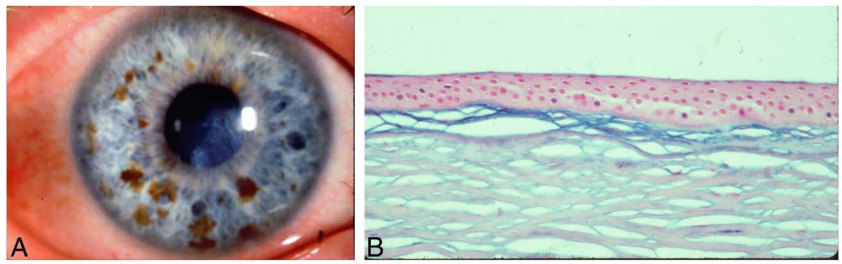

FIGURE 3. Subepithelial mucinous corneal dystrophy (SMCD). A, Slit lamp biomicroscopy reveals that diffuse subepithelial opacities and haze are densest centrally. B, Light microscopy: a band of increased staining is present beneath the epithelium. The Bowman layer is thin (Alcian blue, ×40). Photograph courtesy of Robert Feder MD. Figures 3A and B from Figures 3A and B in Weiss JS, Møller HU, Aldave AJ, et al. IC3D Classification of Corneal Dystrophies—Edition 2. *Cornea*. 2015;34:117–159.

BIBLIOGRAPHY

- Feder RS, Jay M, Yue BY, et al. Subepithelial mucinous corneal dystrophy. Clinical and pathological correlations. *Arch Ophthalmol*. 1993;111:1106–1114.

Meesmann Corneal Dystrophy (MECD)

MIM #122100.

Former Alternative Names and Eponyms

Juvenile hereditary epithelial dystrophy.
Stocker-Holt dystrophy.

Inheritance

Autosomal dominant.

Genetic Loci

Locus 12q13 (*KRT3*) MIM #148043.
Locus 17q12 *(KRT12*) MIM #601687.

Genes

Keratin 3—*KRT3*.
Keratin 12—*KRT12*.

Onset

Early childhood to young adulthood.

Signs

Multiple, tiny intraepithelial vesicles extend to the limbus. Direct illumination shows varying diffuse gray opacities in different patterns, which may have a distinct border (Fig. 4A). Areas of the central or peripheral cornea may be unaffected, particularly in younger individuals. Whorled and wedge-shaped epithelial patterns have been reported. The gray opacities appear as solitary tiny transparent cysts on indirect illumination (Figs. 4B, C). Approximately 85% of eyes show microcysts affecting the entire epithelium while the remainder are localized to the upper, lower, central, and/or peripheral cornea. Coalescence of several cysts may result in refractile linear opacities with intervening clear cornea. The cornea may be slightly thinned, and corneal sensation may be reduced.

Symptoms

Patients are typically asymptomatic or may have mild visual reduction, although some patients complain of glare and light sensitivity. Patients may note foreign body sensation or tearing. Recurrent painful punctiform epithelial erosions may occur. Rarely, blurred vision results from corneal irregularity and scarring.

Course

Stationary or slowly progressive.

Light Microscopy

The thickened and disorganized epithelium demonstrates intraepithelial cysts (Fig. 4D) filled with periodic acid–Schiff (PAS)-positive cellular debris, which autofluoresces. The cells also contain moderate amounts of PAS-positive and diastase-sensitive material (glycogen). A thickened multilaminar basement membrane projects into the basal epithelium.

Transmission Electron Microscopy

Intracytoplasmic "peculiar substance" represents a focal collection of fibrogranular material surrounded by tangles of cytoplasmic filaments (Fig. 4E). The intraepithelial cysts are round and uniform (10–50 μm). Some lesions with reflective points in the cytoplasm probably correspond to cell nuclei.

Confocal Microscopy

Hyporeflective areas in the basal epithelium ranging from 40 to 150 μm in diameter, some with reflective spots inside (Fig. 4F). Numerous corneal intraepithelial microcysts and hyperreflective material, believed to represent degenerated cells, have been detected closer to the basal layer of the corneal epithelium in older patients. Compared with the basal epithelial layer, the superficial layer contains larger microcysts with atrophic changes of the hyperreflective material.

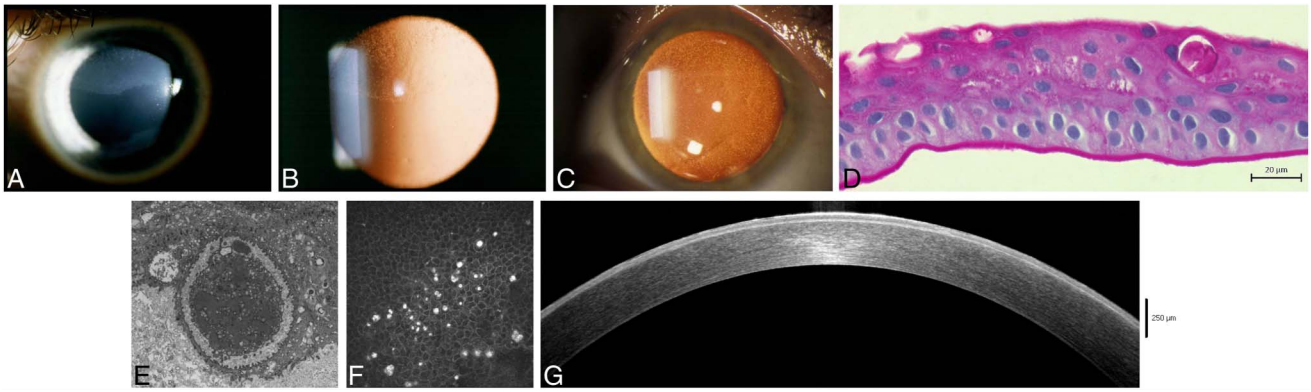

FIGURE 4. Meesmann corneal dystrophy (MECD). A, In direct illumination, diffuse gray, superior opacity with a distinct border is apparent. B, With retroillumination, the same eye demonstrates that the opacity pattern is composed of multiple, solitary transparent microcysts. C, Multiple, solitary transparent microcysts in retroillumination. D, Light microscopy: intraepithelial cysts, sometimes extruding onto the corneal surface, contain amorphous material probably comprised of degenerated epithelial cells. The basement membrane is thickened (Alcian blue and hematoxylin and eosin stain, × 400). E, Electron microscopy: cyst containing intracytoplasmic fibrillar peculiar substance, with surrounding tangles of filaments. F, In vivo confocal microscopy shows hyporeflective areas corresponding to microcysts in the basal epithelial layer and round hyperreflective structures (400 × 400 µm). G, Spectral domain OCT shows an irregular thickness and diffuse hyperreflectivity of the epithelium. Figures 4A and B from Figure 4B in Weiss, JS, Møller HU, Lisch W, et al. The IC3D Classification of the Corneal Dystrophies. *Cornea*. 2008;27(suppl 2):S1–S42. Figures 4C, D, E, and F from Figures 4C, D, E, and F in Weiss JS, Møller HU, Aldave AJ, et al. IC3D Classification of Corneal Dystrophies—Edition 2. *Cornea*. 2015;34:117–159.

Clearly visualized demarcation lines between the microcysts and normal epithelial cells correspond to the biomicroscopically visible demarcation between clear and affected areas observed on slit lamp examination.

Optical Coherence Tomography

Diffuse hyperreflectivity throughout the epithelium, with hyperreflective spots within the superficial layer (Fig. 4G). The epithelial thickness is irregular.

Category

1.

Note: Stocker-Holt dystrophy has been reported to be a variant of Meesmann corneal dystrophy caused by an R19L mutation in *KRT12*.

BIBLIOGRAPHY

- Allen EH, Atkinson SD, Liao H, et al. Allele-specific siRNA silencing for the common keratin 12 founder mutation in Meesmann epithelial corneal dystrophy. *Invest Ophthalmol Vis Sci*. 2013;54:494–502.
- Behnke H, Thiel HJ. On hereditary epithelial dystrophy of the cornea (type Meesmann-Wilke) in Schleswig-Holstein. *Klin Monbl Augenheilkd*. 1965;147:662–672.
- Burns RP. Meesmann's corneal dystrophy. *Trans Am Ophthalmol Soc*. 1968;66:530–635.
- Cao W, Yan M, Hao Q, et al. Autosomal-dominant Meesmann epithelial corneal dystrophy without an exon mutation in the keratin-3 or keratin-12 gene in a Chinese family. *J Int Med Res*. 2013;41:511–518.
- Clausen I, Duncker GI, Grünauer-Kloevekorn C. Identification of a novel mutation in the cornea specific keratin 12 gene causing Meesmann's corneal dystrophy in a German family. *Mol Vis*. 2010;16:954–960.
- Cremona FA, Ghosheh FR, Laibson PR, et al. Meesmann corneal dystrophy associated with epithelial basement membrane and posterior polymorphous corneal dystrophies. *Cornea*. 2008;27:374–377.
- Ehlers N, Hjortdal J, Nielsen K, et al. Phenotypic variability in Meesmann's dystrophy: clinical review of the literature and presentation of a family genetically identical to the original family. *Acta Ophthalmol*. 2008;86:40–44.
- Fine BS, Yanoff M, Pitts E, et al. Meesmann's epithelial dystrophy of the cornea. *Am J Ophthalmol*. 1977;83:633–642.
- Hassan H, Thaung C, Ebenezer ND, et al. Severe Meesmann's epithelial corneal dystrophy phenotype due to a missense mutation in the helix-initiation motif of keratin 12. *Eye (Lond)*. 2013;27:367–373.
- Javadi MA, Rezaei-Kanavi M, Javadi A, et al. Meesmann corneal dystrophy; a clinico-pathologic, ultrastructural, and confocal scan report. *J Ophthalmic Vis Res*. 2010;5:122–126.
- Meesmann A. Über eine bisher nicht beschriebene dominant vererbte Dystrophia epithelialis corneae. *Ber Zusammenkunft Dtsch Ophthalmol Ges*. 1938;52:154–158.
- Nielsen K, Orntoft T, Hjortdal J, et al. A novel mutation as the basis for asymptomatic Meesmann dystrophy in a Danish family. *Cornea*. 2008;27:100–102.
- Nishino T, Kobayashi A, Mori N, et al. In vivo histology and p.L132V mutation in *KRT12* gene in Japanese patients with Meesmann corneal dystrophy. *Jpn J Ophthalmol*. 2019;63:46–55.

- Ogasawara M, Matsumoto Y, Hayashi T, et al. KRT12 mutations and in vivo confocal microscopy in two Japanese families with Meesmann corneal dystrophy. *Am J Ophthalmol*. 2014;157:93–102.
- Seto T, Fujiki K, Kishishita H, et al. A novel mutation in the cornea-specific Keratin 12 gene in Meesmann corneal dystrophy. *Jpn J Ophthalmol*. 2008;52:224–226.
- Stocker FW, Holt LB. A rare form of hereditary epithelial dystrophy of the cornea: a genetic, clinical and pathologic study. *Trans Am Ophthalmol Soc*. 1954;52:133–144.
- Sullivan LS, Baylin EB, Font R, et al. A novel mutation of the Keratin 12 gene responsible for a severe phenotype of Meesmann's corneal dystrophy. *Mol Vis*. 2007;13:975–980.
- Szaflik JP, Ołdak M, Maksym RB, et al. Genetics of Meesmann corneal dystrophy: a novel mutation in the keratin 3 gene in an asymptomatic family suggests genotype-phenotype correlation. *Mol Vis*. 2008;14:1713–1718.
- Thiel HJ, Behnke H. On the extent of variation of hereditary epithelial corneal dystrophy (Meesmann-Wilke type). *Ophthalmologica*. 1968;155:81–86.
- Tuft S, Bron AJ. Imaging the microstructural abnormalities of Meesmann corneal dystrophy by in vivo confocal microscopy. *Cornea*. 2006;25:868–870.
- Wittebol-Post D, van-Bijsterveld OP, Delleman JW. Meesmann's epithelial dystrophy of the cornea. Biometrics and a hypothesis. *Ophthalmologica*. 1987;194:44–49.
- Yeung JY, Hodge WG. Recurrent Meesmann's corneal dystrophy: treatment with keratectomy and mitomycin C. *Can J Ophthalmol*. 2009;44:103–104.

Lisch Epithelial Corneal Dystrophy (LECD)

MIM #300778.

Former Alternative Names and Eponyms

Band-shaped and whorled microcystic dystrophy of the corneal epithelium.

Inheritance

Autosomal dominant

Note: Although formerly believed to be X-chromosomal dominant, the gene discovery demonstrated that LECD is inherited in autosomal dominant fashion.

Genetic Locus

19p13.2.

Gene

Mucolipin 1—*MCOLN1*

Onset

Childhood.

Signs

Direct illumination shows localized gray opacities in different patterns: whorl-like, radial, band-shaped flame/feathery and club-shaped (Figs. 5A, B). Indirect illumination demonstrates multiple, tiny, densely crowded clear cysts (Fig. 5C). All familial cases are bilateral. Sporadic cases can be unilateral or bilateral. LECD may or may not extend to the corneal limbus. Opacities can be minimal or asymmetric with clear surrounding epithelium. Similar appearance in male and female patients.

Symptoms

Asymptomatic or blurred vision if the pupillary axis is involved.

Course

Slow progression of opacities with possible visual deterioration. Can also slowly regress.

Light Microscopy

Epithelial basal cells are cuboidal with low nuclear to cytoplasmic ratio. Intraepithelial vacuolated cells (Fig. 5D) progress to the epithelial surface, where they adopt elongated flat squamous shapes. These vacuoles are PAS-positive, diastase-labile, Luxol fast blue and Sudan black-negative consistent with glycogen. Intercellular cysts, parakeratosis, orthokeratosis, and hyperkeratosis are not identified.

Transmission Electron Microscopy

Basal epithelial cells with intact basement membrane and hemidesmosomes are unremarkable. In the midlevel and superficial epithelium, there are cells with myriad vacuoles and inclusions (Fig. 5E) of either of the following forms: vaguely flocculent or lamellar material with or without a circumscribing membrane and more electron-dense whorled or membranous structures.

Confocal Microscopy

There are 4 characteristic features of the abnormal epithelial cells: highly hyperreflective cytoplasm and hyporeflective nuclei (Fig. 5F), uniform involvement of all epithelial layers within the affected areas, well-demarcated borders with adjacent normal epithelium, and involvement of the limbal area. No distinct intracellular deposits are present, although the cytoplasm has granular hyperreflectivity.

Category

1.

BIBLIOGRAPHY

- Butros S, Lang GK, Alvarez de Toledo J, et al. Die verschiedenen Trübungsmuster der Lisch-

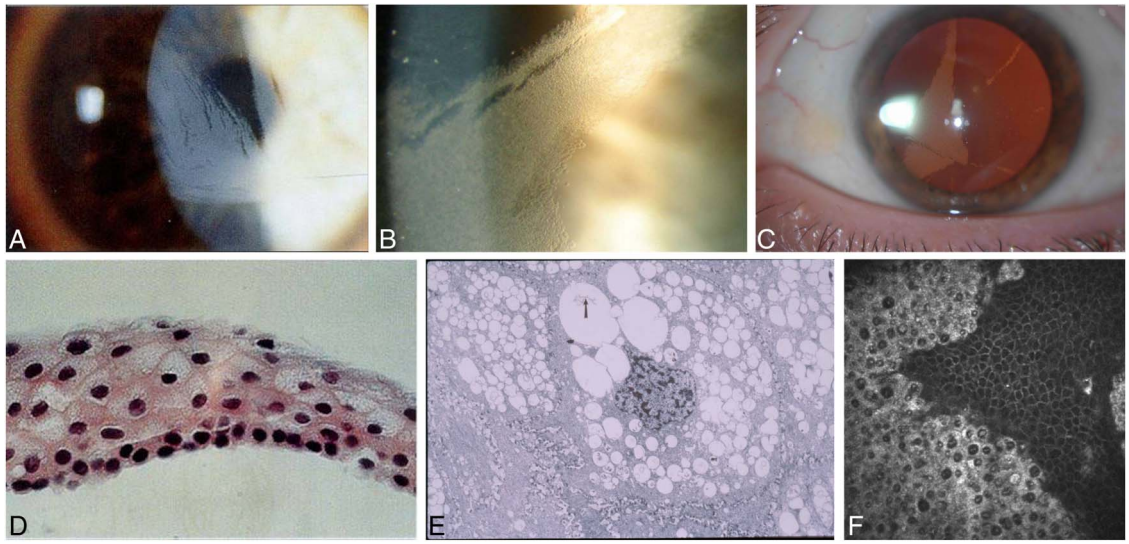

FIGURE 5. Lisch epithelial corneal dystrophy (LECD). A and B, Diffuse grayish epithelial opacities form radial, feathery, or club-shaped patterns. C, Opacification consists of crowded, transparent microcysts in retroillumination. D, Light microscopy: pronounced vacuolization of the epithelial cells, particularly in outer layers (hematoxylin and eosin stain, ×250). E, Electron microscopy: discloses coalescent intracellular vacuolization of the wing cells. Some of these vacuoles coalesce to form empty spaces within the cytoplasm of the epithelial cells (×4000). F, In vivo confocal microscopy shows intraepithelial hyperreflective dystrophic areas containing hyporeflective round structures, sharply demarcated from normal epithelial areas (400 × 400 μm). Figures 5A, B, D, E, and F from Figures 5A, B, D, E, and F in Weiss JS, Møller HU, Aldave AJ, et al. IC3D Classification of Corneal Dystrophies—Edition 2. *Cornea*. 2015;34:117–159.

Hornhautdystrophie. *Klin Monbl Augenheilkd*. 2006;223:837–840.
- Charles NC, Young JA, Kumar A, et al. Band-shaped and whorled microcystic dystrophy of the corneal epithelium. *Ophthalmology*. 2000;107:1761–1764.
- Kurbanyan K, Sejpal KD, Aldave AJ, et al. In vivo confocal microscopic findings in Lisch corneal dystrophy. *Cornea*. 2012;31:437–441.
- Lisch W, Steuhl KP, Lisch C, et al. A new, band-shaped and whorled microcystic dystrophy of the corneal epithelium. *Am J Ophthalmol*. 1992;114:35–44.
- Lisch W, Büttner A, Offner F, et al. Lisch corneal dystrophy is genetically distinct from Meesmann corneal dystrophy and maps to Xp22.3. *Am J Ophthalmol*. 2000;130:461–468.
- Patterson K, Chong JX, Chung DD, et al. Lisch epithelial corneal dystrophy is caused by heterozygous loss-of-functions variants in *MCOLN1*. *Am J Ophthalmol*. 2024;258:183–195.
- Robin SB, Epstein RJ, Kornmehl EW. Band-shaped, whorled microcystic corneal dystrophy. *Am J Ophthalmol*. 1994;117:543–544.
- Wessel MM, Sarkar JS, Jakobiec FA, et al. Treatment of Lisch corneal dystrophy with photorefractive keratectomy and Mitomycin C. *Cornea*. 2011;30:481–485.

Gelatinous Drop-Like Corneal Dystrophy (GDLD)

MIM #204870.

Former Alternative Names and Eponyms

Subepithelial amyloidosis.
Primary familial amyloidosis (Grayson).

Inheritance

Autosomal recessive.

Genetic Locus

1p32.

Gene

Tumor-associated calcium signal transducer 2—*TACSTD2*, previously *M1S1*.

Onset

First to second decade.

Signs

Initially, the subepithelial lesions may appear similar to band-shaped keratopathy (Fig. 6A), or there may be groups of small multiple nodules, that is, mulberry configuration (Fig. 6B). They may stain with fluorescein (Fig. 6C), indicating epithelial hyperpermeability. Recurrent corneal epithelial erosion or superficial vascularization is frequently seen. In later life, patients may also develop stromal opacification or develop larger nodular, kumquat-like lesions (Fig. 6D) although it is

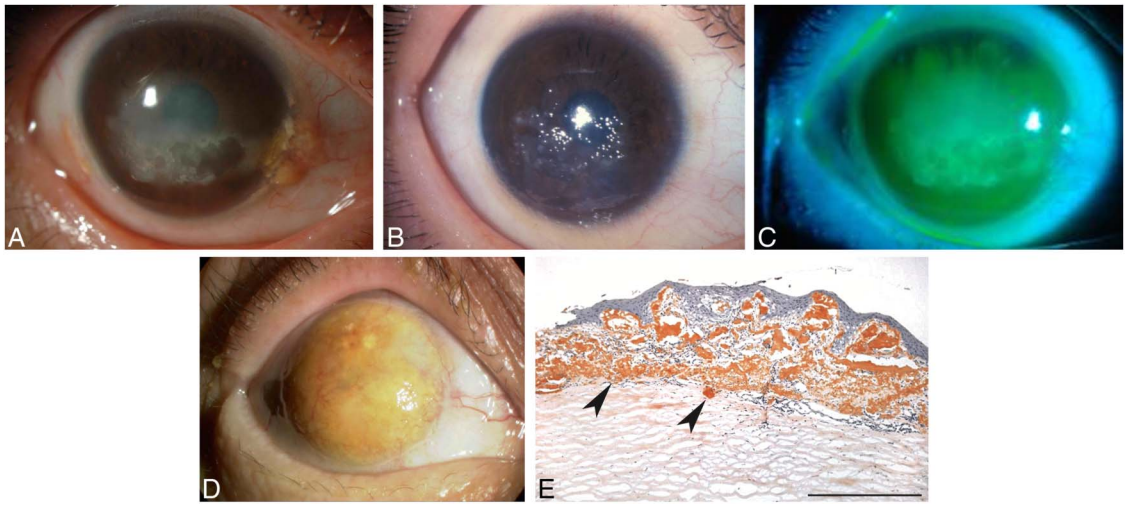

FIGURE 6. Gelatinous drop-like corneal dystrophy (GDLD). A, Band keratopathy type. B, Mulberry type. C, Fluorescein staining shows an extremely hyperpermeable corneal epithelium, here without superficial punctate keratopathy or erosion. D, Kumquat-like diffuse stromal opacity. E, Light microscopy: massive amyloid in a subepithelial lesion (arrowheads) extending to the mid-stromal cornea, bar = 400 μm (direct fast scarlet, ×10). Figures 6A, B, and D from Figures 6B, A, and C in Weiss, JS, Møller HU, Lisch W, et al. The IC3D Classification of the Corneal Dystrophies. *Cornea*. 2008;27(suppl 2):S1–S42. Figures 6C and E from Figures 6C and E in Weiss JS, Møller HU, Aldave AJ, et al. IC3D Classification of Corneal Dystrophies—Edition 2. *Cornea*. 2015;34:117–159.

uncertain whether there is a transition of the 4 different phenotypes, from one to the other, with time.

Symptoms

Irritation, photophobia, tearing, redness, blepharospasm, and significant progressive decrease in vision.

Course

Progression of protruding subepithelial deposits and stromal opacity. Most patients develop recurrence after superficial keratectomy, lamellar keratoplasty, or penetrating keratoplasty, typically within a few years.

Light Microscopy

Corneal epithelium of variable thickness with or without destruction of the epithelial basement membrane and disruption or absence of the Bowman layer. Subepithelial and stromal amyloid deposits have a band-shaped or nodular appearance (Fig. 6E).

Transmission Electron Microscopy

The epithelium varies in thickness with enlarged intercellular spaces and intact desmosomes. Degeneration of epithelial tight junctions in the superficial epithelium. Amyloid is noted in the basal epithelial layer and anterior stroma, consisting of nonbranched, irregularly arranged fibrils with spherical shapes. In early stages, the basement membrane and the Bowman layer may still be intact, which may change with further progression. Amyloid deposits in stromal collagen fibrils may cause stromal disorganization.

Immunohistochemistry

Deposits stain with antibodies to lactoferrin.

Confocal Microscopy

Epithelial cells are irregular in shape and often elongated. The overall epithelial architecture is mildly disorganized. Large accumulations of brightly reflective materials are noted within or beneath the epithelium and within the anterior stroma. No evident abnormalities can be detected in the posterior cornea.

Category

1.

BIBLIOGRAPHY

- Fujiki K, Nakayasu K, Kanai A. Corneal dystrophies in Japan. *J Hum Genet*. 2011;46:431–435.
- Ide T, Nishida K, Maeda N, et al. A spectrum of clinical manifestations of gelatinous drop-like corneal dystrophy in Japan. *Am J Ophthalmol*. 2004;137:1081–1084.
- Kaji Y, Oshika T, Takazawa Y, et al. Co-localization of advanced glycation end products and D-beta-aspartic acid-containing proteins in gelatinous drop-like corneal dystrophy. *Br J Ophthalmol*. 2012;96:1127–1131.
- Kaza H, Barik MR, Reddy MM, et al. Gelatinous drop-like corneal dystrophy: a review. *Br J Ophthalmol*. 2017;101:10–15.
- Kinoshita S, Nishida K, Dota A, et al. Epithelial barrier function and ultrastructure of gelatinous drop-like corneal dystrophy. *Cornea*. 2000;19:551–555.

- Kitazawa K, Kawasaki S, Shinomiya K, et al. Establishment of a human corneal epithelial line lacking the functional TACSTD2 gene as an in vitro model for gelatinous drop-like dystrophy. *Invest Ophthalmol Vis Sci*. 2013:5701–5711.
- Klintworth GK, Valnickova Z, Kielar RA, et al. Familial subepithelial corneal amyloidosis - a lactoferrin-related amyloidosis. *Invest Ophthalmol Vis Sci*. 1997;38:2756–2763.
- Maeno S, Soma T, Tsujikawa M, et al. Efficacy of therapeutic soft contact lens in the management of gelatinous drop-like corneal dystrophy. *Br J Ophthalmol*. 2020;104:241–246.
- Maeno S, Soma T, Nishida K. A case of clinically atypical gelatinous drop-like corneal dystrophy with unilateral recurrent amyloid depositions. *Cornea*. 2022;41:1447–1450.
- Nagahara Y, Tsujikawa M, Koto R, et al. Corneal opacity induced by light in a mouse model of gelatinous drop-like corneal dystrophy. *Am J Pathol*. 2020;190:2330–2342.
- Nakaizumi GA. A rare case of corneal dystrophy. *Acta Soc Ophthalmol Jpn*. 1914;18:949–950.
- Nakatsukasa M, Kawasaki S, Yamasaki K, et al. Tumor-associated calcium signal transducer 2 is required for the proper subcellular localization of claudin 1 and 7: implications in the pathogenesis of gelatinous drop-like corneal dystrophy. *Am J Pathol*. 2010;177:1344–1355.
- Nakatsukasa M, Kawasaki S, Yamasaki K, et al. Two novel mutations of TACSTD2 found in three Japanese gelatinous drop-like corneal dystrophy families with their aberrant subcellular localization. *Mol Vis*. 2011;19:965–970.
- Paliwal P, Gupta J, Tandon R, et al. Identification and characterization of a novel TACSTD2 mutation in gelatinous drop-like corneal dystrophy. *Mol Vis*. 2010;16:729–739.
- Ren Z, Lin PY, Klintworth GK, et al. Allelic and locus heterogeneity in autosomal recessive gelatinous drop-like corneal dystrophy. *Hum Genet*. 2002;110:568–577.
- Tsujikawa M, Kurahashi H, Tanaka T, et al. Identification of the gene responsible for gelatinous drop-like corneal dystrophy. *Nat Genet*. 1999;21:420–423.
- Tsujikawa M. Gelatinous drop-like corneal dystrophy. *Cornea*. 2012;31(suppl 1):S37–S40.
- Yoshida S, Kumano Y, Yoshida A, et al. Two brothers with gelatinous drop-like dystrophy at different stages of the disease: role of mutational analysis. *Am J Ophthalmol*. 2002;133:830–832.

EPITHELIAL-STROMAL *TGFBI* DYSTROPHIES

Reis–Bücklers Corneal Dystrophy (RBCD)

MIM #608470.

Former Alternative Names and Eponyms

Corneal dystrophy of Bowman layer, type 1 (CDB 1).
Geographic corneal dystrophy (Weidle).
Atypical granular corneal dystrophy.
Granular corneal dystrophy, type 3.
Anterior limiting membrane dystrophy, type 1.
Superficial variant of granular corneal dystrophy.

Inheritance

Autosomal dominant.

Genetic Locus

5q31.

Gene

Transforming growth factor beta–induced—*TGFBI*.

Onset

Childhood.

Signs

Confluent irregular and coarse geographic-like opacities with varying densities develop at the level of the Bowman layer and the superficial stroma, initially more central and discrete (Fig. 7A) and subsequently extending to the limbus and deeper stroma (Fig. 7B). Can easily be confused with Thiel–Behnke corneal dystrophy (TBCD), especially in the first 2 decades, as well as early-onset lattice corneal dystrophy variants (LCD variants) with superficial geographic opacification in Bowman layer secondary to amyloid deposition (see Introduction and Table 2). After the early stages, RBCD shows more irregular diffuse opacities with clear interruptions whereas TBCD exhibits multiple flecks with reticular formation especially in the center of the cornea.

Symptoms

Vision is impaired from childhood. Painful recurrent corneal erosions can occur throughout life, starting in early childhood. The erosions may occur before observable corneal opacities.

Course

Slowly progressive deterioration of vision. Recurrent corneal erosions tend to abate with time. Similar but frequently more aggressive course than TBCD but may not be able to distinguish in an individual case. Multiple erosions can result in corneal scarring.

Light Microscopy

The Bowman layer is replaced by a sheet-like layer of granular Masson trichrome-positive deposits (Fig. 7C), which can extend to subepithelial stroma. In advanced cases, sparse round deposits appear in the middle and posterior stroma.

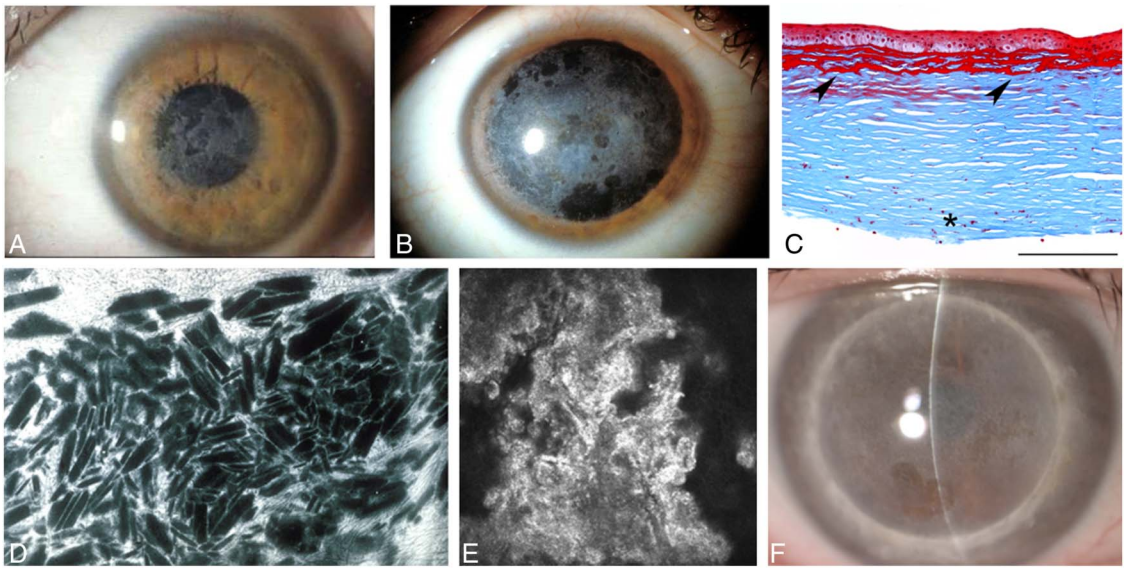

FIGURE 7. Reis–Bücklers corneal dystrophy (RBCD). A, Confluent irregular, geographic-like opacities. B, Geographic opacities extend to the limbus and deeper stroma in a more advanced case. C, Light microscopy: Masson trichrome stains keratohyalin intensely red beneath the epithelium and between superficial stromal lamellae. Note characteristic destruction of the Bowman layer. Deeper red spots (asterisk) are an artifact of lamellar keratoplasty (R124L *TGFBI* mutation), bar = 200 μm. D, Electron microscopy: broad band of irregularly arranged, subepithelial rod-shaped bodies (×3000). E, In vivo confocal microscopy shows a granular, highly reflective material without any shadow within the basal epithelium (R124L *TGFBI* mutation) (400 × 400 μm). F, Recurrent deposits within the corneal graft 15 years after penetrating keratoplasty. Figure 7A from Figure 7A in Weiss, JS, Møller HU, Lisch W, et al. The IC3D Classification of the Corneal Dystrophies. *Cornea*. 2008;27(suppl 2):S1–S42. Figures 7B, C, D, and E from Figures 7B, C, D, and E in Weiss JS, Møller HU, Aldave AJ, et al. IC3D Classification of Corneal Dystrophies—Edition 2. *Cornea*. 2015;34:117–159.

Transmission Electron Microscopy

Subepithelial electron-dense, rod-shaped, or trapezoidal-shaped bodies identical to those in GCD1 (Fig. 7D) replace Bowman layer and extend from basal epithelial cell level to anterior stroma and, sparsely, to deeper stroma. Basal epithelial cells may contain vesicles with similar rods. Transmission electron microscopy can definitively distinguish RBCD from TBCD. RBCD demonstrates rod-shaped bodies in the region of the Bowman layer, unlike TBCD which demonstrates curly fibers in the region of the Bowman layer.

Immunohistochemistry

Rod-shaped bodies are immunopositive for transforming growth factor beta–induced protein (keratoepithelin).

Confocal Microscopy

Distinct deposits are found in the epithelium and the Bowman layer. The deposits in the suprabasal and basal epithelial cell layer show extremely high reflectivity from small granular or amorphous material without shadows (Fig. 7E). The Bowman layer is replaced by highly reflective irregular material, even more reflective than in TBCD. Fine diffuse round or spindle-shaped deposits may be noted in the anterior and sparsely even in the posterior stroma.

Optical Coherence Tomography

A homogenous confluent layer of hyperreflective deposits often with a serrated anterior border is apparent at the level of the Bowman layer and the anterior stroma. It is thickest in the center (72–132 μm), becomes thinner in midperiphery, and disappears toward the limbus.

Category

1.

Note: Patients with RBCD have a R124L *TGFBI* mutation. RBCD may recur within the corneal graft within 5 to 10 years after lamellar or penetrating keratoplasty (Fig. 7F). Latency is shorter after lamellar keratectomy and excimer laser phototherapeutic keratectomy (PTK).

BIBLIOGRAPHY

- Bücklers M. Über eine weitere familiäre Hornhautdystrophie. *Klin Monbl Augenkeilkd*. 1949;114:386–397.
- Dinh R, Rapuano CJ, Cohen EJ, et al. Recurrence of corneal dystrophy after excimer laser phototherapeutic keratectomy. *Ophthalmology*. 1999;106:1490–1497.
- Kobayashi A, Sugiyama K. In vivo laser confocal microscopy findings for Bowman's layer dystrophies (Thiel-Behnke and Reis-Bücklers corneal dystrophies). *Ophthalmology*. 2007;114:69–75.

- Konishi M, Yamada M, Nakamura Y, et al. Immunohistology of keratoepithelin in corneal stromal dystrophies associated with R124 mutations of the BIGH3 gene. *Curr Eye Res*. 2000;21:891–896.
- Küchle M, Green WR, Völcker HE, et al. Reevaluation of corneal dystrophies of Bowman's layer and the anterior stroma (Reis-Bücklers and Thiel-Behnke types): a light and electron microscopic study of 8 corneas and a review of the literature. *Cornea*. 1995;14:333–354.
- Liang Q, Pan Z, Sun X, et al. Reis-Bücklers corneal dystrophy: a reappraisal using in vivo and ex vivo imaging techniques. *Ophthalmic Res*. 2014;51:187–195.
- Munier FL, Korvatska E, Djemaï A, et al. Keratoepithelin mutations in 4 5q31-linked corneal dystrophies. *Nat Genet*. 1997;15:247–251.
- Reis W. Familiäre, fleckige Hornhautentartung. *Dtsch Med Wochenschr*. 1917;43:575.
- Ridgway AE, Akhtar S, Munier FL, et al. Ultrastructural and molecular analysis of Bowman's layer corneal dystrophies: an epithelial origin? Invest *Ophthalmol Vis Sci*. 2000;41:3286–3292.
- Small KW, Mullen L, Barletta J, et al. Mapping of Reis-Bücklers corneal dystrophy to chromosome 5q. *Am J Ophthalmol*. 1996;121:384–390.
- Stone EM, Mathers WD, Rosenwasser GO, et al. Three autosomal dominant corneal dystrophies map to chromosome 5q. *Nat Genet*. 1994;6: 47–51.
- Streeten BW, Qi Y, Klintworth GK, et al. Immunolocalization of beta ig-h3 protein in 5q31-linked corneal dystrophies and normal corneas. *Arch Ophthalmol*. 1999;117:67–75.
- Weidle EG. Klinische und feingewebliche Abgrenzung der Reis-Bücklers'schen Hornhautdystrophie. *Klin Monbl Augenheilkd*. 1989;194:217–226.
- Wittebol-Post D, Pels E. The dystrophy described by Reis and Bücklers. *Ophthalmologica*. 1989;199:1–9.

Thiel–Behnke Corneal Dystrophy (TBCD)

MIM #602082.

Former Alternative Names and Eponyms

Corneal dystrophy of Bowman layer, type II (CDB2).
Honeycomb-shaped corneal dystrophy.
Anterior limiting membrane dystrophy, type II.
Curly fibers corneal dystrophy.
Waardenburg–Jonkers corneal dystrophy.

Inheritance

Autosomal dominant.

Genetic Locus

5q31.

Gene

Transforming growth factor beta–induced—*TGFBI*.

Onset

Early childhood.

Signs

Initial signs are solitary flecks or irregularly shaped scattered opacities at the level of the Bowman layer, followed by symmetrical subepithelial honeycomb opacities (Figs. 8A–C) with peripheral cornea typically uninvolved. In older patients, opacities can progress to deeper stromal layers and corneal periphery. It is difficult to distinguish from Reis-Bücklers corneal dystrophy (RBCD) in early or individual cases.

Rare alleles, which combine R555Q with other *TGFBI* mutations, lead to variants of TBCD with atypical opacities.

Symptoms

Recurrent corneal erosions may be painful in the first and second decade. Gradual visual impairment develops later. Erosions are less frequent, and the onset of visual impairment is later than in RBCD.

Course

Slowly progressive deterioration of vision results from increasing corneal scarring. Recurrent corneal erosions diminish with time. Similar but frequently less aggressive course than RBCD but difficult to distinguish individual cases.

Light Microscopy

Alternating irregular thickening and thinning of the epithelial layer to compensate for ridges and furrows of underlying stroma, with focal absence of epithelial basement membrane (Fig. 8D). Bowman layer is replaced by a superficial fibrocellular pannus with a pathognomonic wavy saw-toothed pattern.

Transmission Electron Microscopy

Presence of curly collagen fibers with 9 to 15 nm diameter (Fig. 8E), importantly distinguishes TBCD from RBCD.

Immunohistochemistry

Curly fibers are immunopositive for transforming growth factor beta–induced protein (keratoepithelin).

Confocal Microscopy

Distinct deposits are found in the epithelium and the Bowman layer (Fig. 8F). The deposits in the basal epithelial cell layer show homogeneous reflectivity with round edges accompanying dark shadows. The Bowman layer is replaced with reflective irregular material that is less reflective than in RBCD.

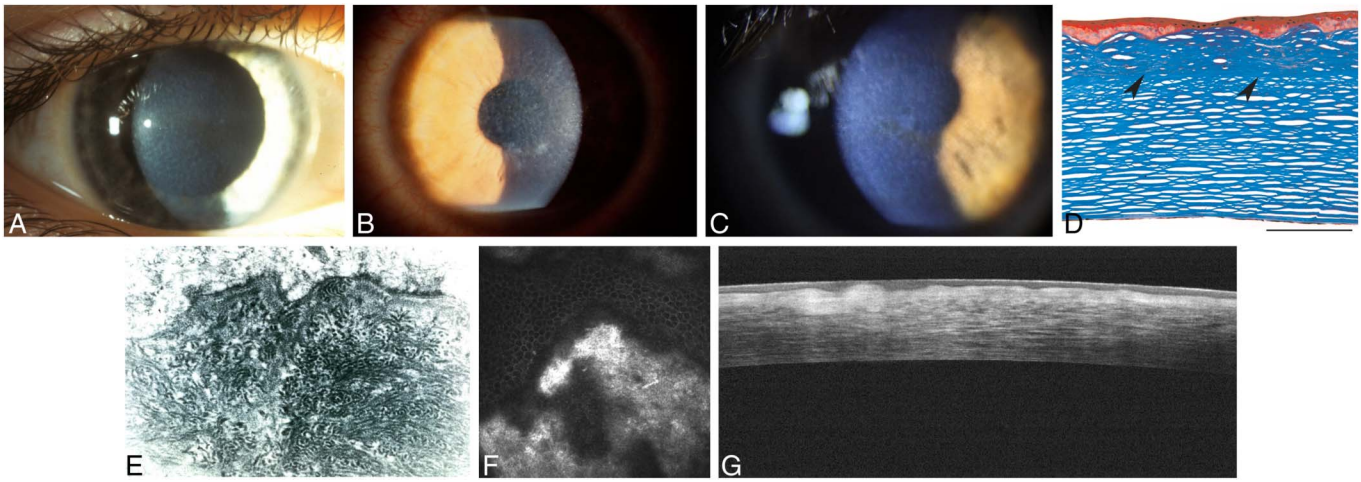

FIGURE 8. Thiel–Behnke corneal dystrophy (TBCD). A, Initial signs of mild honeycomb appearance. B, Intensive honeycomb opacity pattern in advanced disease (R555Q *TGFBI* mutation). C, Corneal honeycomb opacity in a 42-year-old with genetically confirmed TBCD (R555Q *TGFBI* mutation). D, Light microscopy: varying thickness of the epithelium because of a thickened abnormal subepithelial fibrous layer (arrowheads) that replaces the Bowman layer and has a characteristic sawtooth-like surface. Masson trichrome, bar = 200 μm. E, Transmission electron microscopy: subepithelial curly filaments with a thickness of 10 nm (x 50,000). F, In vivo confocal microscopy shows abnormal hyperreflective material with homogeneous reflectivity, round edges, and dark shadows within the basal epithelium (400 × 400 μm). G, Anterior segment OCT from the same 42-year-old in (C) demonstrates a sawtooth pattern of hyperreflective material in the Bowman layer. Figures 8A, B, C, D, E, F, and G from Figures 8A, B, Ci, D, E, F, and Cii in Weiss JS, Møller HU, Aldave AJ, et al. IC3D Classification of Corneal Dystrophies—Edition 2. *Cornea*. 2015;34:117–159.

Optical Coherence Tomography

Prominent hyperreflective material at the level of the Bowman layer extending into the epithelium in a characteristic saw-tooth pattern is a major feature in distinguishing TBCD from RBCD (Fig. 8G).

Category

1.

Note: Patients with TBCD have a R555Q *TGFBI* mutation. Chromosome 10q23-q24 linked corneal abnormality, which had been interpreted as a variant of TBCD, is now classified as epithelial recurrent erosion dystrophy (ERED) associated with the c.3156C>T variant in *COL17A1*.

BIBLIOGRAPHY

- Chen YJ, Chen JT, Lu DW, et al. In vivo corneal confocal microscopic findings and gene analysis of three patients with Thiel-Behnke corneal dystrophy. *Br J Ophthalmol*. 2010;94:262–264.
- Cho KJ, Mok JW, Na KS, et al. *TGFBI* gene mutations in a Korean population with corneal dystrophy. *Mol Vis*. 2012;18:2012–2021.
- Kobayashi A, Sugiyama K. In vivo laser confocal microscopy findings for Bowman's layer dystrophies (Thiel-Behnke and Reis-Bücklers corneal dystrophies). *Ophthalmology*. 2007;114:69–75.
- Küchle M, Green WR, Völcker HE, et al. Reevaluation of corneal dystrophies of Bowman's layer and the anterior stroma (Reis-Bücklers and Thiel-Behnke types): a light and electron microscopic study of 8 corneas and a review of the literature. *Cornea*. 1995;14:333–354.
- Lin BR, Le DJ, Chen Y, et al. Whole exome sequencing and segregation analysis confirms that a mutation in *COL17A1* Is the cause of epithelial recurrent erosion dystrophy in a large dominant pedigree previously mapped to chromosome 10q23-q24. *PLoS One*. 2016;11:1–10.
- Lohse E, Stock EL, Jones JC, et al. Reis-Bücklers' corneal dystrophy. Immunofluorescent and electron microscopic studies. *Cornea*. 1989;8:200–209.
- Munier FL, Korvatska E, Djemaï A, et al. Keratoepithelin mutations in four 5q31-linked corneal dystrophies. *Nat Genet*. 1997;15:247–251.
- Niel-Butschi F, Kantelip B, Iwaszkiewicz J, et al. Genotype-phenotype correlations of *TGFBI* p.Leu509Pro, p.Leu509Arg, p.Val613Gly, and the allelic association of p.Met502Val-p.Arg555Gln mutations. *Mol Vis*. 2011;17:1192–1202.
- Nowińska AK, Wylegala E, Janiszewska DA, et al. Genotype-phenotype correlation of *TGFBI* corneal dystrophies in Polish patients. *Mol Vis*. 2011;17:2333–2342.
- Ridgway AE, Akhtar S, Munier FL, et al. Ultrastructural and molecular analysis of Bowman's layer corneal dystrophies: an epithelial origin? *Invest Ophthalmol Vis Sci*. 2000;41:3286–3292.
- Streeten BW, Qi Y, Klintworth GK, et al. Immunolocalization of beta igh3 protein in 5q31-linked corneal dystrophies and normal corneas. *Arch Ophthalmol*. 1999;117:67–75.

- Thiel HJ, Behnke H. Eine bisher unbekannte subepitheliale hereditäre Hornhautdystrophie. *Klin Monbl Augenheilkd*. 1967;150:862–874.
- Vajzovic LM, Karp CL, Haft P, et al. Ultra high-resolution anterior segment optical coherence tomography in the evaluation of anterior corneal dystrophies and degenerations. *Ophthalmology*. 2011;118:1291–1296.
- Weidle EG. Die wabenförmige Hornhautdystrophie (Thiel-Behnke) Neubewertung und Abgrenzung gegenüber der Reis-Bücklerschen Hornhautdystrophie. *Klin Monbl Augenheilkd*. 1999;214:125–135.
- Wittebol-Post D, Van Schooneveld MJ, Pels E. The corneal dystrophy of Waardenburg and Jonkers. *Ophthalmic Paediatr Genet*. 1989;10:249–255.

Lattice Corneal Dystrophies (LCDs)

MIM #122200 (classic LCD), MIM #608471 (LCD variants).

Former Alternative Names and Eponyms

Classic LCD

LCD, type 1.
Biber-Haab-Dimmer.

LCD Variants

LCD type III.
LCD type IIIA.
LCD type I/IIIA.
LCD type IV.
LCDi.
Atypical LCD.
Deep LCD.
Polymorphic corneal amyloidosis.

Inheritance

Autosomal dominant.

Genetic Locus

5q31.

Gene

Classic LCD

Transforming growth factor beta–induced—*TGFBI* (R124C mutation).

LCD Variants

Transforming growth factor beta–induced—*TGFBI* (mutations other than R124C) (Table 2).

Onset

Classic LCD

Early (first to second decade).

LCD Variants

May have similarly early (first to second decade), intermediate (third to fourth decade), or late (fifth to ninth decade) onset of symptoms compared with classic LCD (Table 2).

Signs

Classic LCD

The first signs are central, superficial, fleck-like opacities that usually emerge by the end of the first decade (Fig. 9A). In retroillumination, a few isolated, subtle, and peripheral lattice lines in deeper layers are visible (Fig. 9B). Simultaneously, thin branching refractile lines and/or subepithelial, whitish, ovoid dots are also evident. These lines start centrally and more superficially and spread centrifugally and deeply but leave the far peripheral stroma clear. Descemet membrane and the endothelium are uninvolved (Figs. 9C, D). Diffuse, subepithelial, ground-glass haze of the central and paracentral cornea develops concurrently with the central and paracentral lattice lines and subsequently progresses (Fig. 9C), accompanied by recurrent epithelial erosions. Progression of diffuse central haze in the second to third decade may obscure visualization of lattice lines and reduce vision sufficiently to necessitate surgical intervention. Asymmetric corneal involvement is common, and unilateral involvement has been described.

LCD Variants

At least 5 major phenotypes of variant LCD can be distinguished by appearance and depth of the amyloid deposits (Figs. 10A–K, also see Introduction for more detailed description). As with classic LCD, there may be phenotypic variation between both eyes and among individual patients carrying the same pathogenic *TGFBI* variant. Overlapping phenotypes also exist in which lattice lines and granular deposits are whitish and contain both amyloid and red Masson trichrome-staining keratohyalin. In late cases, it may be impossible to determine the phenotype because of anterior stromal scarring. Table 2 lists published variants including mutation, age of onset, the published phenotypic descriptions, countries with reported patients, and shorthand PMID references for clinical and experimental articles.

Symptoms

Classic LCD

Ocular discomfort, pain, and visual impairment, sometimes starting as early as the first decade secondary to frequent recurrent erosive attacks. Visual impairment occurs by the fourth decade.

LCD Variants

Ocular discomfort may or may not occur, depending on the depth of the deposits. This can range from severe discomfort in those with anterior geographic amyloid deposition to minimal or no pain in those with predominantly deep deposits. The level of visual impairment also varies significantly: from

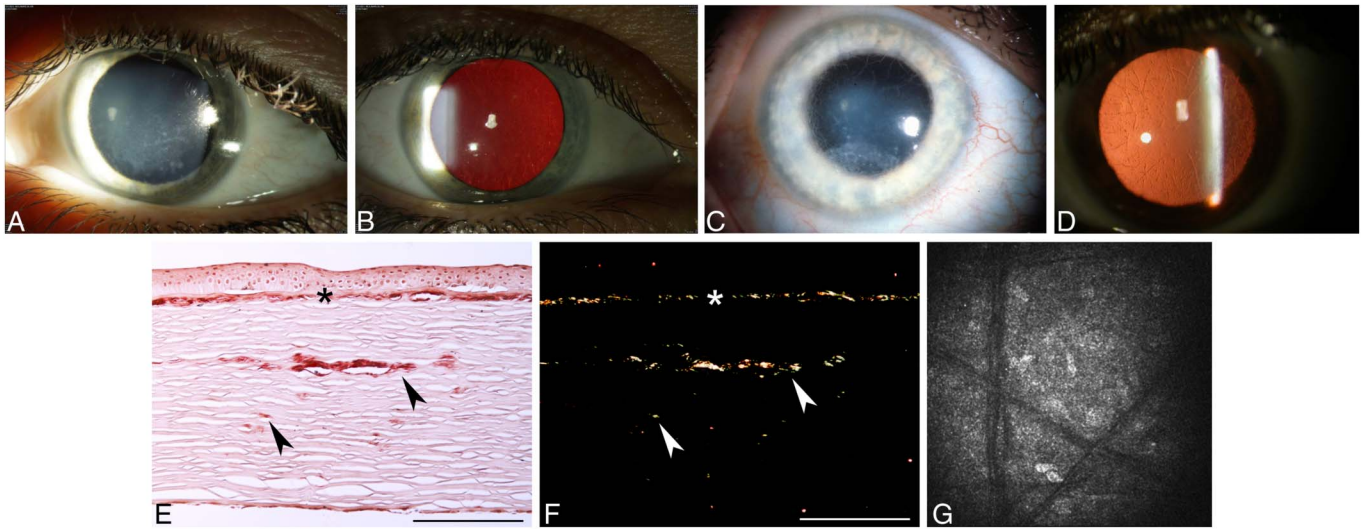

FIGURE 9. Classic lattice corneal dystrophy (classic LCD). Direct (A) and retroillumination (B) of early lattice corneal dystrophy with dots and fine lattice lines (R124C *TGFBI* mutation). C, Subepithelial ground glass haze of the central and inferior cornea and diffuse lattice lines in advanced LCD (R124C *TGFBI* mutation). D, Dots and paracentral lattice lines in retroillumination (R124C *TGFBI* mutation). E, Light microscopy: Congo red prominently stains a continuous layer of amyloid (asterisk) that underlies and partially destroys the Bowman layer and intrastromal amyloid deposits (arrowheads) corresponding to lattice lines (R124C *TGFBI* mutation). F, Light microscopy: this same section viewed with polarized light confirms deposits are birefringent and red–green dichroic, thus amyloid, bar = 200 μm. G, In vivo confocal microscopy image shows filaments corresponding to lattice lines within the stroma (400 × 400 μm). Figure 9D from Figure 10A in Weiss, JS, Møller HU, Lisch W, et al. The IC3D Classification of the Corneal Dystrophies. *Cornea*. 2008;27(suppl 2):S1-S42. Figures 9A, B, C, E, F, and G from Figures 9A, B, C, E, F, and G in Weiss JS, Møller HU, Aldave AJ, et al. IC3D Classification of Corneal Dystrophies—Edition 2. *Cornea*. 2015;34:117–159.

early and marked in the early-onset variant dystrophies to late and mild or even normal vision in late-onset variants (incidentally detected on slit lamp biomicroscopy).

Course

Classic LCD

Progressive, often with marked visual decrease by the fourth decade.

LCD Variants

Progressive but often much slower with later onset of symptoms and later diagnosis.

Light Microscopy

Classic LCD

Eosinophilic amyloid material accumulates between the epithelial basement membrane and the Bowman layer. Stromal deposition of amyloid distorts the architecture of corneal lamellae. Epithelial atrophy and disruption with degeneration of the basal epithelial cells plus focal thinning, later absence of the Bowman layer develops with age. Amyloid deposits characteristically stain positive with Congo red (Fig. 9E) and display birefringence (Fig. 9F) and red-green dichroism under polarized light (Fig. 9F). Deposits also exhibit metachromasia with crystal violet and fluorescence when stained with thioflavin T.

LCD Variants

Same, but findings depend on the depth, breadth, and size of amyloid deposits. Larger deposits may incite a focal stromal scarring reaction. Posterior deposits may indent Descemet membrane. In addition to amyloid, there may be minor deposition of keratohyalin (seen sometimes even in classic LCD).

Transmission Electron Microscopy

Extracellular masses of fine, electron-dense, randomly aligned fibrils of uniform 8–10 nm diameter are characteristic of amyloid protein. There are fewer keratocytes in the areas of amyloid deposition, and some are degenerated with cytoplasmic vacuolization, whereas others seem metabolically active. Descemet membrane and the endothelium are normal.

Confocal Microscopy

Linear and branching structures (Fig. 9G) or other forms of stromal deposits with changing reflectivity and poorly demarcated margins.

Category

Genotype and Variant Nomenclature

For consistency of reporting and to facilitate literature searches, from here on IC3D recommends referring to the specific pathogenic variant, when known, by appending the mutation using 1-letter amino acid abbreviations (for example, LCD-H626R results from the His626Arg missense mutation, and former LCD type IV with variant L527R could be referred to as LCD-L527R).

For this classification, we define classic LCD as LCD-R124C. This mutation has been detected in every country reporting on genotyped patients with LCD across 5 continents, whereas LCD variants are geographically more restricted, suggesting founder mutations (for discussion of founder mutations, see Introduction); some have been reported only from single families. The most common LCD variant is LCD-H626R, reported from more than 10 countries across 3 continents.

Most LCD variants result from point mutations, but short deletions and insertions also have been reported, as well as compound heterozygous mutations, in which case, the second mutation may or may not alter the phenotype.

Systemic Amyloidosis with Corneal Findings: Lattice Corneal Amyloidosis

Systemic amyloidosis with corneal lattice lines derived from gelsolin is properly termed familial amyloidosis, Finnish type, or gelsolin type. Eponymously, it is known as Meretoja syndrome (Fig. 11A). The prior name, lattice corneal dystrophy type 2 (LCD2) is a misnomer because this condition is not a corneal dystrophy but a systemic disease with corneal findings. More recently, the corneal findings have been referred to as lattice corneal amyloidosis to distinguish this systemic disease with corneal findings from the true corneal dystrophies.

An important additional clinical feature is that of reduced or absent corneal sensation such that the resultant neurotrophic keratopathy is subject to epithelial erosions and persistent defects. This carries a risk of major surface healing issues after keratoplasty.

Signs in Systemic Amyloidosis with Corneal Findings

On slit lamp examination, Meretoja syndrome has less numerous lattice lines than classic LCD. The lattice lines are denser in the periphery than in the central cornea (Fig. 11B). This typically results in later and less dense central corneal opacification and better visual acuity for a longer time when compared with classic LCD.

BIBLIOGRAPHY

- Aldave AJ, Yellore VS, Sonmez B, et al. A novel variant of combined granular-lattice corneal dystrophy associated with the Met619Lys mutation in the TGFBI gene. *Arch Ophthalmol*. 2008;126:371–377.
- Biber H. Ueber einige seltene Hornhauterkrankungen: IV. Die oberflächliche gittrige Keratitis [Inaugural dissertation]. Zurich; 1890.
- Chiou AG, Beuermann RW, Kaufman SC, et al. Confocal microscopy in lattice corneal dystrophy. *Graefes Arch Clin Exp Ophthalmol*. 1999;237:697–701.
- Dighiero P, Drunat S, Ellies P, et al. A new mutation (A546T) of the big-h3 gene responsible for a French lattice corneal dystrophy type IIIA. *Am J Ophthalmol*. 2000;129:248–251.
- Dighiero P, Niel F, Ellies P, et al. Histologic phenotype-genotype correlation of corneal dystrophies associated with eight distinct mutations in the TGFBI gene. *Ophthalmology*. 2001;108:818–823.
- Eifrig DE Jr, Afshari NA, Buchanan HW 4th, et al. Polymorphic corneal amyloidosis: a disorder due to a novel mutation in the transforming growth factor beta-induced (BIGH3) gene. *Ophthalmology*. 2004;111:1108–1114.
- Ellies P, Renard G, Valleix S, et al. Clinical outcome of eight BIGH3-linked corneal dystrophies. *Ophthalmology*. 2002;109:793–797.
- Fujiki K, Hotta Y, Nakayasu K, et al. A new L527R mutation of the beta IGH3 gene in patients with lattice corneal dystrophy with deep stromal opacities. *Hum Genet*. 1998;103:286–289.
- Fukuoka H, Kawasaki S, Yamasaki K, et al. Lattice corneal dystrophy type IV (p.Leu527Arg) is caused by a founder mutation of the TGFBI gene in a single Japanese ancestor. *Invest Ophthalmol Vis Sci*. 2010;51:4523–4530.
- Funayama T, Mashima Y, Kawashima M, et al. Lattice corneal dystrophy type III in patients with a homozygous L527R mutation in the TGFBI gene. *Jpn J Ophthalmol*. 2006;50:62–64.
- Gruenauer-Kloevekorn C, Clausen I, Weidle E, et al. TGFBI (BIGH3) gene mutations in German families: two novel mutations associated with unique clinical and histopathological findings. *Br J Ophthalmol*. 2009;93:932–937.
- Hida T, Proia AD, Kigasawa K, et al. Histopathologic and immunochemical features of lattice corneal dystrophy type III. *Am J Ophthalmol*.1987;104:249–254.
- Hirano K, Hotta Y, Nakamura M, et al. Late-onset form of lattice corneal dystrophy caused by Leu527Arg mutation of the TGFBI gene. *Cornea*. 2001;20:525–529.
- Hotta Y, Fujiki K, Ono K, et al. Arg124Cys mutation of the betaig-h3 gene in a Japanese family with lattice corneal dystrophy type I. *Jpn J Ophthalmol*. 1998;42:450–455.
- Irusteta L, Ramírez-Miranda A, Navas-Pérez A, et al. Detailed phenotypic description of stromal corneal dystrophy in a large pedigree carrying the uncommon TGFBI p.Ala546Asp pathogenic variant. *Ophthalmic Genet*. 2022;43:589–593.
- Jaakkola AM, Kivelä TT. Clinical and histopathologic characteristics and template of the TGFBI p.(His626Arg) missense variant lattice corneal dystrophy. *Cornea*. 2023;42:1124–1132.
- Kannabiran C, Klintworth GK. TGFBI gene mutations in corneal dystrophies. *Hum Mutat*. 2006;27:615–625.
- Kawamoto K, Morishige N, Yamada N, et al. Delayed corneal epithelial wound healing after penetrating keratoplasty in individuals with lattice corneal dystrophy. *Am J Ophthalmol*. 2006;142:173–174.

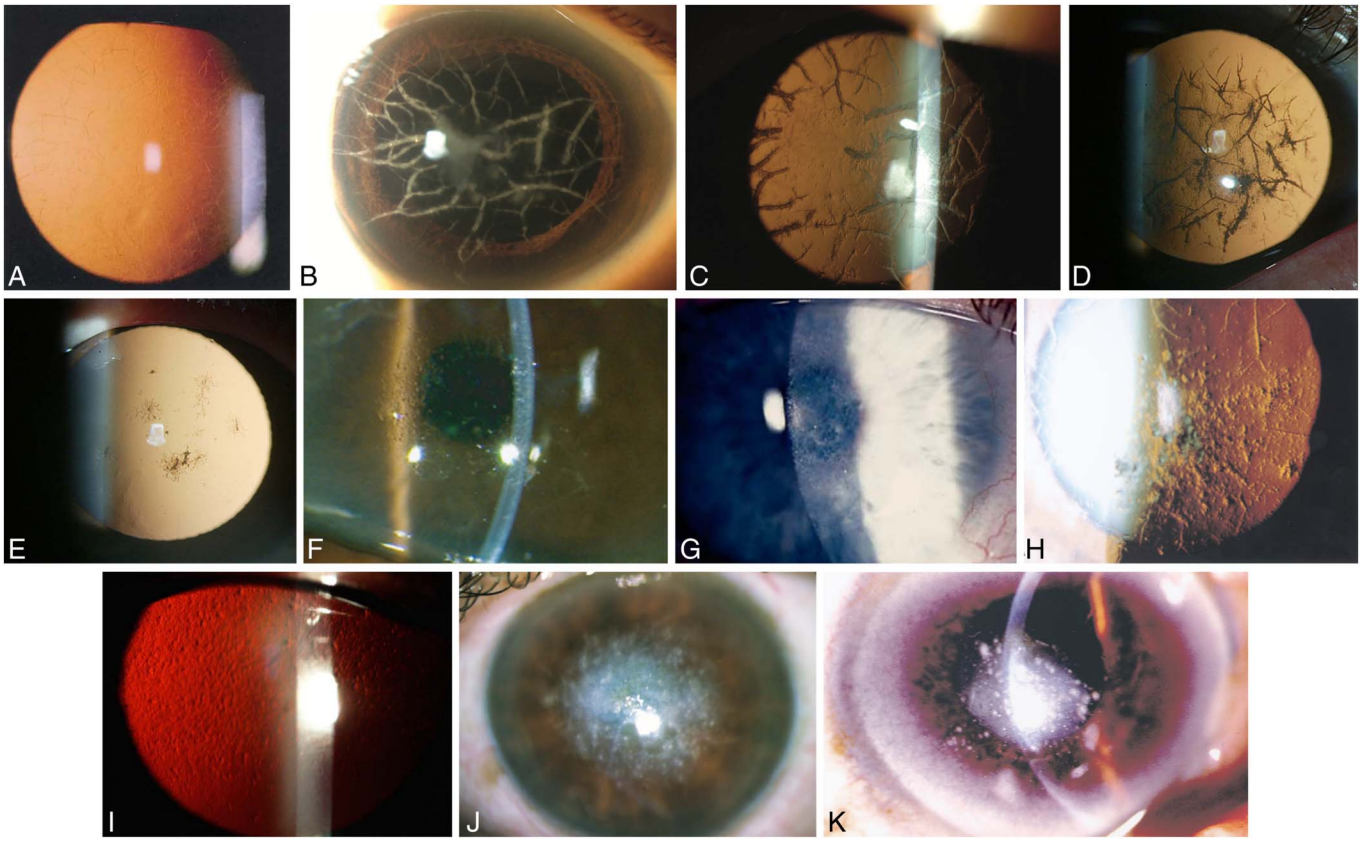

FIGURE 10. Lattice corneal dystrophy (LCD) variants. Five broad phenotypes. A, LCD variant phenotype that recapitulates the early onset and fine lattice lines of classic LCD in a 7-year-old (LCD-L569R *TGFBI* mutation). B, Intermediate sometimes late-onset LCD variant phenotype demonstrating lattice lines that are thick, ropy, and more prominent than in classic LCD, as seen in direct (B) and retroillumination (C), in a 50-year-old (LCD-T621P *TGFBI* mutation). D and E, Same phenotype as (B and C) but with asymmetric progression between the 2 eyes of 1 patient (LCD-H626R *TGFBI* mutation, the second most common and geographically widespread LCD variant). F, Late-onset LCD variant phenotype demonstrating amyloid deposits primarily located in the deep stroma, thus not leading to corneal erosions, with lattice lines that are infrequent or inconspicuous in an 85-year-old (LCD-R496W *TGFBI* mutation). G, Intermediate-onset superficial LCD variant phenotype in which amyloid is mainly deposited at Bowman layer level resulting in a geographic pattern that may be misdiagnosed as EBMD, RBCD, or TBCD, with infrequent or indistinct lattice lines in a 40-year-old (LCD-H626P *TGFBI* mutation). H, Intermediate to late-onset LCD variant phenotype in which amyloid deposits are mostly dot-shaped and comma-shaped and show variation in form and depth, with lattice lines in a 74-year-old (LCD-L527R *TGFBI* mutation). I, Same phenotype as (H) but with infrequent and indistinct lattice lines in a 65-year-old (LCD-L565P *TGFBI* mutation). J and K, Same phenotype as (H and I), late stage with opacification of central cornea from white more granular-like deposits in a 60- and 82-year-old (LCD-L527R *TGFBI* mutation and LCD-A546D *TGFBI* mutation, respectively). Figure 10A reprinted from Figure 2C in Warren JF, Abbott RL, Yoon MK, et al. A new mutation (Leu569Arg) within exon 13 of the *TGFBI (BIGH3)* gene causes lattice corneal dystrophy type I. *Am J Ophthalmol*. 2003;136:872–878 with permission from Elsevier. Figures 10B and C used with permission of Slack, Inc. from Figures A(a) and A(b) in Lee J, Ji YW, Park SY, et al. Delayed onset of lattice corneal dystrophy Type IIIA due to a novel T621P mutation in *TGFBI*. *J Refract Surg*. 2016;32:356; permission conveyed through Copyright Clearance Center, Inc. Figures 10D and E reprinted from Figures 1A and B in Zenteno JC, Correa-Gomez-V, Santacruz-Valdez C, et al. Clinical and genetic features of *TGFBI*-linked corneal dystrophies in Mexican population: description of novel mutations and novel genotype–phenotype correlations. *Exp Eye Res*. 2009;89:172–177 with permission from Elsevier. Figure 10F reproduced from Figure 1B in Kawasaki S, Yagi H, Yamasaki K, et al. A novel mutation of the *TGFBI* gene causing a lattice corneal dystrophy with deep stromal involvement. *Br J Ophthalmol*. 2011;95:150–151, with permission from BMJ Publishing Group Ltd. Figure 10 G from Figure 1A in Liskova P, Klintworth GK, Bowling BL, et al. Phenotype associated with the H626P mutation and other changes in the *TGFBI* gene in Czech families. *Ophthalmic Res*. 2008;40:105–108. Copyright 2008 Karger Publishers, Basel, Switzerland. Figure 10H and K from Figures 1A and 3A in Hirano K, Hotta Y, Nakamura M, et al. Late-onset form of lattice corneal dystrophy caused by Leu527Arg mutation of the *TGFBI* gene. *Cornea*. 2001;20:525–529. Figure 10I from Figure 1B in Ołdak M, Szaflik JP, Ścieżyńska A, et al. Late-onset lattice corneal dystrophy without typical lattice lines caused by a novel mutation in the *TGFBI* gene. *Cornea*. 2014;33:294–299. Figure 10J from Figure 3A in Irusteta L, Ramírez-Miranda A, Navas-Pérez A, et al. Detailed phenotypic description of stromal corneal dystrophy in a large pedigree carrying the uncommon *TGFBI* p.Ala546Asp pathogenic variant. *Ophthalmic Genet*. 2022;43:589–593. Reprinted by permission of Taylor & Francis Ltd.

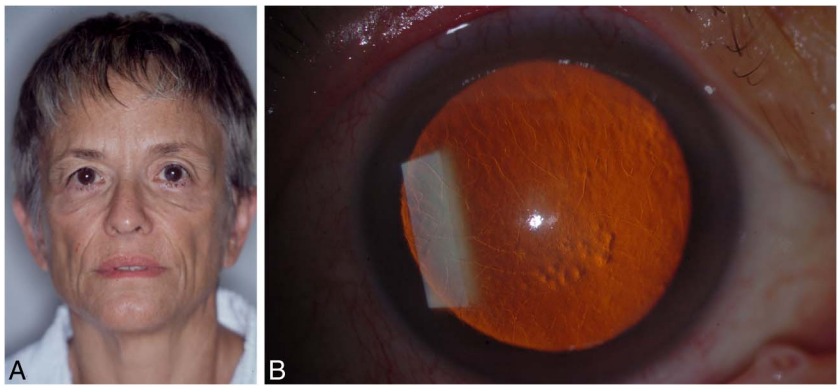

FIGURE 11. Systemic amyloidosis with corneal findings (Meretoja syndrome). A, Lax, mask-like facies consequent to cranial nerve VII palsy. B, Lattice lines are less numerous than in classic and variant LCD, start peripherally and spread centrally. Figures 11A and B from Figures 11A and B in Weiss JS, Møller HU, Aldave AJ, et al. IC3D Classification of Corneal Dystrophies—Edition 2. *Cornea*. 2015;34:117-159.

- Kawasaki S, Yagi H, Yamasaki K, et al. A novel mutation of the TGFBI gene causing a lattice corneal dystrophy with deep stromal involvement. *Br J Ophthalmol*. 2011;95:150–151.
- Kim J, Lee KA, Kim EK, et al. A Korean patient with lattice corneal dystrophy type IV with Leu527Arg mutation in the TGFBI gene. *Korean J Ophthalmol*. 2014;28:83–85.
- Klintworth GK, Bao W, Afshari NA, et al. Two mutations in the TGFBI (BIGH3) gene associated with lattice corneal dystrophy in an extensively studied family. Invest *Ophthalmol Vis Sci*. 2004;45:1382–1388.
- Lee J, Ji YW, Park SY, et al. Delayed onset of lattice corneal dystrophy type IIIA due to a novel T621P mutation in TGFBI. *J Refract Surg*. 2016;32:356.
- Liskova P, Klintworth GK, Bowling BL, et al. Phenotype associated with the H626P mutation and other changes in the TGFBI gene in Czech families. *Ophthalmic Res*. 2008;40:105–108.
- Munier FL, Frueh BE, Othenin-Girard P, et al. BIGH3 mutation spectrum in corneal dystrophies. *Invest Ophthalmol Vis Sci*. 2002;43:949–954.
- Munier FL, Korvatska E, Djemaï A, et al. Keratoepithelin mutations in four 5q31-linked corneal dystrophies. *Nat Genet*. 1997;15:247–251.
- Nakagawa AS, Fujiki K, Enomoto Y, et al. Case of late onset and isolated lattice corneal dystrophy with Asn544Ser (N544S) mutation of transforming growth factor beta-induced (TGFBI, BIGH3) gene. *Nippon Ganka Gakkai Zasshi*. 2004;108:618–620.
- Ołdak M, Szaflik JP, Ścieżyńska A, et al. Late-onset lattice corneal dystrophy without typical lattice lines caused by a novel mutation in the TGFBI gene. *Cornea*. 2014;33:294–299.
- Schmitt-Bernard CF, Guittard C, Arnaud B, et al. BIGH3 exon 14 mutations lead to intermediate type I/IIIA of lattice corneal dystrophies. *Invest Ophthalmol Vis Sci*. 2000;41:1302–1308.
- Seitz B, Weidle E, Naumann GOH. Einseitige gittrige stromale Hornhautdystrophie Typ III (Hida). *Klin Monbl Augenheilkd*. 1993;203:279–285.
- Snead DR, Mathews BN. Differences in amyloid deposition in primary and recurrent corneal lattice dystrophy type 1. *Cornea*. 2002;21:308–311.
- Starck T, Kenyon KR, Hanninen LA, et al. Clinical and histopathologic studies of two families with lattice corneal dystrophy and familial systemic amyloidosis (Meretoja syndrome). *Ophthalmology*. 1991;98:1197–1206.
- Stewart H, Black GCM, Donnai D, et al. A mutation within exon 14 of the TGFBI (BIGH3) gene on chromosome 5q31 causes an asymmetric, late-onset form of lattice corneal dystrophy. *Ophthalmology*. 1999;106:964–970.
- Stix B, Leber M, Bingemer P, et al. Hereditary lattice corneal dystrophy is associated with corneal amyloid deposits enclosing C-terminal fragments of keratoepithelin. *Invest Ophthalmol Vis Sci*. 2005;46:1133–1139.
- Tian X, Fujiki K, Wang W, et al. Novel mutation (V505D) of the TGFBI gene found in a Chinese family with lattice corneal dystrophy, type I. *Jpn J Ophthalmol*. 2005;49:84–88.
- Tsujikawa K, Tsujikawa M, Yamamoto S, et al. Allelic homogeneity due to a founder mutation in Japanese patients with lattice corneal dystrophy type IIIA. *Am J Med Genet*. 2002;113:20–22.
- Warren JF, Abbott RL, Yoon MK, et al. A new mutation (Leu569Arg) within exon 13 of the TGFBI (BIGH3) gene causes lattice corneal dystrophy type I. *Am J Ophthalmol*. 2003;136:872–878.
- Wheeldon CE, de Karolyi BH, Patel DV, et al. A novel phenotype-genotype relationship with a TGFBI exon 14 mutation in a pedigree with a unique corneal dystrophy of Bowman's layer. *Mol Vis*. 2008;14:1503–1512.
- Yamada N, Chikama TI, Morishige N, et al. Homozygous mutation (L527R) of TGFBI in an individual with lattice corneal dystrophy. *Br J Ophthalmol*. 2005;89:771–773.
- Yamamoto S, Okada M, Tsujikawa M, et al. A keratoepithelin (big-h3) mutation in lattice corneal dystrophy type IIIA. *Am J Hum Genet*. 1998;62:719–722.
- Yamamoto S, Okada M, Tsujikawa M, et al. The spectrum of beta ig-h3 gene mutations in Japanese patients with corneal dystrophy. *Cornea*. 2000;19(3 suppl):S21–S23.
- Zenteno JC, Correa-Gomez V, Santacruz-Valdez C, et al. Clinical and genetic features of TGFBI-linked corneal dystrophies in Mexican population: description of novel mutations and novel genotype-phenotype correlations. *Exp Eye Res*. 2009;89:172–177.

Granular Corneal Dystrophy, Type 1 (Classic) (GCD1)

MIM #121900.

Former Alternative Names and Eponyms

Corneal dystrophy Groenouw type 1.

Inheritance

Autosomal dominant.

Genetic Locus

5q31.

Gene

Transforming growth factor beta–induced—*TGFBI* (typically R555W mutation).

Onset

Childhood, as early as age 2 years.

Signs

In children, a vortex pattern (Fig. 12A) of very small brownish granules in the form of lines develops superficial to the Bowman layer. As the patient ages, well-defined discrete granules appear grayish-white on direct illumination with clear intervening stroma. Granules increase in size and number and may coalesce resulting in a snowflake appearance (Figs. 12B, C). On retroillumination (Fig. 12D), these granules are composed of extremely small, translucent dots with the appearance of vacuoles, glassy splinters, or crushed breadcrumbs. Opacities can involve the more peripheral stroma but do not extend to the limbus. In later life, granules extend into the deeper stroma approaching Descemet membrane. Homozygotes have more severe manifestations.

Symptoms

Glare and photophobia are early symptoms. Visual acuity decreases as opacification progresses with age. Recurrent erosions associated with pain may occur. Homozygous cases have more severe symptoms.

Course

With progression, the opacities become more confluent especially in the superficial cornea and reduce visual acuity by the fifth decade. Serial observation demonstrates in both GCD1 and GCD2 that granule dropout after epithelial erosions may result in stromal clearing. Patterns of recurrence are highly variable, with recurrence appearing as early as 1 year after surgery. Recurrent GCD1 deposits typically occur in superficial subepithelial areas (Fig. 12E), deep posterior graft–host interface (Fig. 12F) or along suture tracks (Fig. 12G).

Light Microscopy

Multiple stromal deposits may extend from the deep epithelium to Descemet membrane. The keratohyalin opacities stain with Masson trichrome (Fig. 12H).

Transmission Electron Microscopy

Dense, rod-shaped bodies are similar in appearance to those in RBCD.

Immunohistochemistry

Abnormal deposits react with antibodies to transforming growth factor beta–induced protein (keratoepithelin).

Confocal Microscopy

Abnormal hyperreflective opacities in snowflake and trapezoidal shapes (Fig. 12I).

Optical Coherence Tomography

Multiple hyperreflective opacities in the stroma, corresponding to deposits, with well-defined borders. Deposits may be located throughout the stroma from deep epithelium up to Descemet membrane (Fig. 12J).

Category

1.

Note: Patients with GCD1 typically have R555W *TGFBI* mutation. GCD variants have been reported with other *TGFBI* mutations such as R124S, which demonstrate more severe signs and symptoms with an earlier onset compared with classic GCD1.

BIBLIOGRAPHY

- Bücklers M. Die erblichen Hornhautdystrophien. *Klin Monbl Augen-heilkd*. 1938;Beiheft 3:1–135.
- Eiberg E, Møller HU, Berendt I, et al. Assignment of granular corneal dystrophy Groenouw type I (CDGG1) to Chromosome 5q. *Eur J Hum Genet*. 1994;2:132–138.
- Groenouw A. Knötchenförmige Hornhauttrübungen (Noduli corneae). *Arch Augenheilkd*. 1890;21:281–289.
- Han KE, Choi Sl, Kim TI, et al. Pathogenesis and treatments of TGFBI corneal dystrophies. *Prog Retin Eye Res*. 2016;50:67–88.
- Jones ST, Zimmerman LE. Histopathologic differentiation of granular, macular and lattice dystrophies of the cornea. *Am J Ophthalmol*. 1961;51:394–410.
- Matsuo N, Fujiwara H, Ofuchi Y. Electron and light microscopic observations of a case of Groenouw' s nodular corneal dystrophy. *Folia Ophthalmol Jpn*. 1967;18:436–447.
- Møller HU. Granular corneal dystrophy Groenouw type I. Clinical and genetic aspects. *Acta Ophthalmol*. 1991;69 (suppl 198):1–40.

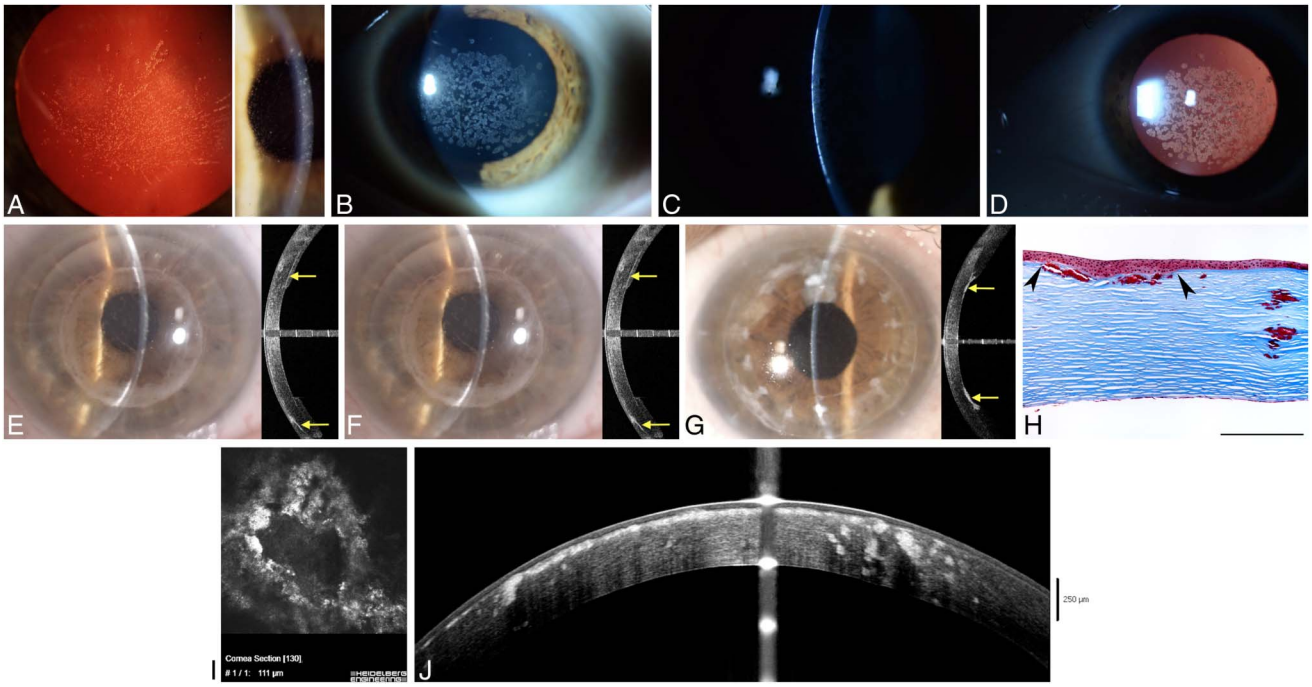

FIGURE 12. Granular corneal dystrophy, type 1 (GCD1). A, In a child, early subepithelial verticillate-like opacities are evident by retroillumination and direct illumination. With (B) full direct illumination, (C) slit-beam illumination, and (D) retroillumination, "snowflake" stromal deposits are both discrete and confluent and are axially distributed within the clear intervening stroma. E, After PTK, GCD1 deposits (arrows) are noted to recur in the subepithelial area on slit lamp and OCT. F and G, After DALK, GCD1 deposits (arrows) are noted to recur (F) centrally in the deep posterior graft–host interface (arrows) or (G) peripherally along suture tracks (arrows) on slit lamp and OCT. H, Light microscopy: Masson trichrome highlights full-thickness deposits of keratohyalin in the corneal stroma (R555W *TGFBI* mutation, bar = 240 μm). I, In vivo confocal microscopy (400 × 400 μm) shows abnormal hyperreflective opacities in snowflake and trapezoidal shapes within the stroma. J, Spectral domain OCT shows multiple hyperreflective stromal deposits, with well-defined borders, located from deep epithelium to Descemet membrane, in a 32-year-old male patient with GCD1. Figures 12A and H from Figures 12A and E in Weiss JS, Møller HU, Aldave AJ, et al. IC3D Classification of Corneal Dystrophies—Edition 2. *Cornea*. 2015;34:117–159.

- Munier FL, Korvatska E, Djemaï A, et al. Kerato-epithelin mutations in four 5q31-linked corneal dystrophies. *Nat Genet*. 1997;15:247–251.
- Seitz B, Behrens A, Langenbucher A, et al: Morphometric analysis of deposits in granular and lattice corneal dystrophy: histopathologic implications for phototherapeutic keratectomy. *Cornea*. 2004;23:380–385.
- Stone E M, Mathers WD, Rosenwasser GOD, et al. Three autosomal dominant corneal dystrophies map to chromosome 5q. *Nat Genet*. 1994;6: 47–51.
- Weidle EG, Lisch W. Die verschiedenen Trübungsformen der bröckeligen Hornhautdystrophie. *Klin Monbl Augenheilkd*. 1984;185:167–173.
- Wittebol-Post D, van der Want JJL, van Bijsterveld OP. Granular dystrophy of the cornea (Groenouw's type I). *Ophthalmologica*. 1987;195:169–177.

Granular Corneal Dystrophy, Type 2 (GCD2)

MIM #607541.

Former Alternative Names and Eponyms

Avellino dystrophy.

Combined granular-lattice dystrophy.

Note: For nearly a century, this entity was considered a mild GCD variant (Groenouw type I). Bücklers, as early as 1938, described and depicted a large family with this phenotype. Fifty years later, Weidle published the same patients and subdivided granular dystrophy according to subtle clinical differences. In 1988, Folberg et al described the histopathology of both amyloid and keratohyalin deposits in such patients. In 1992, the clinical findings of these patients were published and termed Avellino corneal dystrophy (from the district of Italy where the initially published pedigree originated). The term, Avellino, came into popular usage but is now considered obsolete because of the dystrophy's global occurrence. Others have used the term combined granular-lattice dystrophy, but although amyloid is deposited in both GCD2 and LCDs, the lines in GCD2 have a different appearance and rarely crisscross in a lattice configuration while the lines in LCDs crisscross in a lattice configuration.

Inheritance

Autosomal dominant.

Genetic Locus

5q31.

Gene

Transforming growth factor beta–induced—*TGFBI*.

Onset

Homozygous patients have an earlier onset with dystrophy diagnosed as early as age 18 months, compared with heterozygotes, who may be diagnosed as early as age 8 years. Most GCD2 is diagnosed during adolescence or early adulthood.

Signs

In heterozygotes, initial signs are subtle, superficial, stromal tiny whitish dots (Fig. 13A) which typically develop small spokes or thorns. Some may be arranged linearly like a string of pearls. Later, all eyes show superficial whitish round patches that have moth-eaten centers to the extent of even appearing to be discoid or ring-shaped. Most patients also develop spiky anterior to midstromal deposits (Fig. 13B) that are star, icicle, or spider-shaped (i) and partially translucent in retroillumination (ii). Patients may also have entirely translucent, short, dash-like linear or dot-like deposits in the posterior stroma deep to the branching stromal opacities.

The short lines or dashes sometimes observed in GCD2 do not resemble the lattice lines of LCD (classic). The lines or dashes in GCD2 are thicker and whiter, less commonly cross each other, and may have attached bulbs or spikes. In comparison, the thinner lattice lines in LCD classic may be more refractile and characteristically intersect, resulting in the pathognomonic lattice configuration (defined as an "open framework consisting of a crisscrossed pattern of strips"). In the previously named LCDIIIA (LCD variant), lattice lines may be thicker and less refractile with less intersections (see Table 2 and Introduction for a more detailed description).

Ultimately, more superficial translucent flattened breadcrumb opacities coalesce in the sub-Bowman anterior stroma (Fig. 13C).

Phenotypic expressivity varies considerably, with some patients manifesting only a few white dots and others demonstrating deposits throughout the stroma. Patients with GCD2 with heterozygous mutations have fewer stromal opacities than those with GCD1. Homozygous patients initially demonstrate numerous small dots in the superficial cornea in early childhood. By adulthood, these progress to larger, very dense, irregularly shaped opacities that may become deeper with time (Fig. 13D).

Symptoms

Vision decreases with age as the central cornea becomes more affected. Pain accompanies epithelial erosions. In comparison with GCD1, there are fewer erosive episodes, less corneal opacification, and consequently less resultant decrease in vision, provided that the corneal haze which occurs late in the disease does not involve the central cornea.

Course

Slowly progressive.

Homozygotes demonstrate more rapid progression.

Light Microscopy

Corneal opacities extend from the basal epithelium to the deep stroma. There is deposition of both keratohyalin and amyloid; therefore, individual opacities stain with Masson trichrome and/or Congo red (Fig. 13E). Homozygotes demonstrate more severe findings.

Transmission Electron Microscopy

Anterior stromal rod-shaped, very electron-dense deposits are similar to those noted in GCD1. On higher magnification, each rod-shaped deposit is composed of extracellular masses of fine, electron-dense, highly aligned fibrils. Enlarged keratocytes of heterozygous corneal tissue demonstrate intracellular organelles while details of the intracellular organelles are barely discernible in normal cell cytoplasm. In heterozygous tissue, keratocytes contain many dilated or degenerative mitochondria and vesicles containing amorphous material. An extremely common ultrastructural finding is the presence of randomly aligned fibrils of amyloid (see LCDs template). Homozygotes demonstrate more severe findings.

Confocal Microscopy

Reflective, breadcrumb-like round deposits with well-delineated borders or highly reflective, irregular trapezoidal deposits are present in the anterior stroma (similar to GCD1). Linear and branching deposits with changing reflectivity (Fig. 13F) are observed (reminiscent of lattice lines in LCDs).

Optical Coherence Tomography

Multiple irregular hyperreflective deposits located in the Bowman layer and the anterior stroma (Fig. 13G). Descemet membrane and the endothelium are preserved.

Category

1.

Note: Patients with GCD2 have a R124H *TGFBI* mutation. Injury to the central cornea results in exacerbation of this corneal dystrophy with accelerated opacification. Hence, laser in situ keratomileusis (LASIK), photorefractive keratectomy (PRK), laser-assisted subepithelial keratomileusis (LASEK), and small incision lenticule extraction (SMILE) procedures are strongly contraindicated in this dystrophy.

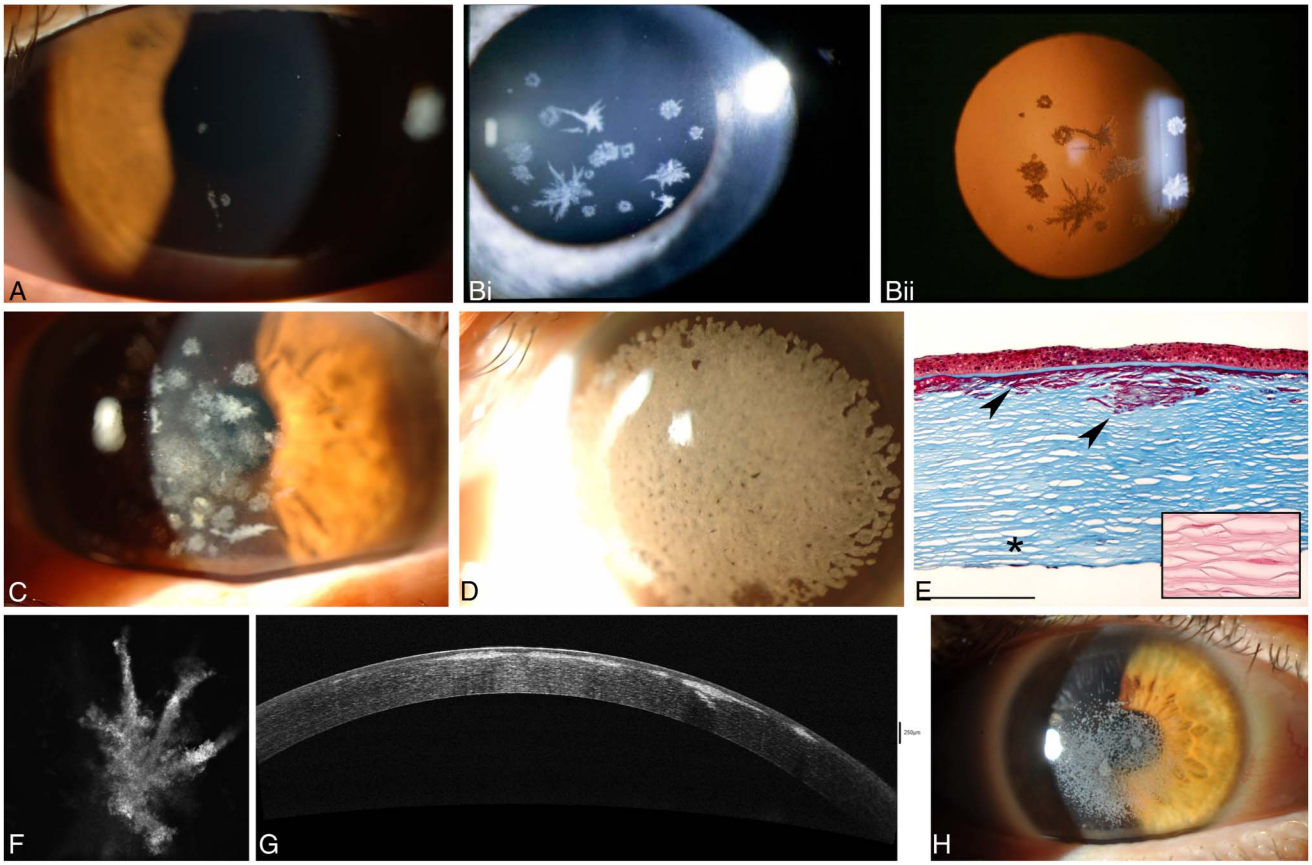

FIGURE 13. Granular corneal dystrophy, type 2 (GCD2). A, A 13-year-old with sparse white dots and genetic confirmation of GCD2. B, Direct illumination (i) and retroillumination (ii) demonstrate branching, star-shaped, spiny, and ring-like deposits. C, GCD2 with superficial, translucent flattened breadcrumb opacities beneath the Bowman layer. Denser icicles and disc-like and ring-like opacities are also present (R124H *TGFBI* mutation). D, Homozygote with denser and confluent opacities (R124H *TGFBI* mutation). E, Light microscopy: sub-Bowman and anterior stromal keratohyalin deposits (arrowheads) stain red with Masson trichrome (R124H *TGFBI* mutation). Note that the deeper stromal layers do not have keratohyalin granules (asterisk). In the deep stroma, small amyloid deposits stain with Congo red (inset) (bar = 300 μm, inset = 200 μm). F, In vivo confocal microscopy shows abnormal hyperreflective stromal deposits with a snowflake or trapezoidal shape within the corneal stroma (400 × 400 μm). G, Spectral domain OCT shows irregular hyperreflective deposits located in the Bowman layer and in the anterior stroma in a 34-year-old patient with GCD2. H, GCD2 exacerbated status post-LASIK with prominent stromal opacities. Figures 13Bi and Bii from Figure 13B in Weiss, JS, Møller HU, Lisch W, et al. The IC3D Classification of the Corneal Dystrophies. *Cornea*. 2008;27(suppl 2):S1–S42. Figures 13A, C, D, E, and F from Figures 13A, C, D, E, and F in Weiss JS, Møller HU, Aldave AJ, et al. IC3D Classification of Corneal Dystrophies—Edition 2. *Cornea*. 2015;34:117–159.

GCD2 is usually much more exacerbated after LASIK (Fig. 13H) than after LASEK or PRK.

In GCD2 patients with significant superficial opacities, excimer laser phototherapeutic keratectomy (PTK) may be judiciously used to reduce visually significant anterior stromal opacities, recognizing that repeated PTK treatments and possibly keratoplasty may be eventually required. In the exacerbated cornea after LASIK, PTK with flap removal shows better results than PTK with flap conservation in terms of visual acuity and recurrence. In homozygous GCD2, PTK results in more rapid recurrence than in heterozygous GCD2. However, when intervention is indicated, repeated PTK can be used to postpone definitive intervention by keratoplasty. PTK can also be performed for postkeratoplasty recurrences which tend to be located in the superficial stroma.

BIBLIOGRAPHY

- Banning CS, Kim WC, Randleman JB, et al. Exacerbation of Avellino corneal dystrophy after LASIK in North America. *Cornea*. 2006;25:482–484.
- Bücklers M. Die erblichen Hornhautdystrophie. *Klin Monbl Augenheilkd*. 1938;3:1–135.
- Folberg R, Alfonso E, Croxatto JO, et al. Clinically atypical granular corneal dystrophy with pathologic features of lattice-like amyloid deposits: a study of three families. *Ophthalmology*. 1988;95:46–51.
- Han KE, Choi SI, Chung WS, et al: Extremely varied phenotypes in granular corneal dystrophy type 2 heterozygotes. *Mol Vis*. 2012;18:1755–1762.

- Han KE, Chung WS, Kim T, et al. Changes of clinical manifestation of granular corneal deposits because of recurrent corneal erosion in granular corneal dystrophy types 1 and 2. *Cornea*. 2013;32:e113–e120.
- Holland EJ, Daya SM, Stone EM, et al. Avellino corneal dystrophy. Clinical manifestations and natural history. *Ophthalmology*. 1992;99:1564–1568.
- Hong JP, Kim TI, Chung JL, et al. Analysis of deposit depth and morphology in granular corneal dystrophy type 2 using Fourier domain optical coherence tomography. *Cornea*. 2011;30:729–738.
- Jones ST, Zimmerman LE. Histopathologic differentiation of granular, macular and lattice dystrophies of the cornea. *Am J Ophthalmol*. 1961;51:394–410.
- Jun I, Jung JW, Choi YJ, et al. Long-term clinical outcomes of phototherapeutic keratectomy in corneas with granular corneal dystrophy type 2 exacerbated after LASIK. *J Refract Surg*. 2018;34:132–139.
- Jun RM, Tchah H, Kim TI, et al. Avellino corneal dystrophy after LASIK. *Ophthalmology*. 2004;111:463–468.
- Kim TI, Kim T, Kim SW, et al. Comparison of corneal deposits after LASIK and PRK in eyes with granular corneal dystrophy type II. *J Refract Surg*. 2008;24:392–395.
- Kim TI. Kim H, Lee DJ, et al. Altered mitochondrial function in type 2 granular corneal dystrophy. *Am J Pathol*. 2011;179:684–692.
- Kwak JJ, Yoon SH, Seo KY, et al. Exacerbation of granular corneal dystrophy Type 2 after small incision lenticule extraction. Cornea. 2021;40:519–524.
- Lee JH, Chung SH, Stulting RD, et al. Effects of corneal neovascularization on the manifestations of Avellino corneal dystrophy (granular corneal dystrophy type II) *Cornea*. 2006;25:914–918.
- Lee JH, Stulting RD, Lee DH, et al. Exacerbation of granular corneal dystrophy type II (Avellino corneal dystrophy) after LASEK. *J Refract Surg*. 2008;24:39–45.
- Matsuo N, Fujiwara H, Ofuchi Y. Electron and light microscopic observations of a case of Groenouw's nodular corneal dystrophy. *Folia Ophthalmol Jpn*. 1967;18:436–447.
- Møller HU, Ridgway AEA. Granular corneal dystrophy Groenouw type I. A Report of a probable homozygous case. *Acta Ophthalmol (Copenh)*. 1990;68:97–101.
- Moon JW, Kim SW, Kim T, et al. Homozygous granular corneal dystrophy type II (Avellino corneal dystrophy): natural history and progression after treatment. *Cornea*. 2007;26:1095–1100.
- Munier FL, Korvatska E, Djemaï A, et al. Kerato-epithelin mutations in four 5q31-linked corneal dystrophies. *Nat Genet*. 1997;15:247–251.
- Nielsen NS, Poulsen ET, Lukassen MV, et al. Biochemical mechanisms of aggregation in TGFBI-linked corneal dystrophies. *Prog Retin Eye Res*. 2020;77:1–20.
- Roh MI, Chung SH, Stulting RD, et al. Preserved peripheral corneal clarity after surgical trauma in patients with Avellino corneal dystrophy. *Cornea*. 2006;25:497–498.
- Roh MI, Grossniklaus HE, Chung SH, et al. Avellino corneal dystrophy exacerbated after LASIK: scanning electron microscopic findings. *Cornea*. 2006;25:306–311.
- Weidle EG. Granular corneal dystrophy: two variants. In: Ferraz de Olivera LN, editor. *Ophthalmology Today*. Elsevier; Amsterdam, The Netherlands: 1988. pp. 617–619.

STROMAL DYSTROPHIES

Macular Corneal Dystrophy (MCD)

MIM #217800.

Former Alternative Names and Eponyms

Groenouw corneal dystrophy type II.
Fehr speckled dystrophy.

Inheritance

Autosomal recessive.

Genetic Locus

16q22.1.

Gene

Carbohydrate sulfotransferase 6—*CHST6*.

Onset

Childhood.

Signs

Initially, central, superficial, irregular whitish fleck-like opacities (macules) develop which give the condition its name (Fig. 14A); and unlike granular corneal dystrophy, these flecks can later involve the limbus and the deep stroma down to Descemet membrane (Fig. 14B). Simultaneously, a progressive diffuse haze develops to involve the entire corneal stroma (Fig. 14C). The larger central "macules" are located in the superficial stroma while the smaller and more discrete peripheral opacities are located in the deep stroma. The epithelium remains smooth but occasionally develops erosions.

The cornea is thinner than normal. As the disorder progresses, Descemet membrane becomes grayer and develops guttate excrescences, although frank endothelial decompensation rarely occurs.

Symptoms

Severe visual impairment occurs between age 10 and 30 years. Corneal sensitivity is reduced. Photophobia and painful recurrent erosions can rarely occur.

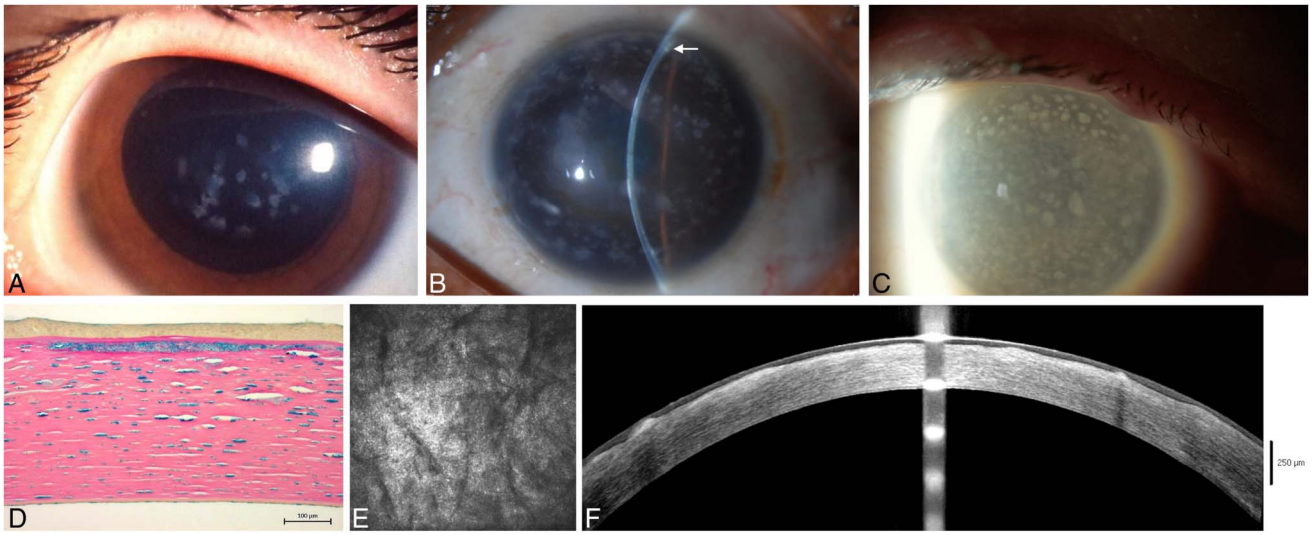

FIGURE 14. Macular corneal dystrophy (MCD). A, Early stage with few central macular opacities. B, Slit lamp photograph demonstrates anterior deposits centrally as well as extension of the deposits to the limbus (arrow) and to the deep stroma down to Descemet membrane peripherally (arrow). C, More diffuse opacities and haze involving the entire stroma in an individual with type 2 MCD (L276P *CHST6* mutation). D, Light microscopy: intracellular and extracellular accumulation of glycosaminoglycans (GAGs) at all levels of stroma and corneal endothelium. Subepithelial fibrous tissue also contains GAGs. Colloidal iron, ×20. E, In vivo confocal microscopy image (400 × 400 µm) showing hyperreflective abnormal areas within the stroma. Some dark striae can be observed within the hyperreflective material. F, Spectral domain OCT shows hyperreflective throughout the corneal stroma (at the site of the stromal deposits), associated with hyperreflective opacities in the Bowman layer and irregular stromal surface, in a 29-year-old patient with MCD. Figure 14A from Figure 14A in Weiss, JS, Møller HU, Lisch W, et al. The IC3D Classification of the Corneal Dystrophies. *Cornea*. 2008;27(suppl 2):S1-S42. Figures 14C, D, and E from Figures 14C, D, and E in Weiss JS, Møller HU, Aldave AJ, et al. IC3D Classification of Corneal Dystrophies—Edition 2. *Cornea*. 2015;34:117–159.

Course

Slowly progressive.

Light Microscopy

Breaks in Bowman layer. Glycosaminoglycans (GAGs) diffusely accumulate intracellularly and extracellularly throughout the corneal stroma. Unique to stromal dystrophies, Descemet membrane and the endothelium are primarily involved, as evidenced by Descemet thickening and corneal guttae plus endothelial staining with colloidal iron or Alcian blue (Fig. 14D).

Transmission Electron Microscopy

Keratocytes and endothelial cells stain positively for GAGs and contain vacuoles and lamellar bodies. The extracellular matrix contains focal and diffuse fibrillogranular GAGs.

Confocal Microscopy

Blurred limited accumulations of highly reflective deposits are seen in the basal epithelium and anterior stroma and midstroma (Fig. 14E). Some of these may have dark striae-like images. Normal keratocytes are not seen.

Optical Coherence Tomography

Hyperreflectivity throughout the corneal stroma corresponds to diffuse corneal clouding together with diffuse hyperreflective opacities especially in the Bowman layer (Fig. 14F). Spectral domain OCT can visualize early changes in the Bowman layer while time domain OCT reveals hyperreflective accumulations in the anterior corneal stroma and peripheral posterior cornea stroma.

Additional Findings

Although clinically indistinguishable, 3 variants of macular corneal dystrophy are distinguished based on immunoreactivity of specific sulfated epitopes of antigenic keratan sulfates (AgKS) in the cornea and the serum.

- MCD type I: no AgKS reactivity in the cornea or in the serum.
- MCD type IA: Keratocytes manifest AgKS reactivity, but the extracellular material does not. Serum lacks AgKS.
- MCD type II: All the abnormal deposits react positively with AgKS, and the serum has normal or lower levels of AgKS.

Note: Electron microscopic corneal findings in systemic mucopolysaccharidoses are similar to findings that are seen in macular dystrophy. However, on clinical examination and light microscopy, cornea demonstrates more diffuse and

earlier opacification without flecks in mucopolysaccharidoses that show corneal involvement (especially Hurler, Hurler-Scheie, and Maroteaux–Lamy types). The decisive phenotypic difference between MCD and the mucopolysaccharidoses are the flecks/macules, which appear in MCD.

Category

1.

BIBLIOGRAPHY

- Aggarwal S, Peck T, Golen J, et al. Macular corneal dystrophy: A review. *Surv Ophthalmol*. 2018;63:609–617.
- Akama TO, Nishida K, Nakayama J, et al. Macular corneal dystrophy type I and type II are caused by distinct mutations in a new sulphotransferase gene. *Nat Genet*. 2000;26:237–241.
- Fehr O. Über familiäre, fleckige Hornhautentartung. *Zentralbl Prakt Augenheilkd*. 1904;28:1–11.
- Groenouw A. Knötchenförmige Hornhauttrübungen (Noduli corneae). *Arch Augenheilk*. 1890;21:237–241.
- Klintworth GK, Vogel FS. Macular corneal dystrophy: an inherited acid mucopolysaccharide storage disease of the corneal fibroblast. *Am J Pathol*. 1964;45:565–586.
- Klintworth GK. Research into the pathogenesis of macular corneal dystrophy. *Trans Ophthalmol Soc U K*. 1980;100:186–194.
- Klintworth GK, Smith CF, Bowling BL. CHST6 mutations in North American subjects with macular corneal dystrophy: a comprehensive molecular genetic review. *Mol Vis*. 2006;12:159–176.
- Micali A, Pisani A, Puzzolo D, et al, et al. Macular corneal dystrophy: in vivo confocal and structural data. *Ophthalmology*. 2014;121:1164–73.
- Nowinska AK, Wylegala E, Teper S, et al. Phenotype and genotype analysis in patients with macular corneal dystrophy. *Br J Ophthalmol*. 2014;98:1514–1521.
- Nowińska A, Chlasta-Twardzik E, Dembski M, et al. Detailed corneal and genetic characteristics of a pediatric patient with macular corneal dystrophy: case report. *BMC Ophthalmol*. 2021;21:285.
- Singh S, Das S, Kannabiran C, et al. Macular corneal dystrophy: An updated review. *Curr Eye Res*. 2021;46:765–770.
- Snip RC, Kenyon KR, Green WR. Macular Corneal dystrophy: Ultrastructural pathology of corneal endothelium and Descemet's membrane. *Invest Ophthalmol*. 1973;12:88–97.
- Vance JM, Jonasson F, Lennon F, et al. Linkage of a gene for macular corneal dystrophy to chromosome 16. *Am J Hum Genet*. 1996;58:757–762.

Schnyder Corneal Dystrophy (SCD)

MIM #121800.

Former Alternative Names and Eponyms

Schnyder crystalline corneal dystrophy (SCCD).
Schnyder crystalline dystrophy sine crystals.
Hereditary crystalline stromal dystrophy of Schnyder.
Crystalline stromal dystrophy.
Central stromal crystalline corneal dystrophy.
Corneal crystalline dystrophy of Schnyder.
Schnyder corneal crystalline dystrophy.

Genetic Locus

1p36.

Gene

UbiA prenyltransferase domain-containing protein 1—*UBIAD1*.

Inheritance

Autosomal dominant.

Onset

May be as early as childhood, but diagnosis is usually made by the second or third decade. Diagnosis may be further delayed in patients who have the acrystalline form of the disease.

Signs

Corneal changes are predictable on the basis of age. Patients aged 23 years or younger have ring-like or disc-like central corneal opacity (Fig. 15A) and/or central crowded comma-shaped subepithelial crystals (Fig. 15B). Between age 23 and 38 years, arcus lipoides is also noted (Fig. 15C). After age 38 years, midperipheral panstromal haze also develops, causing the entire cornea to appear hazy (Figs. 15D-F). Despite the now obsolete, former name, Schnyder crystalline corneal dystrophy, only 50% of patients demonstrate corneal crystals. Crystals may be unilateral, may rarely regress, and can occur late in the disease.

Symptoms

Visual acuity decreases and complaints of glare increase with age. Although scotopic vision may be remarkably good (considering the slit lamp appearance), photopic vision may be disproportionately decreased. Corneal sensation decreases with age. Both affected and unaffected members of the pedigrees may have hyperlipoproteinemia (type IIa, Ill, or IV).

Course

Although slowly progressive, most patients older than 50 years have severe reduction of photopic vision.

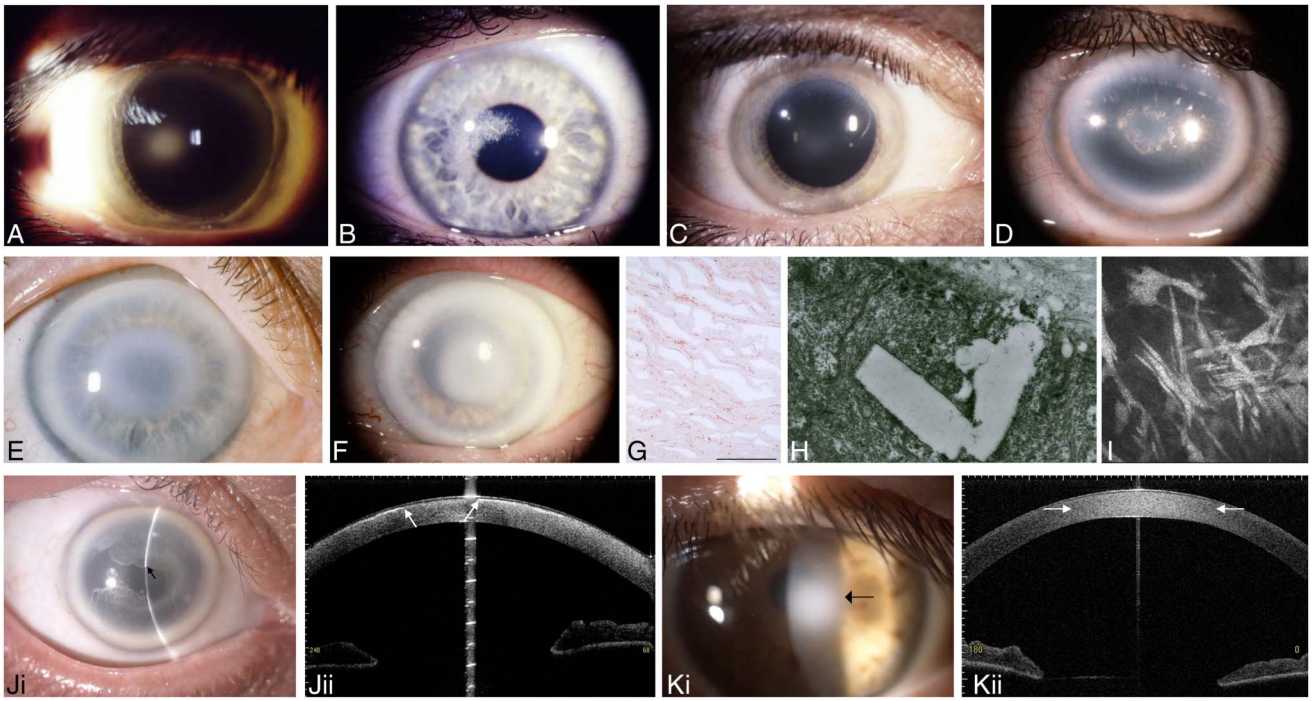

FIGURE 15. Schnyder corneal dystrophy (SCD). A, Central stromal opacity in early SCD without crystals (*UBIAD1* mutation). B, Early subepithelial central crystalline deposit (*UBIAD1* mutation). C, Central corneal opacity with arcus lipoides. D, Central corneal opacity, subepithelial crystalline ring, midperipheral haze, and arcus lipoides. E, Noncrystalline central diffuse opacity pattern with clearer area centrally, midperipheral haze, and prominent arcus lipoides in 39-year-old patient (*UBIAD1* mutation). F, Non-crystalline disc-like central opacity, midperipheral haze, and prominent arcus lipoides in a 72-year-old patient with SCD with *UBIAD1* mutation. G, Light microscopy: Oil Red O stains innumerable tiny lipid droplets within the corneal stroma in a frozen section that has not undergone processing for paraffin embedding, which would dissolve the lipids and make the staining negative, bar = 100 μm. H, Electron microscopy: empty crystalline space within a basal cell representing cholesterol deposit dissolved during dehydration stage of embedding process (×10,000) (SCD with crystals). I, In vivo confocal microscopy (400 × 400 μm) shows abnormal hyperreflective homogeneous spindle-shaped deposits within the subepithelial zone (SCD with crystals). J, Right cornea of a 66-year-old patient with SCD (i) with nonconfluent subepithelial crystals (arrow) sparing the visual axis. OCT (ii) demonstrates corresponding areas of subepithelial lucency (arrows) representing subepithelial cholesterol crystalline deposits. K, Left cornea of a 57-year-old patient with SCD (i) with panstromal opacification (arrow) and no crystals with corresponding OCT (ii) showing panstromal hyperlucency representing panstromal lipid deposits (flanked by arrows). Figures 15B and C from Figures 15B and A in Weiss, JS, Møller HU, Lisch W, et al. The IC3D Classification of the Corneal Dystrophies. *Cornea*. 2008; 27(suppl 2):S1–S42. Figures 15A, D, E, F, G, H, and I from Figures 15A, D, E, F, G, H, and I in Weiss, JS, Møller HU, Aldave AJ, et al. The IC3D Classification of the Corneal Dystrophies—Edition 2. *Cornea*. 2015 34:117–159.

Light Microscopy

Abnormal deposition of intracellular and extracellular esterified and unesterified phospholipids and cholesterol in basal epithelial cells, Bowman layer, and stroma. Because organic solvents and resins (such as alcohol) can dissolve lipids, staining for lipids [such as Oil Red O (Fig. 15G) or Sudan black] is facilitated by submitting fresh tissue for pathology and ensuring appropriate fixation for special stains. In addition, there is a published report of SCD corneas with positive Congo red staining, suggesting secondary amyloid deposition and another reporting Alcian blue staining, suggesting secondary deposition of glycosaminoglycans.

Transmission Electron Microscopy

Abnormal accumulations of intracellular and extracellular esterified and unesterified phospholipids and cholesterol are deposited in the epithelium (Fig. 15H), the Bowman layer, and throughout the stroma. Endothelial lipid has rarely been reported.

Confocal Microscopy

Confocal microscopy shows abnormal hyperreflective homogeneous spindle-shaped deposits within the subepithelial zone if subepithelial crystals are present. Intracellular and extracellular highly reflective deposits may lead to eventual disruption of the basal epithelial/subepithelial nerve plexus (Fig. 15I).

Optical Coherence Tomography

Spectral domain OCT can demonstrate subepithelial hyperreflectivity if subepithelial crystals are present

(Fig. 15J). Diffuse hyperreflectivity of the anterior, mid and posterior stroma also can be noted indicating the diffuse panstromal opacification associated with lipid deposition (Fig. 15K). However, in the presence of subepithelial hyperreflectivity, it may not be possible to assess either the presence or the amount of underlying panstromal hyperreflectivity.

Category

1.

Note: Although Schnyder crystalline corneal dystrophy has been the more commonly used name for this entity in the past, this has caused diagnostic confusion because only 50% of the patients exhibit corneal crystals. Consequently, Schnyder corneal dystrophy is the preferred name. If the ophthalmologist does not suspect SCD when performing keratoplasty, the opportunity to perform lipid stains may be lost if the corneal specimen is not preserved correctly (as specified above).

BIBLIOGRAPHY

- Delleman JW, Winkelman JE. Degeneratio corneae cristallinea hereditaria. A clinical, genetical and histological study. *Ophthalmologica*. 1968;155:409–426.
- Eiferman RA, Rodrigues MM, Laibson PR, et al. Schnyder's crystalline dystrophy associated with amyloid deposition. *Metab Ophthalmol*. 1979;3:15.
- Evans CJ, Dudakova L, Skalicka P, et al. Schnyder corneal dystrophy and associated phenotypes caused by novel and recurrent mutations in the UBIAD1 gene. *BMC Ophthalmol*. 2018:18:250
- Gaynor PM, Zhang WY, Weiss JS, et al. Accumulation of HDL apolipoproteins accompanies abnormal cholesterol accumulation in Schnyder's corneal dystrophy. *Arterioscler Thromb Vase Biol*. 1996;16:993–999.
- Ghazal W, Georgeon C, Grieve K, et al. Multimodal imaging features of Schnyder corneal dystrophy. *J Ophthalmol*. 2020:2020:1–12.
- Lisch W, Weidle EG, Lisch C, et al. Schnyder's dystrophy. Progression and metabolism. *Ophthalmic Paediatr Genet*. 1986;7:45–56.
- Orr A, Sube MP, Marcadier, et al. Mutations in the *UBIAD1* gene encoding a potential prenyltransferase are causal for Schnyder crystalline corneal dystrophy. *PLoS One*. 2007:2:e685.
- Pameijer JK. Über eine fremdartige familiäre oberflächliche Hornhautveränderung. *Klin Monbl Augenheilkd*. 1935;95:516–517.
- Schnyder WF. Mitteilung über einen neuen Typus von familiärer Hornhauterkrankung. *Schweiz Med Wschr*. 1929;10:559–571.
- Schnyder WF. Scheibenförmige Kristalleinlagerungen in der Hornhautmitte als Erbleiden. *KIin Monbl Augenheilkd*. 1939;103:494–502.
- van Went JM, Wibaut F. En zeldzame erfelijke hoornvliessandoening. *Niederl Tijdschr Geneesk*. 1924;68:2996–2997.
- Vesaluoma MH, Linna TU, Sankila EM, et al. In vivo confocal microscopy of a family with Schnyder crystalline corneal dystrophy. *Ophthalmology*. 1999;106:944–951.
- Weiss JS. Schnyder's dystrophy of the cornea. A Swede-Finn connection. *Cornea*. 1992;11:93–101.
- Weiss JS, Rodrigues MM, Kruth HS, et al. Panstromal Schnyder's corneal dystrophy. Ultrastructural and histochemical studies. *Ophthalmology*.1992;99:1072–1081.
- Weiss JS. Schnyder crystalline dystrophy sine crystals. Recommendation for a revision of nomenclature. *Ophthalmology*. 1996;103:465–473.
- Weiss JS. Visual morbidity in thirty-four families with Schnyder's corneal dystrophy. *Trans Am Soc Ophthamol*. 2007;105:1–33.
- Weiss JS, Kruth HS, Kuivaniemi H, et al. Mutations in the *UBIAD1* gene on chromosome short arm 1, region 36 cause Schnyder crystalline corneal dystrophy. *Invest Ophthalmol Vis Sci*. 2007;48:5007–5012.
- Weiss JS, Khemichian AJ. Differential diagnosis of Schnyder corneal dystrophy. *Dev Ophthalmol*. 2011;48:67–96.

Congenital Stromal Corneal Dystrophy (CSCD)

MIM #610048.

Former Alternative Names and Eponyms

Congenital hereditary stromal dystrophy.

Inheritance

Autosomal dominant.

Genetic Locus

12q21.33.

Gene

Decorin—*DCN*.

Onset

Congenital.

Signs

Diffuse, bilateral, corneal clouding with flake-like, whitish stromal opacities throughout the stroma (Fig. 16A). The changes are equally pronounced in all areas of the cornea. The corneal surface is normal and without fluorescein staining or vascularization. Pachymetry demonstrates increased stromal thickness.

Symptoms

Moderate-to-severe visual loss. Photophobia occurs in a minority of patients.

Course

Nonprogressive or slowly progressive.

Light Microscopy

The stromal lamellae are irregularly separated and may contain amorphous material (Fig. 16B).

Transmission Electron Microscopy

Amorphous areas consisting of thin filaments randomly arranged in an electron-lucent ground substance separated by lamellae of normal appearance (Fig. 16C). The changes can be seen at all levels of the stroma. The abnormal layers are broader in the posterior stroma. The keratocytes and endothelium are normal, although absence of the anterior banded zone of Descemet membrane has been reported. Immunoelectron microscopy identifies accumulation of decorin, in the amorphous areas.

Optical Coherence Tomography

Increased corneal thickness. Diffuse higher reflectivity in the stroma.

Confocal Microscopy

Epithelial cells appear normal. Increased reflectivity from the anterior stroma prevents further studies.

Category

1.

Note: While CSCD is typically associated with truncating mutations in *DCN*, a missense mutation in the same gene has been reported in a mother and son who presented with later-onset and milder corneal changes.

BIBLIOGRAPHY

- Bredrup C, Knappskog PM, Majewski J, et al. Congenital stromal dystrophy of the cornea caused by a mutation in the decorin gene. *Invest Ophthalmol Vis Sci*. 2005;46:420–426.
- Bredrup C, Stang E, Bruland O, et al. Decorin accumulation contributes to the stromal opacities found in congenital stromal corneal dystrophy. *Invest Ophthalmol Vis Sci*. 2010;51:5578–5582.
- Desvignes P, Vigo. A propos d'un cas de dystrophie cornéenne parenchymateuse familiale à hérédité dominante. *Bull Soc Ophtalmol Fr*. 1955;4:220–225.
- Jing Y, Kumar RP, Zhu L, et al. Novel decorin mutation in a Chinese family with congenital stromal corneal dystrophy. *Cornea*. 2014;33:288–293.
- Kim JH, Ko JM, Lee I, et al. A novel mutation of the decorin gene identified in a Korean family with congenital hereditary stromal dystrophy. *Cornea*. 2011;30:1473–1477.
- Lee JH, Ki CS, Chung ES, et al. A novel decorin gene mutation in congenital hereditary stromal dystrophy: a Korean family. *Korean J Ophthalmol*. 2012;26:301–305.
- Odland M. Dystrophia corneae parenchymatosa congenita. A clinical, morphological and histochemical examination. *Acta Ophthalmol (Copenh)*. 1968;46:477–485.
- Pouliquen Y, Lacombe E, Schreinzer C, et al. La dystrophie congénitale héréditaire du stroma cornéen de Turpin. *J Fr Ophtalmol*. 1979;2:115–125.
- Turpin R, Tisserand M, Sérane J. Opacités cornéennes héréditaires et congénitales réparties sur trois générations et atteignant deux jumelles monozygotes. *Arch Ophtalmol*.1939;3:109–111.
- Van Ginderdeuren R, De Vos R, Casteels I, et al. Report of a new family with dominant congenital hereditary stromal dystrophy of the cornea. *Cornea*. 2002;21:118–120.

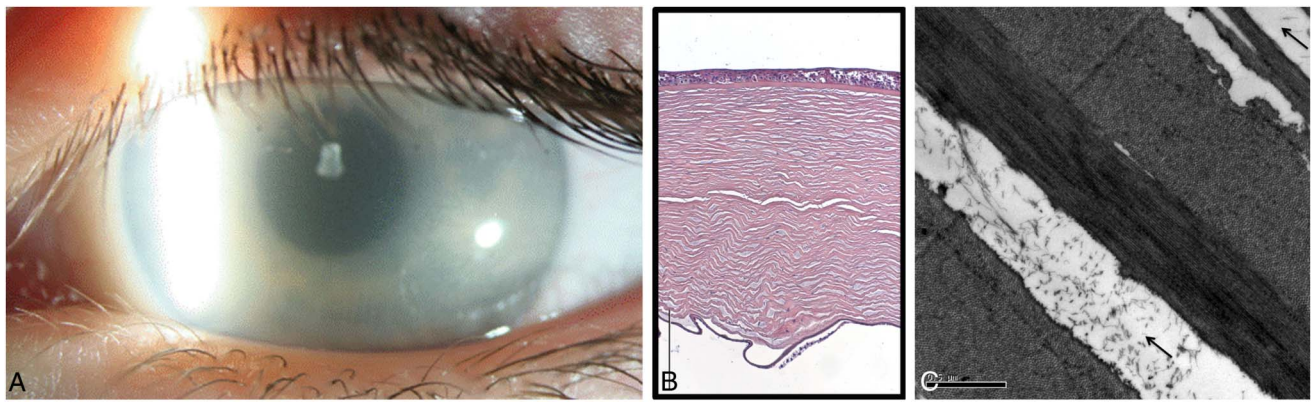

FIGURE 16. Congenital stromal corneal dystrophy (CSCD). A, Diffuse clouding with flake-like opacities throughout the stroma in a 4-year-old patient (c.967delT *DCN* frameshift mutation). B, Light microscopy: The cornea is markedly thickened with stromal lamellae that are separated from each other in a regular manner with some areas of deposition, bar = 200 μm. C, Electron microscopy: Apparently normal collagen lamellae are separated by areas of amorphous substance with small filaments (arrows) characteristic for the condition (original magnification ×20). Figures 16A, B, and C from Figures 16A, B, and C in Weiss, JS, Møller HU, Aldave AJ, et al. The IC3D Classification of the Corneal Dystrophies—Edition 2. *Cornea.* 2015 34:117–159.

• Witschel H, Fine BS, Grützner P, et al. Congenital hereditary stromal dystrophy of the cornea. *Arch Ophthalmol*. 1978;96:1043–1051.

Fleck Corneal Dystrophy (FCD)

MIM #121850.

Former Alternative Names and Eponyms

François-Neetens speckled (mouchetée) corneal dystrophy.

Inheritance

Autosomal dominant.

Genetic Locus

2q34.

Gene

Phosphoinositide kinase, FYVE finger—*PIKFYVE*. Typically, frameshift mutation and copy number variation.

Previously known as phosphatidylinositol-3-phosphate/phosphatidylinositol 5-kinase type III—*PIP5K3*.

Onset

Congenital or first years of life.

Signs

Subtle but distinctive, small, discoid opacities or discrete, flat, gray–white, dandruff-like, and sometimes ring-shaped opacities scattered sparsely throughout any level of the otherwise clear stroma (Figs. 17A, B). Flecks may extend to the limbus and are best detected with broad oblique slit-beam illumination or retroillumination. The epithelium, the Bowman layer, Descemet membrane, and the endothelium are not involved. Asymmetric or unilateral corneal involvement is possible.

Symptoms

Asymptomatic, occasionally slight photophobia or decreased corneal sensitivity.

Course

Nonprogressive.

Light Microscopy

Swollen, vacuolated keratocytes, which contain glycosaminoglycans (GAGs) (staining with Alcian blue and colloidal iron) and complex lipids (demonstrated by Sudan black and Oil red O).

Transmission Electron Microscopy

Some keratocytes show membrane-based inclusions with delicate granular material.

Confocal Microscopy

Accumulation of hyperreflective 2 to 18 μm dot-like material in normal-sized and enlarged stromal keratocyte nuclei. Inclusions in basal nerves and donut-shaped or kidney-shaped 70 × 110 μm deposits have variably been reported.

Optical Coherence Tomography

Flecks correspond to slightly brighter small areas.

Category

1.

BIBLIOGRAPHY

• Assi A, Ebenezer N, Ficker L. Corneal fleck dystrophy in an English family. *Br J Ophthalmol*. 1999;83:1407–1408.
• Can E, Kan E, Akgün Hİ. Clinical features and in vivo confocal microscopic imaging of fleck corneal dystrophy. *Semin Ophthalmol*. 2013;28:239–241.
• François J, Neetens A. Nouvelle dystrophie hérédofamiliale du parenchyme cornéen (hérédo-dystrophie mouchetée). *Bull Soc Belge Ophtal*. 1957;114:641–646.
• Gee J, Frausto R, Chung D-W, et al. Identification of novel PIKFYVE gene mutations associated with Fleck corneal dystrophy. *Mol Vis*. 2015;21:1093–1100.
• Gillespie F, Covelli B. Fleck (mouchetée) dystrophy of the cornea. Report of a family. *South Med J*. 1963;56:1265–1267.
• Holopainen JM, Moilanen JA, Tervo TM. In vivo confocal microscopy of fleck dystrophy and pre-Descemet membrane corneal dystrophy. *Cornea*. 2003;22:160–163.
• Jiao X, Munier FL, Schorderet DF, et al. Genetic linkage of François-Neetens fleck (mouchetée) corneal dystrophy to chromosome 2q35. *Hum Genet*. 2003;112:593–599.
• Kawasaki S, Yamasaki K, Nakagawa H, et al. A novel mutation (p.Glu1389AspfsX16) of the phosphoinositide kinase, FYVE finger containing gene found in a Japanese patient with fleck corneal dystrophy. *Mol Vis*. 2012;18:2954–2960.
• Li S, Tiab L, Jiao X, et al. Mutations in PIP5K3 are associated with François-Neetens mouchetée fleck corneal dystrophy. *Am J Hum Genet*. 2005;77:54–63.
• Nicholson DH, Green WR, Cross HE, et al. A clinical and histopathological study of François-Neetens speckled corneal dystrophy. *Am J Ophthalmol*. 1977;83:554–560.
• Patten JT, Hyndiuk RA, Donaldson DD, et al. Fleck (mouchetée) dystrophy of the cornea. *Ann Ophthalmol*. 1976;8:25–32.
• Purcell JJ Jr, Krachmer JH, Weingeist TA. Fleck corneal dystrophy. *Arch Ophthalmol*. 1977;95:440–444.

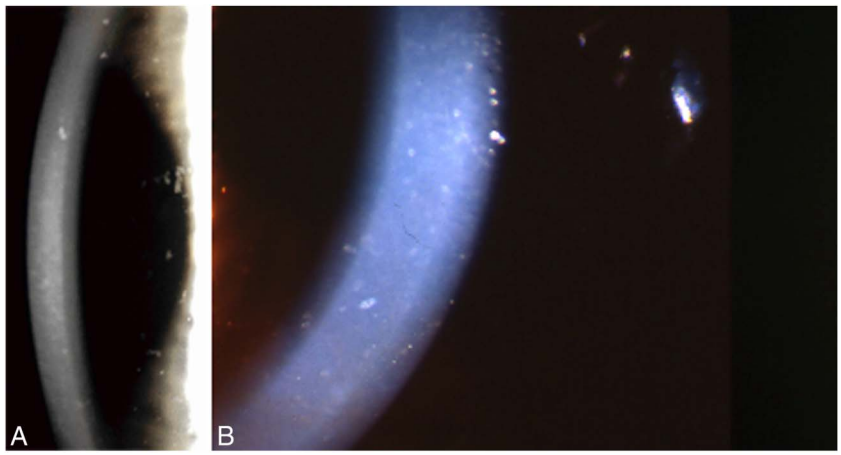

FIGURE 17. Fleck corneal dystrophy (FCD). In 2 different patients, dandruff-like opacities are visualized throughout the stroma using (A), broad oblique illumination and indirect illumination and (B), at varying depths in the slit lamp photograph. Figures 17A and B from Figures 17A and B in Weiss, JS, Møller HU, Lisch W, et al. The IC3D Classification of the Corneal Dystrophies. *Cornea*. 2008;27(suppl 2):S1–S42.

Posterior Amorphous Corneal Dystrophy (PACD)

MIM #612868.

Former Alternative Names and Eponyms

Posterior amorphous stromal dystrophy.

Inheritance

Autosomal dominant.

Genetic Locus

12q21.33.

Gene

Deletion of keratocan—*KERA*, lumican—*LUM*, decorin—*DCN*, and epiphycan—*EPYC*.

Onset

Often diagnosed in the first decade of life and has been noted as early as 16 weeks, suggesting a congenital origin.

Signs

Diffuse gray-white, sheet-like opacities that can involve any layer of the stroma but are most prominent posteriorly (Fig. 18A). The lesions can be centroperipheral, extending to the limbus, or peripheral, the latter with less pronounced findings and symptoms. Transparent stromal breaks often exist within the opacification. Less-than-average corneal thickness (as thin as 380 μm) (Fig. 18B) and corneal flattening to less than 41 diopters with associated hyperopia are characteristic, particularly in the centroperipheral form. Descemet membrane and the endothelium may be indented by the opacities, and focal endothelial abnormalities have been observed. Prominent Schwalbe line, fine iris processes, pupillary remnants, iridocorneal adhesions, corectopia, pseudopolycoria, and anterior stromal tags have been reported, particularly in patients with the centroperipheral pattern, but there is no association with glaucoma. It remains possible that the extent of the deletion, which varies, may modify the clinical findings.

Symptoms

Visual acuity is mildly reduced and usually better than 20/40.

Course

No or slow progression.

Light Microscopy

Irregularity of the posterior stromal lamellae with colloidal iron staining, anterior to a thin Descemet membrane, and focal attenuation of endothelial cells (Fig. 18C).

Transmission Electron Microscopy

Abnormally oriented collagen fibers and abnormal keratocytes with disorganization of the posterior stromal lamellae. A fibrillar layer resembling stromal collagen fibers interrupts Descemet membrane. These findings are not pathognomonic. In 1 patient with more pronounced changes, additional subepithelial deposits and a thick collagenous layer posterior to Descemet membrane were present.

Confocal Microscopy

Normal anterior and middle stroma. Microfolds and diffuse hyperreflective sheet-like opacities with spikes extend from the posterior stroma to immediately adjacent to the endothelium. Pinpoint reflective deposits that appear to be primarily extracellular, some reaching the endothelium. Keratocytes with an enlarged nucleus anterior to Descemet membrane.

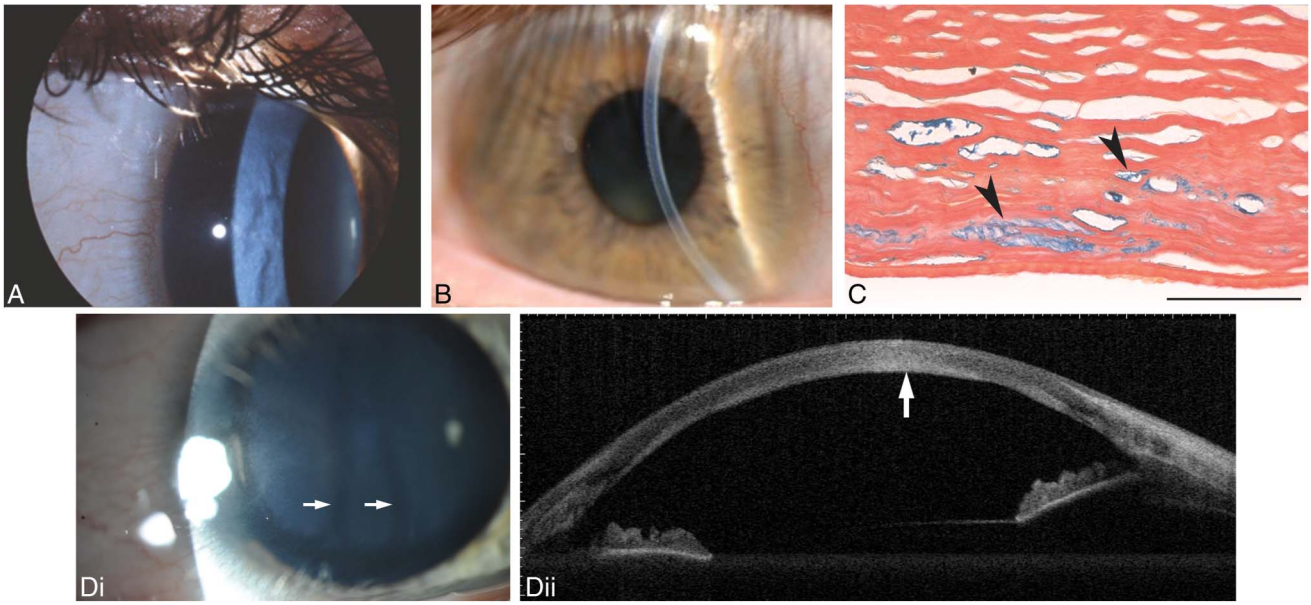

FIGURE 18. Posterior amorphous corneal dystrophy (PACD). A, Central deep stromal/pre-Descemet opacity with some degree of peripheral extension interrupted by a few clear bands in the midperipheral cornea. B, Slit beam demonstrates decreased corneal thickness and posterior stromal lamellar opacification. C, Light microscopy: colloidal iron-positive material (arrowheads) accumulates extracellularly in the posterior stroma, bar = 100 μm. D, (i), Central deep stromal/pre-Descemet opacity interrupted with 2 clearer bands (arrows) and a clear ring in the more peripheral cornea (a 3.0 Mb deletion including 12q12.32-q21.33). (ii) Spectral domain OCT in this patient reveals a continuous hyperreflective band in the posterior stroma anterior to the endothelium (arrow). Figures 18A, B, and C from Figures 18A, B, and C in Weiss JS, Møller HU, Aldave AJ, et al. IC3D Classification of Corneal Dystrophies—Edition 2. *Cornea*. 2015;34:117–159.

Optical Coherence Tomography

A continuous hyperreflective line exists in the posterior stroma next to Descemet membrane without skip areas (Figs. 18Di and Dii).

Category

1.

Note: The likely congenital onset, lack of progression, and association with iris abnormalities of this contiguous gene deletion disorder leading to haploinsufficiency of 1 or more of the deleted genes raises the possibility of mesodermal dysgenesis rather than a progressive corneal dystrophy. Sporadic cases from *de novo* deletions have been reported, in which case, family history will be negative (see Introduction for discussion of sporadic dystrophies and *de novo* mutations).

BIBLIOGRAPHY

- Aldave AJ, Rosenwasser GO, Yellore VS, et al. Linkage of posterior amorphous corneal dystrophy to chromosome 12q21.33 and exclusion coding region mutations in KERA, LUM, DCN and EPYC. *Invest Ophthalmol Vis Sci*. 2010;51:4006–4102.
- Basbus FJ, Cremona FA, Lucero Saá F, et al. Posterior amorphous corneal dystrophy: new chromosomal breakpoints in the small leucine-rich proteoglycan-coding region. *Cornea*. 2022;41:491–495.
- Carpel EF, Sigelman RJ, Doughman DJ. Posterior amorphous corneal dystrophy. *Am J Ophthalmol*. 1977;83:629–632.
- Cervantes AE, Gee KM, Whiting MF, et al. Confirmation and refinement of the heterozygous deletion of the small leucine-rich proteoglycans associated with posterior amorphous corneal dystrophy. *Ophthalmic Genet*. 2018;39:419–424.
- Dunn SP, Krachmer JH, Ching SS. New findings in posterior amorphous corneal dystrophy. *Arch Ophthalmol*. 1984;102:236–239.
- Erdem U, Muftuoglu O, Hurmeric V. In vivo confocal microscopy findings in a patient with posterior amorphous corneal dystrophy. *Clin Exp Ophthalmol*. 2007;35:99–102.
- Johnson AT, Folberg R, Vrabec MP, et al. The pathology of posterior amorphous corneal dystrophy. *Ophthalmology*. 1990;97:104–109.
- Kim M, Frausto RF, Rosenwasser GOD, et al. Posterior amorphous corneal dystrophy is associated with a deletion of small leucine-rich proteoglycans on chromosome 12. *PLoS One*. 2014 Apr 23; 9:e95037.
- Lenk J, Porrmann J, Smitka M, et al. Posterior amorphous corneal dystrophy in a patient with 12q21.33 deletion. *Ophthalmic Genet*. 2018;39:645–647.
- Moshegov CN, Hoe WK, Wiffen SJ, et al. Posterior amorphous corneal dystrophy. A new pedigree with phenotypic variation. *Ophthalmology*. 1996;103:474–478.

• Odent S, Casteels I, Cassiman C, et al. Posterior amorphous corneal dystrophy caused by a de novo deletion. *Ophthalmic Genet*. 2017;38:167–170.

Central Cloudy Dystrophy of François (CCDF)

MIM #217600.

Former Alternative Names and Eponyms

None.

Inheritance

Most likely degenerative. May be phenotypically indistinguishable from posterior crocodile shagreen, which is a corneal degeneration. Autosomal dominant inheritance has been occasionally reported but is difficult to substantiate.

Genetic Locus

None.

Gene

None.

Onset

First decade (youngest affected patient was aged 8 years).

Signs

Fortuitous finding of cloudy central polygonal or rounded stromal opacities that fade anteriorly and peripherally and are surrounded by clear tissue (Fig. 19). The changes are indistinguishable from Vogt posterior crocodile shagreen.

Symptoms

Mostly asymptomatic.

Course

Nonprogressive.

Light Microscopy

No description in familial cases. Faint undulating appearance of the deep stroma and positive staining for GAGs.

Transmission Electron Microscopy

No description in familial cases; therefore, published pathology may represent posterior crocodile shagreen. Extracellular vacuoles, some containing fibrillogranular material and electron-dense deposits. Endothelial vacuoles with fibrillogranular material and a sawtooth lamellar pattern have also been reported.

Confocal Microscopy

No description in familial cases; therefore, published confocal microscopy may represent posterior crocodile shagreen. In 2 unrelated patients, small highly refractile granules and deposits in the anterior stroma were reported. Multiple dark striae in the extracellular matrix with increased intensity in the deep posterior stroma adjacent to the endothelium.

Category

4.

Note: Many of the publications referenced did not provide documentation that the corneal disease was familial. Consequently, it is entirely possible that these cases reported as CCDF might be posterior crocodile shagreen.

BIBLIOGRAPHY

• Bramsen T, Ehlers N, Baggesen LH. Central cloudy comeal dystrophy of François. *Acta Ophthalmol (Copenh)*. 1976;54:221–226.
• François J. Une nouvelle dystrophie hérédo-familiale de la comée. *J Genet Hum*. 1956;5:189–196.

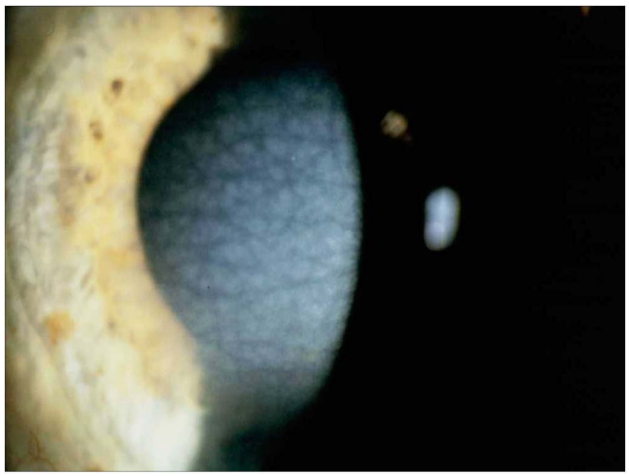

FIGURE 19. Central cloudy dystrophy of François (CCDF) or posterior crocodile shagreen. No information about family history available. Axially distributed, polygonal gray–white stromal opacities separated by linear areas of clear cornea. Figure 19 from Figure 19A in Weiss, JS, Møller HU, Lisch W, et al. The IC3D Classification of the Corneal Dystrophies. *Cornea*. 2008;27(suppl 2):S1–S42.

- Kobayashi A, Sugiyama K, Huang AJ. In vivo confocal microscopy in patients with central cloudy dystrophy of François. *Arch Ophthalmol*. 2004;122:1676–1679.
- Meyer JC, Quantock AJ, Thonar EJ, et al. Characterization of a central corneal cloudiness sharing features of posterior crocodile shagreen and central cloudy dystrophy of François. *Cornea*. 1996;15:347–354.
- Strachan IM. Cloudy central corneal dystrophy of François. Five cases in the same family. *Br J Ophthalmol*. 1969;53:192–194.
- Zaidi A, McLeod SD. Laser in situ keratomileusis in a patient with presumed central cloudy corneal dystrophy of François. *Am J Ophthalmol*. 2005;139:376–377.

Pre-Descemet Corneal Dystrophies (PDCDs)

MIM: PDCD—None
PPPCD—#619871

Former Alternative Names and Eponyms

Deep filiform dystrophy.
Deep punctiform dystrophy.
Polychromatic dystrophy.

Inheritance

Isolated pre-Descemet corneal dystrophy (PDCD) is neither a well-defined entity nor is it clearly a hereditary or degenerative disorder (known as cornea farinata, "flour-like cornea"). Although no definite pattern of inheritance is established, it has been described in families over 2 to 4 generations. The subtype punctiform and polychromatic pre-Descemet corneal dystrophy (PPPCD) has been reported to be autosomal dominant in several pedigrees and may represent a distinct corneal dystrophy.

Genetic Locus

PDCD: Unknown.
PPPCD: 10q26.11.

Gene

PDCD: Unknown.
PPPCD: Peroxiredoxin 3—*PRDX3*.

Onset

Usually after age 30 years; although PPPCD has been found in children as young as age 3 years.

Signs

PDCD has historically been described as having several subgroups, many of which may represent sporadic, age-related degenerative and secondary changes. PDCD only involves the posterior stroma. Focal, fine, polymorphic gray opacities that may be central, annular, or diffuse are visible in the deep stroma immediately anterior to Descemet membrane (Figs. 20A, B). In the degenerative condition, cornea farinata, many fine, dust-like gray–brown to white opacities are best seen on retroillumination and are located bilaterally in the posterior stroma near Descemet membrane.

In PPPCD, the pre-Descemet deposits are more uniform and polychromatic within the otherwise normal cornea. The opacities in PPPCD are larger and more punctate than those of cornea farinata (Fig. 20C). While it is likely that PPPCD is a distinct entity, rare simultaneous presence of polychromatic opacities just beneath the anterior lens capsule raises the question of whether it is a corneal dystrophy in the strict sense. It has been suggested that similar appearing opacities, which occur not only in the posterior stroma where they are denser but also in the panstromal region, should be considered atypical PDCD or even a different dystrophy altogether.

Symptoms

Vision is usually unaffected, and patients are typically asymptomatic. One adult member of a recently described pedigree complained of glare.

Course

PPPCD is nonprogressive or possibly shows mild progression. Other forms of PDCD show progression.

Light Microscopy

Histopathologic studies of PDCD are not consistent. Normal cornea except for enlarged keratocytes in the posterior stroma containing vacuoles and intracytoplasmic inclusions of lipid-like material. There are no published descriptions at this time of light microscopy of PPPCD.

Transmission Electron Microscopy

Membrane-bound intracellular vacuoles containing electron-dense material suggestive of secondary lysosomes and inclusions of a lipofuscin-like lipoprotein consistent with a degenerative process are seen in PDCD. No extracellular deposits are noted. There are no published descriptions at this time of transmission electron microscopy of PPPCD.

Confocal Microscopy

In PDCD, there are intracellular and extracellular hyperreflective inclusions immediately anterior to Descemet membrane with prominent sub-basal nerves. In cornea farinata, the superficial stromal and midstromal layers appear normal with highly reflective small particles found in some keratocytes (cytoplasm) but only in the deep stroma. Descemet and endothelium are normal. In cases of genetically confirmed PPPCD, there are hyperreflective opacities distributed at the level of Descemet membrane (Fig. 20D).

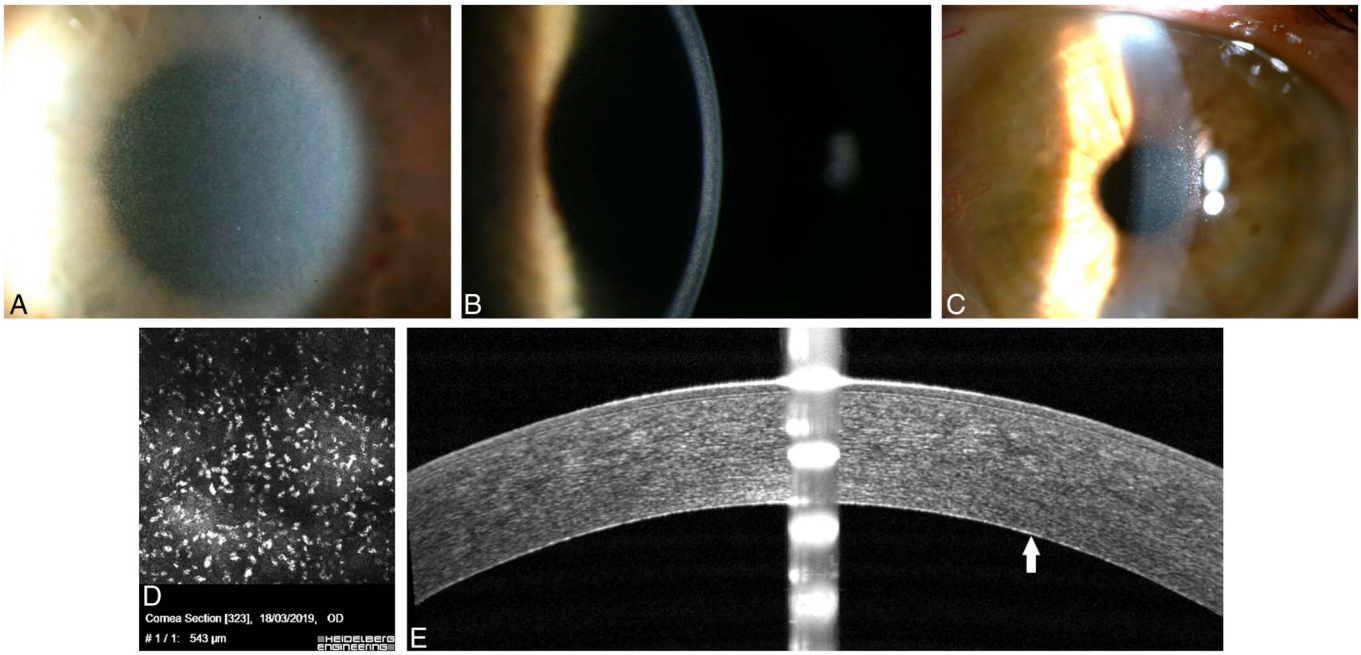

FIGURE 20. Pre-Descemet corneal dystrophy (PDCD). A, With broad-beam illumination, punctate opacities anterior to Descemet membrane are apparent. B, Slit-beam illumination of the same eye demonstrating punctate opacities anterior to Descemet membrane. C, Punctiform and polychromatic pre-Descemet corneal dystrophy (PPPCD, *PRDX3* mutation). Slit-beam illumination demonstrates large uniform pre-Descemet opacities. D, Confocal microscopy of the same patient from (C) demonstrates hyperreflective deposits at the level of Descemet membrane. E, OCT demonstrates hyperreflectivity posteriorly (arrow). Figures 20A and B from Figures 20A and B in Weiss, JS, Møller HU, Aldave AJ, et al. The IC3D Classification of the Corneal Dystrophies—Edition 2. *Cornea*. 2015 34:117–159.

Scheimpflug Imaging

In PPPCD, hyperreflective posterior stromal opacities are more easily seen with Scheimpflug imaging than with OCT (Fig. 20E).

Category

1. PPPCD.
4. PDCD.

Note: Similar opacities have been noted in association with other ocular and systemic diseases such as pseudoxanthoma elasticum, keratoconus, posterior polymorphous corneal dystrophy (PPCD), EBMD, and central cloudy dystrophy of François (CCDF).

Similar deep corneal deposits to PDCD are also frequently seen in X-linked ichthyosis (MIM #308100) which results from mutations in the steroid sulfatase gene (*STS*) at genetic locus Xp22.31. It has been described in the first decade of life. This is a systemic disease with corneal manifestations and therefore is not a corneal dystrophy.

BIBLIOGRAPHY

- Alió Del Barrio JL, Chung DD, Al-Shymali O, et al. Punctiform and polychromatic pre-Descemet corneal dystrophy: Clinical evaluation and identification of the genetic basis. *Am J Ophthalmol*. 2020;212:88–97.
- Choo CH, Boto de Los Bueis A, et al. Confirmation of PRDX3 c.568G>C as the genetic basis of punctiform and polychromatic pre-Descemet corneal dystrophy. *Cornea*. 2022;41:779–781.
- Costagliola C, Fabbrocini G, Illiano GM, et al. Ocular findings in X-linked ichthyosis: a survey on 38 cases. *Ophthalmologica*. 1991;202:152–155.
- Curran RE, Kenyon KR, Green WR. Pre-Descemet's membrane corneal dystrophy. *Am J Ophthalmol*. 1974;77:711–716.
- Fernandez-Sasso D, Acosta JE, Malbran E. Punctiform and polychromatic pre-Descemet's dominant corneal dystrophy. *Br J Ophthalmol*. 1979;63:336–338.
- Friedmann NJ, Kaiser PK, Pineda R. Pre-Descemet's Dystrophy. In: Friedmann NJ, Kaiser PK, Pineda R, editors. *The Massachusetts Eye and Ear Infirmary Illustrated Manual of Ophthalmology*. 3rd ed. Saunders Elsevier; 2009. p. 223.
- Grayson M, Wilbrandt M. Pre-Descemet dystrophy. *Am J Ophthalmol* 1967;64:276–282.
- Hung C, Ayabe RI, Wang C, et al. Pre-Descemet corneal dystrophy and X-linked ichthyosis associated with deletion of Xp22.31 containing the STS gene. *Cornea*. 2013;32:1283–1287.
- Kempster, RC, Hirst, LW, de la Cruz Z, et al. Clinicopathologic study of the cornea in X-linked ichthyosis. *Arch Ophthalmol*. 1997;115:409–415.

- Lanza M, Borrelli M, Benusiglio E, Rosa N. In vivo confocal microscopy of an apparent deep stroma corneal dystrophy: a case report. *Cases J*. 2009;2:9317.
- Lisch W, Weidle EG. Die posteriore kristalline Hornhautdystrophie. *Klin Monbl Augenheilkd*. 1984;185:128–131.
- Ye YF, Yao YF, Zhou P, et al. In vivo confocal microscopy of pre-Descemet's membrane corneal dystrophy. *Clin Experiment Ophthalmol*. 2006;34:614–616.

ENDOTHELIAL DYSTROPHIES

Fuchs Endothelial Corneal Dystrophy (FECD)

MIM #136800 (FECD1), MIM #610158 (FECD2), MIM #613267 (FECD3), MIM #613268 (FECD4), MIM #613269 (FECD5), MIM #613270 (FECD6), MIM #613271 (FECD7), MIM #615523 (FECD8).

Former Alternative Names and Eponyms

Endoepithelial corneal dystrophy.

Inheritance

Cases without known inheritance are most common, but many cases consistent with autosomal dominant inheritance have been reported. The genetic basis of FECD is complex and heterogeneous, demonstrating variable expressivity and incomplete penetrance.

Genetic Locus

Early-onset FECD: 1p34.3 (FECD1).

Late-onset FECD: Association has been reported to the following:

13pter-q12.13 (FECD2).
18q21.2 (FECD3).
20p13 (FECD4).
5q33.1-q35.2 (FECD5).
10p11.22 (FECD6).
9p24.1-p22.1 (FECD7).
15q25.3 (FECD8).

Gene

Early-onset FECD: Alpha 2 subunit of collagen type VIII—*COL8A2* (FECD1).

Late-onset FECD: Variants have been reported or associated with the following:

Transcription factor 4—*TCF4* (CTG18.1 trinucleotide repeat) (FECD3).

Solute carrier family 4, sodium borate cotransporter, member 11—*SLC4A11* (FECD4).

Zinc finger E-box-binding homeobox 1—*ZEB1* (FECD6).

ATP/GTP-binding protein-like 1—*AGBL1* (FECD8).

Onset

FECD is generally a slowly progressive condition. Most cases begin in the fourth decade or later, but the rare early variant starts in the first or second decade. Late-onset FECD has a female predominance ratio of 2.5:1 to 3.5:1. Smoking and ultraviolet light exposure have been associated with increased risk for FECD.

Signs

Corneal guttae start centrally and spread peripherally (Stage 1) (Fig. 21A). Some patients demonstrate guttae but never progress to later stages, whereas others advance to endothelial decompensation and stromal edema (Stage 2). Corneal endothelium may have a beaten metal-like appearance with or without pigment dusting. Descemet membrane is irregularly thickened. Stromal edema may progress to involve the epithelium, causing intraepithelial and interepithelial edema (epithelial bullae) and bullous keratopathy (Stage 3) (Figs. 21B, C). Subepithelial fibrosis (pannus), stromal scarring, and peripheral superficial or deep vascularization from chronic edema can occur in longstanding cases (Stage 4).

Symptoms

Intermittent reduced vision from epithelial/stromal edema or persistently decreased vision from stromal edema. Visual acuity may be worse in the morning because of increased stromal/epithelial edema after overnight eye closure. Pain, photophobia, and epiphora from epithelial erosions resulting from epithelial bullae or their rupture. Progressive visual loss. Guttae alone may not cause corneal edema, and mild corneal edema may not result in symptomatic decreased vision. More severe disease associated with decreased vision often has epithelial and stromal edema and subepithelial fibrosis.

Course

Can be progressive.

Light Microscopy

Diffuse thickening and lamination of Descemet membrane. Sparse and attenuated endothelial cells and hyaline excrescences (guttae) on thickened Descemet membrane (Fig. 21D). Guttae may become buried or confluent or more rarely may not be detected (Fig. 21E). Degeneration, thinning, and reduction of endothelial cells. Increasing waviness of the stromal collagen lamellae.

Transmission Electron Microscopy

Early-Onset FECD

Thickened anterior banded layer of Descemet membrane. Degeneration of endothelial cells. Stromal thickening with severe disorganization and disruption of the lamellar pattern.

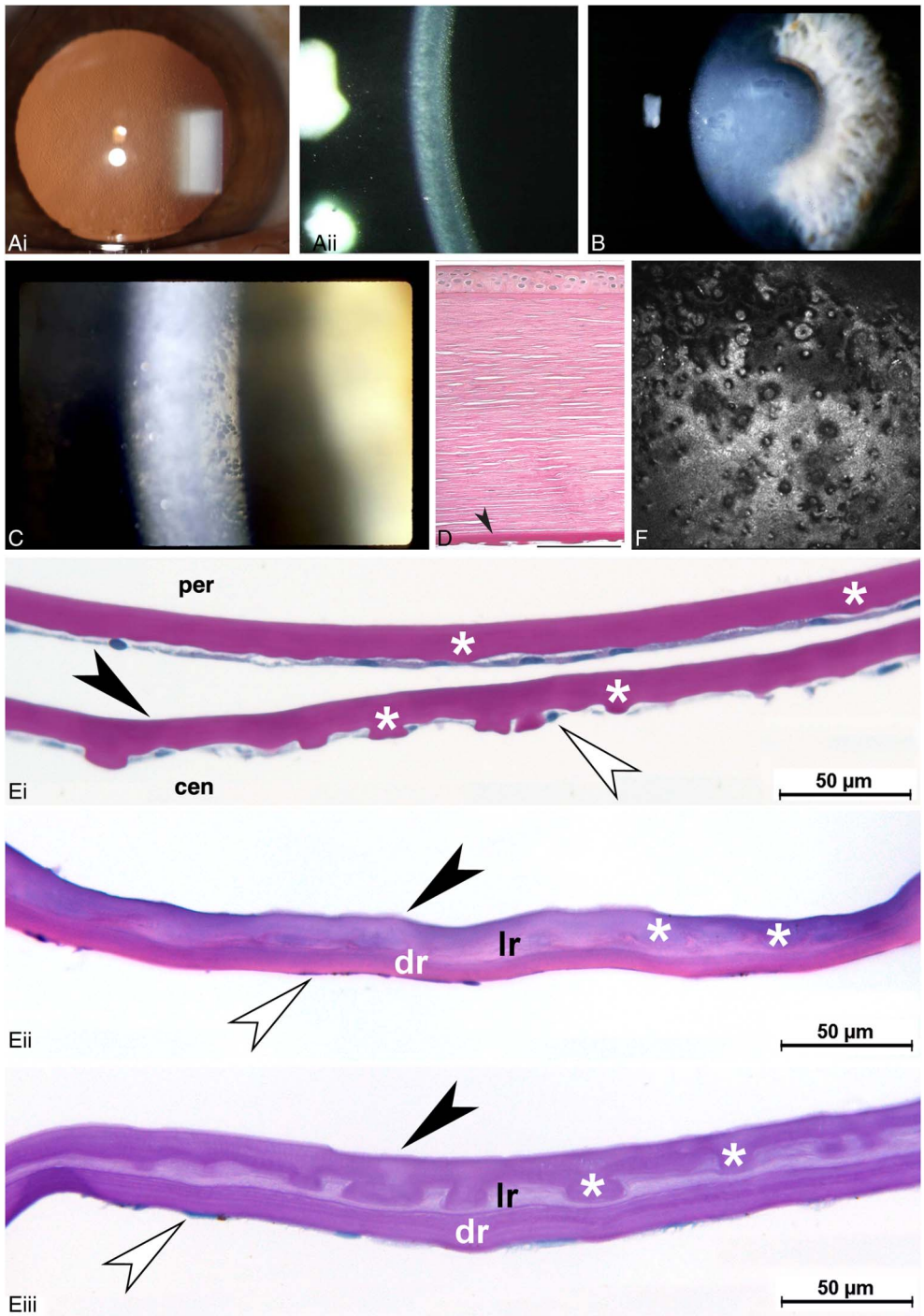

FIGURE 21. Fuchs endothelial corneal dystrophy (FECD). A, Corneal guttae in retroillumination (i) and slit lamp view (ii). B and C, Epithelial edema with bullae and stromal edema due to endothelial decompensation. D, Light microscopy: corneal guttae in the form of focal excrescences at the level of the endothelium; thickening of Descemet membrane (arrowhead); stromal and intraepithelial edema. PAS, bar = 200 μm. E, Light microscopy: Descemet membrane endothelial keratoplasty (DMEK) specimen shows (i) thickened Descemet membrane (black arrowhead) with guttae (asterisks), which are more prominent in the central portion of the DMEK specimen (cen) when compared with the peripheral (per) section, and an attenuated endothelial cell layer (white arrowhead), PAS stain. (ii), In a corneal specimen from a different eye, the original Descemet membrane (black arrowhead) is further thickened by layers of reactively secreted looser (lr) and denser (dr) basement membrane material that buries, and in this routine HE section mostly hides earlier guttae (asterisks), the latter of which are revealed in a PAS-stained section (iii). Note sparse and flattened endothelial cells (white arrowhead); bars = 50 μm. F, In vivo confocal microscopy shows polymegethism and pleomorphism of endothelial cells associated with round hyporeflective structures sometimes containing reflective material and corresponding to guttae (400 × 400 μm). Figures 21B and C from Figures 21D and B in Weiss, JS, Møller HU, Lisch W, et al. The IC3D Classification of the Corneal Dystrophies. *Cornea*. 2008;27(suppl 2):S1–S42. Figures 21D and F from Figures 21D and E in Weiss, JS, Møller HU, Aldave AJ, et al. The IC3D Classification of the Corneal Dystrophies—Edition 2. *Cornea*. 2015;43:117–159.

Late-Onset FECD

Multiple layers of basement membrane–like material on the posterior nonbanded part of Descemet membrane.

Confocal Microscopy

Polymegethism, pleomorphism, decreased hexagonality, and reduced number of endothelial cells (Fig. 21F).

Scheimpflug Imaging

Scheimpflug tomography can identify subclinical corneal edema and light backscatter. It may be useful in monitoring progression of Fuchs dystrophy and may be helpful when evaluating patients for cataract or endothelial keratoplasty surgery.

Category

1. Early-onset FECD.
2. In patients with identified genetic loci.
3. In patients without known inheritance.

Note: Corneal guttae can also occur in aging, inflammation such as uveitis, corneal trauma, and macular corneal dystrophy. Not all patients with corneal guttae have FECD.

BIBLIOGRAPHY

- Afshari NA, Igo RP Jr, Morris NJ, et al. Genome-wide association study identifies three novel loci in Fuchs endothelial corneal dystrophy. *Nat Commun*. 2017;8:14898.
- Aldave AJ, Han J, Frausto RF. Genetics of the corneal endothelial dystrophies: an evidence based review. *Clin Genet*. 2013;84:109–119.
- Baratz KH, Tosakulwong N, Ryu E, et al. E2-2 protein and Fuchs's corneal dystrophy. *N Engl J Med*. 2010;363:1016–1024.
- Biswas S, Munier FL, Yardley J, et al. Missense mutations in COL8A2, the gene encoding the alpha2 chain of type VIII collagen, cause two forms of corneal endothelial dystrophy. *Hum Mol Genet*. 2001;10:2415–2423.
- Chan SWS, Yucel Y, Gupta N. New trends in corneal transplants at the University of Toronto. *Can J Ophthalmol*. 2018;53:580–587.
- Fautsch MP, Wieben ED, Baratz KH, et al. TCF4-mediated Fuchs endothelial corneal dystrophy: Insights into a common trinucleotide repeat-associated disease. Prog Retin Eye Res. 2021;81:100883.
- Fuchs E. Dystrophia epithelialis corneae. *Albrecht von Graefes Arch Klin Exp Ophthalmol*. 1910;76:478–508.
- Gottsch JD, Sundin OH, Liu SH, et al. Inheritance of a novel COL8A2 mutation defines a distinct early-onset subtype of Fuchs corneal dystrophy. *Invest Ophthalmol Vis Sci*. 2005;46:1934–1939.
- Hogan MJ, Wood J, Fine M. Fuchs' endothelial dystrophy of the cornea. *Am J Ophthalmol*. 1974;78:363–383.
- Krachmer JH, Purcell JJ Jr, Joung CW, et al. Corneal endothelial dystrophy. A study of 64 families. *Arch Ophthalmol*. 1978;96:2036–2039.
- Liu, X., Zheng, T., Zhao, C. et al. Genetic mutations and molecular mechanisms of Fuchs endothelial corneal dystrophy. *Eye Vis (Lond)*. 2021;8:24.
- Magovern M, Beauchamp GR, McTigue JW, et al. Inheritance of Fuchs' combined dystrophy. *Ophthalmology*. 1979;86:1897–1923.
- Mehta JS, Vithana EN, Tan DT, et al. Analysis of the posterior polymorphous corneal dystrophy 3 gene, TCF8, in late-onset Fuchs endothelial corneal dystrophy. *Invest Ophthalmol Vis Sci*. 2008;49:184–188.
- Mootha VV, Gong X, Ku HC, et al. Association and familial segregation of CTG18.1 trinucleotide repeat expansion of TCF4 gene in Fuchs' endothelial corneal dystrophy. *Invest Ophthalmol Vis Sci*. 2014;55:33–42.
- Ong Tone S, Kocaba V, Böhm M, et al. Fuchs endothelial corneal dystrophy: The vicious cycle of Fuchs pathogenesis. Prog *Retin Eye Res*. 2021;80:100863.
- Patel SV. Imaging Fuchs endothelial corneal dystrophy in clinical practice and clinical trials. *Cornea*. 2021;40:1505–1511.
- Price MO, Mehta JS, Jurkunas UV, et al. Corneal endothelial dysfunction: Evolving understanding and treatment options. *Prog Retin Eye Res*. 2021;82:100904.
- Riazuddin SA, Parker DS, McGlumphy EJ, et al. Mutations in LOXHD1, a recessive-deafness locus, cause dominant late-onset Fuchs corneal dystrophy. *Am J Hum Genet*. 2012;90:533–539.
- Riazuddin SA, Vasanth S, Katsanis N, et al. Mutations in AGBL1 cause dominant late-onset Fuchs corneal dystrophy and alter protein-protein interaction with TCF4. *Am J Hum Genet*. 2013;93:758–764.
- Riazuddin SA, Vithana EN, Seet LF, et al. Missense mutations in the sodium borate cotransporter SLC4A11 cause late-onset Fuchs corneal dystrophy. *Hum Mutat*. 2010;31:1261–1268.
- Riazuddin SA, Zaghloul NA, Al-Saif A, et al. Missense mutations in TCF8 cause late-onset Fuchs corneal dystrophy and interact with FCD4 on chromosome 9p. *Am J Hum Genet*. 2010;86:45–53.
- Sarnicola C, Farooq AV, Colby K. Fuchs endothelial corneal dystrophy: Update on pathogenesis and future directions. *Eye Contact Lens*. 2019;45:1–10.
- Sun SY, Wacker K, Baratz KH, et al. Determining subclinical edema in Fuchs endothelial corneal dystrophy: Revised classification using Scheimpflug tomography for preoperative assessment. Ophthalmology. 2019;126:195–204.
- Sundin OH, Broman KW, Chang HH, et al. A common locus for late-onset Fuchs corneal dystrophy maps to 18q21.2-q21.32. *Invest Ophthalmol Vis Sci*. 2006;47:3919–3926.
- Sundin OH, Jun AS, Broman KW, et al. Linkage of late-onset Fuchs corneal dystrophy to a novel locus at 13pTel-13q12.13. *Invest Ophthalmol Vis Sci*. 2006;47:140–145.
- Tsedilina TR, Sharova E, Iakovets V, et al. Systematic review of SLC4A11, ZEB1, LOXHD1, and AGBL1 variants in the development of Fuchs' endothelial corneal dystrophy. *Front Med*. 2023;10:1153122.

- Vithana EN, Morgan PE, Ramprasad V, et al. SLC4A11 mutations in Fuchs endothelial corneal dystrophy. *Hum Mol Genet*. 2008;17:656–666.
- Wieben ED, Alaff RA, Tosakulwong N, et al. A common trinucleotide repeat expansion within the transcription factor 4 (TCF4, E2-2) gene predicts Fuchs corneal dystrophy. *PLoS One*. 2012;7:e49083.
- Weiss JS, Afshari NA. Cornea guttata alone does not make a diagnosis of Fuchs endothelial corneal dystrophy. Submitted *AJO*.
- Zhang X, Igo RP Jr, Fondran J, et al. Fuchs' Genetics Multi-Center Study Group. Association of smoking and other risk factors with Fuchs' endothelial corneal dystrophy severity and corneal thickness. *Invest Ophthalmol Vis Sci*. 2013 54:5829–5835.

Posterior Polymorphous Corneal Dystrophy (PPCD)

MIM #122000 (PPCD1), MIM #609141 (PPCD3), MIM #618031 (PPCD4).

Former Alternative Names and Eponyms

Posterior polymorphous dystrophy (PPMD).
Schlichting dystrophy.

Inheritance

Autosomal dominant.

Isolated unilateral cases, with similar phenotype but no known heredity.

Genetic Locus

PPCD1: 20p11.2.
PPCD3: 10p11.22.
PPCD4: 8q22.3.

Gene

Posterior polymorphous corneal dystrophy 1: Ovo-like zinc finger 2—*OVOL2*.

Posterior polymorphous corneal dystrophy 3: Zinc finger E-box-binding homeobox 1—*ZEB1*.

Posterior polymorphous corneal dystrophy 4: Grainyhead-like transcription factor 2—*GRHL2*.

Onset

Variable onset.

Signs

Often asymmetric. Opacities of Descemet membrane and the endothelium with a wide variety of characteristic morphologic features: geographic gray opacities; vesicular lesions (typical for PPCD3), either single or grouped, often surrounded by gray circular opacity and parallel gray-white endothelial bands with white "flaky" material along the bands (railroad tracks), which may extend across the entire cornea (Figs. 22A–C). Occasional cases may be associated with diffuse opacification of Descemet membrane and multiple larger vesicular endothelial opacities. In advanced stages, particularly PPCD1, severe verrucous lesions of the posterior corneal surface may occur (Fig. 22D). Corneal abnormalities in PPCD are typically better detected with retroillumination (Fig. 22E). Both keratoconic and nonkeratoconic corneal steepening have been reported, with most individuals with PPCD3 demonstrating corneal curvatures greater than 48.0 diopters in both eyes. Corneal edema may develop, necessitating keratoplasty in approximately 20% to 25% of affected individuals. Peripheral iridocorneal adhesions in about 25% of cases and elevated intraocular pressure in about 15% to 35% of cases.

Symptoms

Endothelial alterations are often asymptomatic. Visual impairment and pain may develop secondary to corneal edema.

Course

Rarely congenital corneal clouding, although the course may be more severe in some pedigrees. Endothelial changes often unchanged over years. Possible slow progression of polymorphic vesicles and greater thickness of Descemet membrane over years and decades occasionally causing endothelial decompensation.

Light Microscopy

Descemet membrane with multiple layers of collagen on its posterior surface manifesting focal fusiform or nodular excrescences may be present (Figs. 22F, G). Blebs, discontinuities, or reduplication of the endothelial cell layer may be seen. The endothelial layer in PPCD is typically 1 to 2 cell layers thick but reports of up to six cell layers in loop projections detached from Descemet membrane exist.

Transmission Electron Microscopy

The anterior banded portion of Descemet membrane is normal, although the posterior nonbanded portion may be markedly abnormal, demonstrating alterations in thickness, a multilaminar appearance, and occasional guttae. Two types of collagenous tissue posterior to Descemet membrane form layers up to 25 μm thick. Affected endothelial cells display ultrastructural characteristics of epithelial cells, such as microvilli and desmosomes.

Immunohistochemistry

PPCD1

E-cadherin (E-CAD) and cytokeratin 7 (CK7) are positive in the diseased endothelium while negative in the control endothelium.

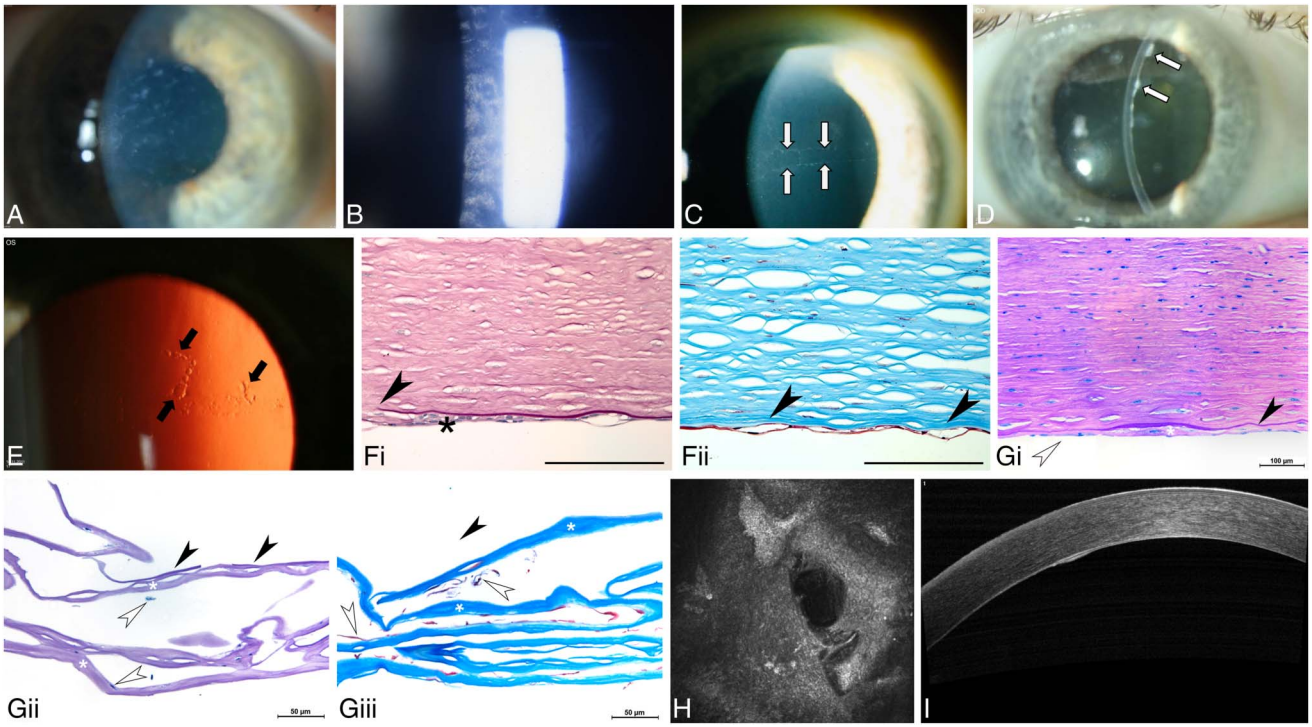

FIGURE 22. Posterior polymorphous corneal dystrophy (PPCD). A, Endothelial plaque-like lesions. B, Irregular crater-like figures on Descemet membrane viewed with specular reflection. C, Endothelial railroad track alteration (arrows). D, Verrucous lesions (arrows) of the posterior corneal surface. E, Changes in PPCD, such as vesicular lesions (arrows), are typically better detected with retroillumination. F, Light microscopy: PAS stain (i) and Masson trichrome (ii) show that the endothelium is replaced with flat epithelial-like cells which grow focally as more than 1 layer of cells (i; asterisk), forming blisters (ii; arrowheads) and occasionally elevated strands. The posterior stroma may show pits or discontinuities in Descemet membrane (i; arrowhead), bar = 100 μm. G, Light microscopy: penetrating keratoplasty specimen (i) shows an uneven, mostly thin, Descemet membrane (black arrowhead) covered by a much thicker collagenous layer (asterisk) secreted by aberrant endothelial cells (white arrowheads), some of which are located within the membrane, in a 6-year-old child with PPCD3 from a *ZEB1* mutation. ii and iii, Corresponding findings at age 8 years in DMEK specimen of the fellow eye, consisting mostly of the thick collagenous layer (asterisks) with sparse endothelial cells (white arrowheads). Some endothelial cells are located within the collagenous membrane or have detached from the membrane, to which fragments of the thin Descemet membrane attach (black arrowheads) (PAS, bar = 100 μm (i); PAS (ii) and Masson trichrome stain (iii), bars = 50 μm). H, In vivo confocal microscopy showing vesicular lesions and band-like structures with irregular edges within the endothelium associated with polymegethism of endothelial cells (400 × 400 μm). I, Spectral domain OCT shows irregular hyperreflectivity within Descemet membrane and endothelial layer, corresponding to abnormal multilayer endothelial cells in a 50-year-old female patient with PPCD. Figure 22B from Figure 22B in Weiss, JS, Møller HU, Lisch W, et al. The IC3D Classification of the Corneal Dystrophies. *Cornea*. 2008;27(suppl 2):S1–S42. Figures 22A, Fi, Fii, and H from Figures 22A, Di, Dii, and E in Weiss, JS, Møller HU, Aldave AJ, et al. The IC3D Classification of the Corneal Dystrophies—Edition 2. *Cornea*. 2015;34:117–159.

Confocal Microscopy

Vesicular lesions: rounded dark areas with some cell detail apparent in the middle giving a donut-like appearance (Fig. 22H). Multilayered nests of cells. "Railroad-track" band-like dark areas with irregular edges enclosing some smaller lighter cells resembling epithelial-like cells. Polymegethism of the endothelium.

Optical Coherence Tomography

OCT shows a thickened Descemet membrane as well as amorphous hyperreflective material and deposits on the backside of the endothelium (Fig. 22I).

Category

1. PPCD1, PPCD3, and PPCD4.

Note: Clinical, histopathologic, and electron microscopic descriptions of two of the five families reported with autosomal dominant congenital hereditary endothelial dystrophy (Kanai A, Kaufman HE. *Invest Ophthalmol*. 1971; Kanai A, Waltman S, Polack FM, et al. *Invest Ophthalmol*. 1971; and Levenson JE, Chandler JW, Kaufman HE. *Am J Ophthalmol*. 1973) are consistent with PPCD, although neither linkage to the PPCD1 locus nor *ZEB1* screening has been performed in either family. Another of the 5 families (Pearce, et al. *Br J Ophthalmol*. 1969; Kirkness, et al. *Br J Ophthalmol*. 1987; and Toma et al. *Hum Mol Genet*. 1995)

may have PPCD based on clinical, histopathologic, and electron microscopic analyses, although a higher percentage of affected individuals in this family demonstrate corneal edema, with an earlier onset and more significant edema compared with most families with PPCD. Because linkage analysis in this family demonstrated linkage to the region of chromosome 20 that is common to 4 families with PPCD, it is probable that the family originally reported by Pearce and colleagues also has PPCD1, with a more severe phenotype than that of other PPCD1 pedigrees. There is no clear evidence that PPCD2 exists because the original article 1) did not have phenotypic descriptions as the two reported individuals had already undergone penetrating keratoplasty and 2) reported association with *COL8A2* missense mutations (Biswas S, Munier FL, Yardley J, et al. *Hum Mol Genet*. 2001).

BIBLIOGRAPHY

- Ahn YJ, Choi SI, Yum HR, et al. Clinical features in children with posterior polymorphous corneal dystrophy. *Optom Vis Sci*. 2017;94:476–481.
- Aldave AJ, Ann LB, Frausto RF, et al. Classification of posterior polymorphous corneal dystrophy as a corneal ectatic disorder following confirmation of associated significant corneal steepening. *JAMA Ophthalmol*. 2013;131:1583–1590.
- Bakhtiari P, Frausto RF, Roldan AN, et al. Exclusion of pathogenic promoter region variants and identification of novel nonsense mutations in the zinc finger E-box-binding homeobox 1 gene in posterior polymorphous corneal dystrophy. *Mol Vis*. 2013;19:575–580.
- Berger T, Seitz B, Löw U, et al. Descemet Membrane Endothelial Keratoplasty (DMEK) for severe verrucous posterior polymorphous corneal dystrophy with uncommon clinical and ultrastructural findings. *Klin Monbl Augenheilkd*. (online ahead of print August 4, 2022).
- Biswas S, Munier FL, Yardley J, et al. Missense mutations in COL8A2, the gene encoding the alpha2 chain of type VIII collagen, cause two forms of corneal endothelial dystrophy. *Hum Mol Genet*. 2001.10:2415–2423
- Chung DD, Zhang W, Jatavallabhula K, et al. Alterations in GRHL2-OVOL2-ZEB1 axis and aberrant activation of Wnt signaling lead to altered gene transcription in posterior polymorphous corneal dystrophy. *Exp Eye Res*. 2019;188:107696.
- Cibis GW, Krachmer JA, Phelps CD, et al. The clinical spectrum of posterior polymorphous dystrophy. *Arch Ophthalmol*. 1977;95:1529–1537.
- Davidson AE, Liskova P, Evans CJ, et al. Autosomal-dominant corneal endothelial dystrophies CHED1 and PPCD1 are allelic disorders caused by non-coding mutations in the promoter of OVOL2. *Am J Hum Genet*. 2016;98:75–89.
- Elhusseiny AM, Saeed HN. Posterior polymorphous corneal dystrophy in a pediatric population. *Cornea*. 2022;41:734–739.
- Frausto RF, Chung DD, Boere PM, et al. ZEB1 insufficiency causes corneal endothelial cell state transition and altered cellular processing. *PLoS One*. 2019;14:e0218279.
- Fung SSM, Sami H, El Hamouly A, et al. Endothelial cell density in children with posterior polymorphous corneal dystrophy: a longitudinal case-control study. *Eye*. 2021;35:3397–3403.
- Gwilliam R, Liskova P, Filipec M, et al. Posterior polymorphous corneal dystrophy in Czech families maps to chromosome 20 and excludes the VSX1 gene. *Invest Ophthalmol Vis Sci*. 2005;46:4480–4484.
- Héon E, Mathers WD, Alward WL, et al. Linkage of posterior polymorphous corneal dystrophy to 20q11. *Hum Mol Genet*. 1995;4:485–488.
- Jirsova K, Merjava S, Martincova R, et al. Immunohistochemical characterization of cytokeratins in the abnormal corneal endothelium of posterior polymorphous corneal dystrophy patients. *Exp Eye Res*. 2007;84:680–686.
- Kanai A, Kaufman HE. Further electron microscopic study of hereditary corneal edema. *Invest Ophthalmol*. 1971;10:545–554.
- Kanai A, Waltman S, Polack FM, et al. Electron microscopic study of hereditary corneal edema. *Invest Ophthalmol*. 1971;10:89–99.
- Kirkness CM, McCartney A, Rice NS, et al. Congenital hereditary corneal oedema of Maumenee: its clinical features, management, and pathology. *Br J Ophthalmol*. 1987;71:130–144.
- Koeppe L. Klinische Beobachtungen mit der Nernstspaltlampe und dem Hornhautmikroskop. *Albrecht von Graefes Arch Klin Exp Ophthalmol*. 1916;91:363–379.
- Krafchak CM, Pawar H, Moroi SE, et al. Mutations in TCF8 cause posterior polymorphous corneal dystrophy and ectopic expression of COL4A3 by corneal endothelial cells. *Am J Hum Genet*. 2005;77:694–708.
- Levenson JE, Chandler JW, Kaufman HE. Affected asymptomatic relatives in congenital hereditary endothelial dystrophy. *Am J Ophthalmol*. 1973:76:967–971.
- Liskova P, Dudakova L, Evans CJ, et al. Ectopic GRHL2 Expression due to non-coding mutations promotes cell state transition and causes posterior polymorphous corneal dystrophy 4. *Am J Hum Genet*. 2018;102:447–459.
- Patel DV, Grupcheva CN, McGhee CNJ. In vivo microscopy of posterior polymorphous dystrophy. *Cornea*. 2005;24:550–554.
- Pearce WG, Tripathi RC, Morgan G. Congenital endothelial corneal dystrophy. Clinical, pathological, and genetic study. *Br J Ophthalmol*.1969;53:577–591.
- Rodrigues MM, Waring GO, Laibson PR, et al. Endothelial alterations in congenital corneal dystrophies. *Am J Ophthalmol*. 1975;80:678–689.
- Schlichting H. Blasen-und dellenförmige Endotheldystrophie der Hornhaut. *Klin Monbl Augenkeilkd*. 1941;107:425–435.
- Shimizu S, Krafchak C, Fuse N, et al. A locus for posterior polymorphous corneal dystrophy (PPCD3) maps to chromosome 10. *Am J Med Genet*. 2004;130:372–377.

- Toma NM, Ebenezer ND, Inglehearn CF, et al. Linkage of congenital hereditary endothelial dystrophy to chromosome 20. *Hum Mol Genet*. 1995;4:2395–2398.
- Yellore VS, Rayner SA, Emmert-Buck L, et al. No pathogenic mutations identified in the COL8A2 gene or four positional candidate genes in patients with posterior polymorphous corneal dystrophy. *Invest Ophthalmol Vis Sci*. 2005;46:1599–1603.
- Zakharevich M, Kattan JM, Chen JL, et al. Elucidating the molecular basis of PPCD: Effects of decreased ZEB1 expression on corneal endothelial cell function. *Mol Vis*. 2017;23:740–752.

Congenital Hereditary Endothelial Dystrophy (CHED)

MIM #217700.

Importantly, as no published evidence convincingly supports the existence of autosomal dominant (AD) CHED, formerly termed CHED1, as a distinct entity, this variant was removed from the IC3D classification system (edition 2, 2015), and autosomal recessive (AR) CHED, formerly known as CHED2, is currently termed CHED.

Former Alternative Names and Eponyms

Maumenee corneal dystrophy.

Genetic Locus

20p13.

Gene

Solute carrier family 4, sodium borate transporter, member 11—*SLC4A11*

Note: Mutations were identified in 76% of CHED pedigrees screened in 1 publication.

Inheritance

Autosomal recessive.

Onset

Congenital.

Signs

Bilateral, often asymmetric. Corneal clouding ranging from a diffuse haze to ground-glass, milky appearance with occasional focal gray spots (Figs. 23A, B). Severe stromal thickening (2–3 times normal but with minimal epithelial edema) (Fig. 23C). Patients are born with significantly decreased corneal endothelial cell (CEC) density (to approximately 10% of age-matched controls), with fibrotic morphology of Descemet membrane. Rarely secondary subepithelial band keratopathy. Rarely elevated intraocular pressure (IOP).

Symptoms

Corneal clouding with blurred vision often accompanied by nystagmus. Minimal to no tearing or photophobia.

Course

Relatively stationary with little or no progression.

Light Microscopy

Diffuse epithelial and stromal edema (Fig. 23D), defects in Bowman layer, degenerated corneal endothelium with sparse and atrophic multinucleated endothelial cells, and uniform Descemet membrane, either thin or massively thickened by posterior fibrous layer (Fig. 23E) because of abnormal secretion by the endothelial cells.

Transmission Electron Microscopy

Edematous stromal thickening with severe disorganization and disruption of the lamellar pattern. Descemet membrane has a normal anterior banded layer, but posterior nonbanded collagenous layer can be thickened to 20 to 40 μm. Endothelial cells are markedly reduced and degenerated with many intracellular vacuoles.

Immunohistochemistry

Distribution of collagen types I and III–V and laminin within the posterior collagenous layer of Descemet membrane.

Confocal Microscopy

Intermediate epithelial cells show no visible nuclei with hyperreflective fibrosis at the level of the basal epithelial cells. Epithelial basement membrane, Bowman layer, and subepithelial nerve plexus are not visible. In the posterior stroma, thin and long hyporeflective bands but no keratocytes. Descemet membrane is gray and homogeneous with remaining endothelial cells showing moderate polymegethism (Fig. 23F).

Optical Coherence Tomography

Thickened epithelial layer with underlying irregular Bowman layer, increased stromal thickness, and abnormally thickened Descemet membrane.

Category

1.

3. For patients without *SLC4A11* mutations.

Note: Harboyan syndrome (HS) or corneal dystrophy and perceptive deafness (CDPD) is a disorder involving CHED and progressive, postlingual sensorineural hearing loss. As some patients with CHED eventually develop HS and as some parents of patients with CHED can have Fuchs endothelial corneal dystrophy (FECD), the presence of all 3 diseases (CHED, HS, and FECD) in the same pedigree

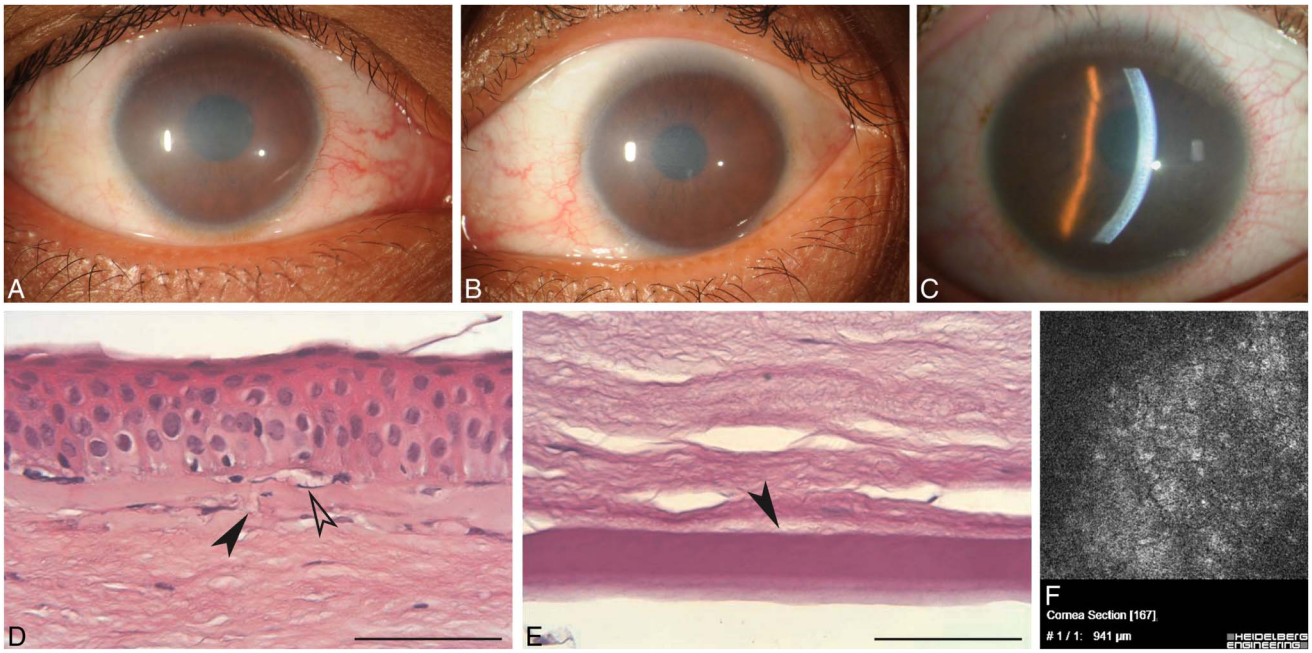

FIGURE 23. Congenital hereditary endothelial dystrophy (CHED). A and B, Right and left corneas, respectively, of a 30-year-old woman with CHED (homozygous T271M *SLC4A11* mutation). Photographs courtesy of Dr. Majid Moshirfar. C, Slit-beam photograph demonstrating diffuse stromal thickening (homozygous *SLC4A11* mutation). D, Light microscopy: edema of basal epithelial cells with subepithelial lacunae (open arrowhead) and breaks (arrowhead) in the Bowman layer, bar = 80 μm. E, Thickened Descemet membrane with no visible endothelial cells, bar = 50 μm. F, In vivo confocal microscopy (400 × 400 μm) shows polymegethism of endothelial cells. Cell cores are enlarged and hyperreflective with poorly defined contours. Figure 23C from Figure 23B in Weiss, JS, Møller HU, Lisch W, et al. The IC3D Classification of the Corneal Dystrophies. *Cornea.* 2008;27(suppl 2):S1–S42. Figures 23A, B, D, and E from Figures 23A, B, D, and E in Weiss JS, Møller HU, Aldave AJ, et al. IC3D Classification of Corneal Dystrophies—Edition 2. *Cornea.* 2015;34:117–159.

suggests that patients with CHED should be monitored for HS and their parents for FECD.

BIBLIOGRAPHY

- Aldahmesh MA, Khan AO, Meyer BF, et al. Mutational spectrum of SLC4A11 in autosomal recessive CHED in Saudi Arabia. *Invest Ophthalmol Vis Sci*. 2009;50:4142–4145.
- Aldave AJ, Han J, Frausto RF. Genetics of the corneal endothelial dystrophies: an evidence based review. *Clin Genet*. 2013;84:109–119.
- Chaurasia S, Ramappa M, Annapurna M, et al. Coexistence of congenital hereditary endothelial dystrophy and Fuchs endothelial corneal dystrophy associated with SLC4A11 mutations in affected families. *Cornea*. 2020;39:354–357.
- Desir J, Moya G, Reish O, et al. Borate transporter SLC4A11 mutations cause both Harboyan syndrome and non-syndromic corneal endothelial dystrophy. *J Med Genet*. 2007; 44:322–326.
- Desir J, Abramowicz M. Congenital hereditary endothelial dystrophy with progressive sensorineural deafness (Harboyan syndrome). *Orphanet J Rare Dis*. 2008;3:28.
- Firasat S, Dur-E-Shawar, Khan WA, et al. SLC4A11 mutations causative of congenital hereditary endothelial dystrophy (CHED) progressing to Harboyan syndrome in consanguineous Pakistani families. *Mol Biol Rep*. 2021;48:7467–7476.
- Georgeon C, Bouheraoua N, Laroche L, et al. Imagerie de la dystrophie endothéliale congénitale héréditaire (CHED) [Optical coherence tomography and in vivo confocal microscopy in congenital hereditary endothelial dystrophy (CHED)]. *J Francais d'Ophtalmol*. 2017;40:148–150.
- Guha S, Chaurasia S, Ramachandran C, et al. SLC4A11 depletion impairs NRF2 mediated antioxidant signaling and increases reactive oxygen species in human corneal endothelial cells during oxidative stress. *Sci Rep*. 2017;7:4074:1–11.
- Guha S, Bhogapurapu B, Ramappa M, et al. Determination of oxidative stress markers in the aqueous humor and corneal tissues of patients with congenital hereditary endothelial dystrophy. *Cornea*. 2021;40:491–496.
- Kenyon KR, Antine B. The pathogenesis of congenital hereditary endothelial dystrophy of the cornea. *Am J Ophthalmol*. 1971;72:787–795.
- Kim JH, Ko JM, Tchah H. Fuchs endothelial corneal dystrophy in a heterozygous carrier of congenital hereditary endothelial dystrophy type 2 with a novel mutation in SLC4A11. *Ophthalmic Genet*. 2015;36:284–286.

- Kirkness CM, McCartney A, Rice NS, et al. Congenital hereditary corneal edema of Maumenee: its clinical features, management, and pathology. *Br J Ophthalmol*. 1987;71:130–144.
- Malhotra D, Jung M, Fecher-Trost C, et al. JR. Defective cell adhesion function of solute transporter, SLC4A11, in endothelial corneal dystrophies. *Hum Mol Genet*. 2020;29:97–116.
- Malhotra D, Casey JR. Molecular mechanisms of Fuchs and congenital hereditary endothelial corneal dystrophies. *Rev Physiol Biochem Pharmacol*. 2020;178:41–81.
- Maumenee AE. Congenital hereditary corneal dystrophy. *Am J Ophthalmol*. 1960;50:1114–1124
- Mehta N, Ramappa M. Novel proposed algorithm in congenital hereditary endothelial dystrophy. *Semin Ophthalmol*. 2022;28:1–8.
- Sekundo W, Marshall GE, Lee WR, et al. Immuno-electron labeling of matrix components in congenital hereditary endothelial dystrophy. *Graefes Arch Clin Exp Ophthalmol*. 1994;232:337–346.
- Siddiqui S, Zenteno JC, Rice A, et al. Congenital hereditary endothelial dystrophy caused by SLC4A11 mutations progresses to Harboyan syndrome. *Cornea*. 2014;33:247–251.
- Sultana A, Garg P, Ramamurthy B, et al. Mutational spectrum of the SLC4A11 gene in autosomal recessive congenital hereditary endothelial dystrophy. *Mol Vis*. 2007;13:1327–1332.
- Vithana EN, Morgan P, Sundaresan P, et al. Mutations in sodium-borate cotransporter SLC4A11 cause recessive congenital hereditary endothelial dystrophy (CHED 2). *Nat Genet*. 2006;38:755–757.
- Zhang J, Dai Y, Wu D, Li Y, et al. Whole exome sequencing identified FAM149A as a plausible causative gene for congenital hereditary endothelial dystrophy, affecting Nrf2-Antioxidant signaling upon oxidative stress. *Free Radic Biol Med*. 2021;173:117–124.

X-Linked Endothelial Corneal Dystrophy (XECD)

MIM #300779.

Former Alternative Names and Eponyms

None.

Inheritance

X-chromosomal dominant.

Genetic Locus

Xq25.

Gene

Unknown.

Onset

Congenital.

Signs

Males

Congenital clouding ranging from a diffuse haze to a ground-glass, milky appearance (Fig. 24A). Possible nystagmus.

Only moon crater–like endothelial changes (Fig. 24B).

Secondary subepithelial band keratopathy combined with moon crater–like endothelial changes.

Females

Only moon crater–like endothelial changes (Fig. 24C).

Symptoms

Males

Often blurred vision.

Females

Asymptomatic.

Course

Males

Minimally progressive.

Females

Nonprogressive.

Light microscopy

Moon crater–like endothelial changes and subepithelial keratopathy. Irregular thinning of the epithelium and Bowman layer. Anterior stroma with irregularly arranged collagen lamellae. Irregular thickening of Descemet membrane with small excavations and pits. Loss of endothelial cells or atypical appearance (Fig. 24D).

Transmission Electron Microscopy

Moon crater–like endothelial changes and subepithelial band keratopathy. Subepithelial accumulations of an amorphous granular material. Irregular thinning of Bowman layer (up to 0.5 μm) with many interruptions and gaps. Thickening of Descemet membrane (20–35 μm) consisting of an abnormal anterior and abnormal posterior banded zone. There is complete absence of the normal posterior nonbanded zone. Discontinuous endothelial layer with partly normal and partly degenerative appearing cells (Fig. 24E). No evidence of desmosome-like adherent junctions between the cells or tonofilament bundles within the cytoplasm.

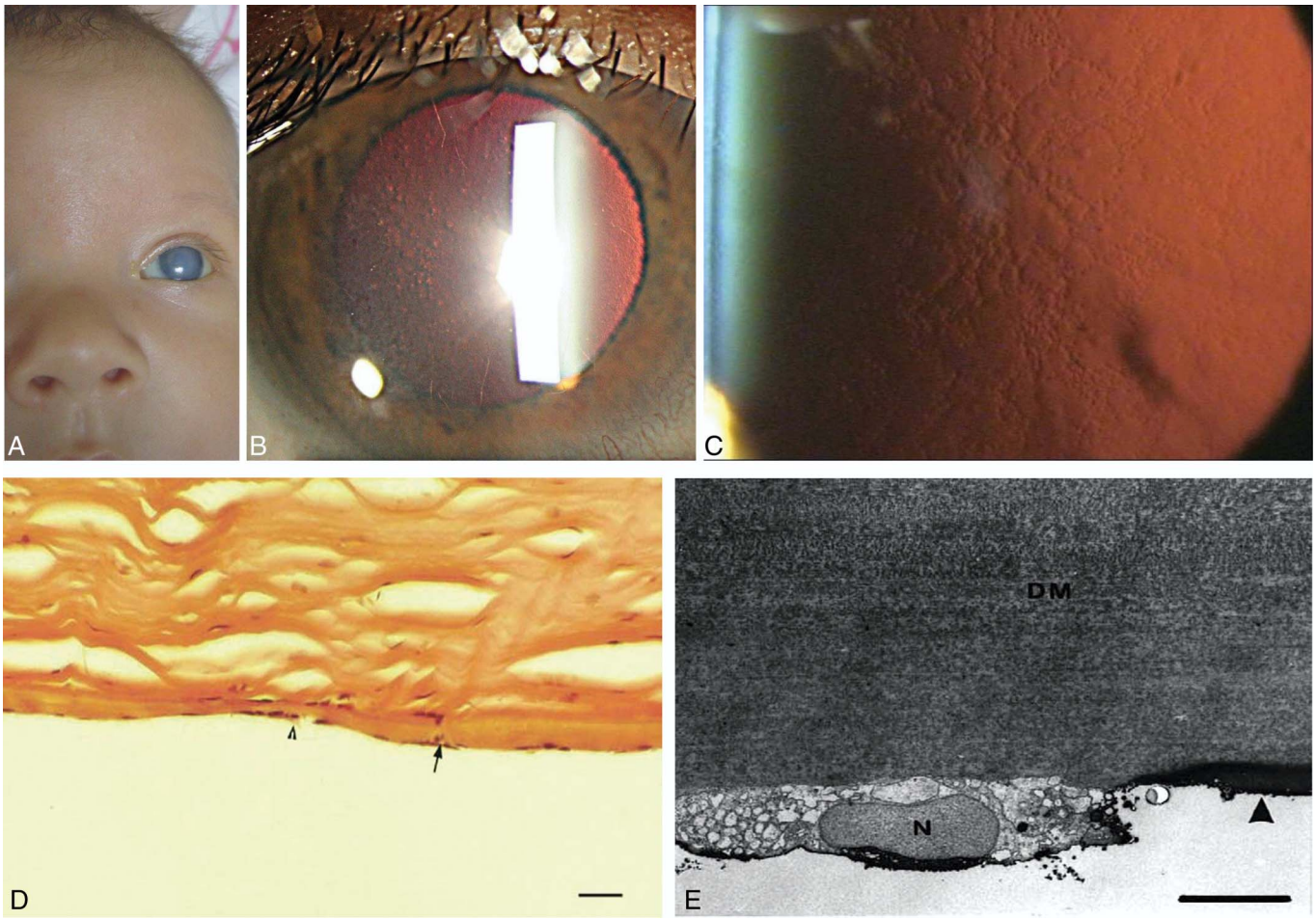

FIGURE 24. X-linked endothelial dystrophy (XECD). A, Male infant with congenital corneal haze. B, The same patient at age 12 years now showing moon crater–like endothelial changes in indirect illumination. C, His mother with moon crater–like endothelial changes in retroillumination. D, Light microscopy: scarce endothelial cells (arrowheads) with an atypical appearance, bar = 100 μm. E, Electron microscopy: degenerative endothelial cell adjacent to denuded area (arrow) of Descemet membrane (DM) (×10,000). N, nucleus. Figures 24A, C, D, and E from Figures 24A, B, C, and D in Weiss JS, Møller HU, Aldave AJ, et al. IC3D Classification of Corneal Dystrophies—Edition 2. *Cornea*. 2015;34:117–159.

Confocal Microscopy

Not reported.

Category

2.

BIBLIOGRAPHY

- Lisch W. Primäre bandförmige Hornhautdegeneration und ihre Assoziation mit anderen erblichen Hornhautveränderungen. *Klin Monbl Augenheilkd*. 1976;169:717–727.
- Schmid E, Lisch W, Philipp W, et al. A new, X-linked endothelial corneal dystrophy. *Am J Ophthalmol*. 2006;141:478–487.

ACKNOWLEDGMENTS

The authors thank the Louisiana Lions Eye Foundation, USA; Wills Eye Hospital, USA; Saarland University, Germany; University of Ferrara, Italy; Helsinki University Hospital, Finland; Norwegian Association of the Blind, Norway; La Fondation Voir et Entendre, France; Ken K. Nischal MD, USA; Cornea Consultants International, USA; Corneal Dystrophy Research Institute, Yonsei University College of Medicine, Korea; and Aarhus University Hospital, Denmark for financial support of photographic publishing charges and/or open access article processing charges. The authors also thank Anthony J. Aldave, MD; Natalie A. Afshari, MD; Petra Lišková, MD, PhD; and Hans Grossniklaus, MD, MBA.

REFERENCES

1. Weiss JS, Møller HU, Lisch W, et al. The IC3D classification of the corneal dystrophies. *Cornea*. 2008;27(suppl 2):S1–S83.

2. Weiss JS. Schnyder crystalline dystrophy sine crystals. Recommendation for a revision of nomenclature. *Ophthalmology*. 1996;103: 465–473.
3. Weiss JS. Visual morbidity in thirty-four families with Schnyder crystalline corneal dystrophy (an American Ophthalmological Society thesis). *Trans Am Ophthalmol Soc*. 2007;105:616–648.
4. Groenouw A. Knoetchenfoermige Hornhauttruebungen (noduli corneae). *Arch Augenheilkd*. 1890;21:281–289.
5. Biber H. Ueber einige seltene Hornhauterkrankungen: die oberflaechliche gittrige Keratitis [Inaugural Dissertation]. A Diggelmann Zuerich; 1890.
6. Weiss JS, Møller HU, Aldave AJ, et al. IC3D classification of corneal dystrophies—edition 2. *Cornea*. 2015;34:117–159.
7. Kanai A, Waltman S, Polack FM, et al. Electron microscopic study of hereditary corneal edema. *Invest Ophthalmol*. 1971;10:89–99.
8. Kanai A, Kaufman HE. Further electron microscopic study of hereditary corneal edema. *Invest Ophthalmol*. 1971;10:545–554.
9. Levenson JE, Chandler JW, Kaufman HE. Affected asymptomatic relatives in congenital hereditary endothelial dystrophy. *Am J Ophthalmol*. 1973;76:967–971.
10. Grayson M, Wilbrandt H. Dystrophy of the anterior limiting membrane of the cornea. (Reis-Buckler type). *Am J Ophthalmol*. 1966;61: 345–349.
11. Jonsson F, Byström B, Davidson AE, et al. Mutations in collagen, type XVII, alpha 1 (COL17A1) cause epithelial recurrent erosion dystrophy (ERED). *Hum Mutat*. 2015;36:463–473.
12. Yee RW, Sullivan LS, Lai HT, et al. Linkage mapping of Thiel-Behnke corneal dystrophy (CDB2) to chromosome 10q23-q24. *Genomics*. 1997; 46:152–154.
13. Lin BR, Le DJ, Chen Y, et al Whole exome sequencing and segregation analysis confirms that a mutation in COL17A1 is the cause of epithelial recurrent erosion dystrophy in a large dominant pedigree previously mapped to chromosome 10q23-q24. *PLoS One*. 2016;11:e0157418.
14. Oliver VF, van Bysterveldt KA, Cadzow M, et al. A COL17A1 Splice-altering mutation Is prevalent in inherited recurrent corneal erosions. *Ophthalmology*. 2016;123:709–722.
15. Vahedi F, Chung DD, Gee KM, et al. Epithelial recurrent erosion dystrophy secondary to COL17A1 c.3156C>T mutation in a non-white family. *Cornea*. 2018;37:909–911.
16. Turunen JA, Tuisku IS, Repo P, et al. Epithelial recurrent erosion dystrophy (ERED) from the splice site altering COL17A1 variant c.3156C>T in families of Finnish-Swedish ancestry. *Acta Ophthalmol*. 2023.
17. Waring GO, Rodrigues MM, Laibson PR. Corneal dystrophies. I. Dystrophies of the epithelium, Bowman's layer and stroma. *Surv Ophthalmol*. 1978;23:71–122.
18. Waring GO, Rodrigues MM, Laibson PR. Corneal dystrophies. II. Endothelial dystrophies. *Surv Ophthalmol*. 1978;23:147–168.
19. Jaakkola AM, Kivelä TT. Clinical and histopathologic characteristics and template of the TGFBI p.(His626Arg) missense variant lattice corneal dystrophy. *Cornea*. 2023;42:1124–1132.
20. Choo CH, Boto de Los Bueis A, Chung DD, et al. Confirmation of PRDX3 c.568G>C as the genetic basis of punctiform and polychromatic pre-Descemet corneal dystrophy. *Cornea*. 2022;41: 779–781.
21. Milman T, Kao AA, Chu D, et al. Paraproteinemic Keratopathy: the expanding diversity of clinical and pathologic manifestations. *Ophthalmology*. 2015;122:1748–1756.
22. Lisch W, Wasielica-Poslednik J, Kivelä T, et al. The hematologic definition of monoclonal gammopathy of undetermined significance in relation to paraproteinemic keratopathy (An American Ophthalmological Society Thesis). *Trans Am Ophthalmol Soc*. 2016;114: T7.
23. Romero PT, Donoso R, López P, et al. Clinical features and possible founder mutation of the 8bp duplication mutation in the SLC4A11 gene causing corneal dystrophy and perceptive deafness in three South American families. *Ophthalmic Genet*. 2019;40:91–98.
24. Fukuoka H, Kawasaki S, Yamasaki K, et al. Lattice corneal dystrophy type IV (p.Leu527Arg) is caused by a founder mutation of the TGFBI gene in a single Japanese ancestor. *Invest Ophthalmol Vis Sci*. 2010;51: 4523–4530.
25. Liskova P, Gwilliam R, Filipec M, et al. High prevalence of posterior polymorphous corneal dystrophy in the Czech Republic; linkage disequilibrium mapping and dating an ancestral mutation. *PLoS One*. 2012;7:e45495.
26. Koizumi N, Okumura N, Ueno M, et al. New therapeutic modality for corneal endothelial disease using Rho-associated kinase inhibitor eye drops. *Cornea*. 2014;33(suppl 11):S25–S31.
27. Syed ZA, Rapuano CJ. Rho kinase (ROCK) inhibitors in the management of corneal endothelial disease. *Curr Opin Ophthalmol*. 2021;32: 268–274.
28. Kanpolat A, Uçakhan OO. Therapeutic use of Focus Night & Day contact lenses. *Cornea*. 2003;22:726–734.
29. Hope-Ross MW, Chell PB, Kervick GN, et al. Oral tetracycline in the treatment of recurrent corneal erosions. *Eye (Lond)*. 1994;8(Pt 4): 384–388.
30. Foulks GN. Treatment of recurrent corneal erosion and corneal edema with topical osmotic colloidal solution. *Ophthalmology*. 1981;88: 801–803.
31. McLean EN, MacRae SM, Rich LF. Recurrent erosion. Treatment by anterior stromal puncture. *Ophthalmology*. 1986;93:784–788.
32. Sridhar MS, Rapuano CJ, Cosar CB, et al. Phototherapeutic keratectomy versus diamond burr polishing of Bowman's membrane in the treatment of recurrent corneal erosions associated with anterior basement membrane dystrophy. *Ophthalmology*. 2002;109: 674–679.
33. Zalentein WN, Holopainen JM, Tervo TMT. Phototherapeutic keratectomy for epithelial irregular astigmatism: an emphasis on map-dot-fingerprint degeneration. *J Refract Surg*. 2007;23:50–57.
34. Pérez-Santonja JJ, Galal A, Cardona C, et al. Severe corneal epithelial sloughing during laser in situ keratomileusis as a presenting sign for silent epithelial basement membrane dystrophy. *J Cataract Refract Surg*. 2005;31:1932–1937.
35. Orndahl MJ, Fagerholm PP. Treatment of corneal dystrophies with phototherapeutic keratectomy. *J Refract Surg*. 1998;14:129–135.
36. Wessel MM, Sarkar JS, Jakobiec FA, et al. Treatment of Lisch corneal dystrophy with photorefractive keratectomy and mitomycin C. *Cornea*. 2011;30:481–485.
37. Ashena Z, Niestrata M, Tavassoli S. Management of stromal corneal dystrophies; Review of the literature with a focus on phototherapeutic keratectomy and keratoplasty. *Vision (Basel, Switzerland)*. 2023;7:22.
38. McDonnell PJ, Seiler T. Phototherapeutic keratectomy with excimer laser for Reis-Bückler's corneal dystrophy. *Refract Corneal Surg*. 1992;8: 306–310.
39. Fogla R, Knyazer B. Microkeratome-assisted two-stage technique of superficial anterior lamellar keratoplasty for Reis–Bücklers corneal dystrophy. *Cornea*. 2014;33:1118–1122.
40. Dinh R, Rapuano CJ, Cohen EJ, et al. Recurrence of corneal dystrophy after excimer laser phototherapeutic keratectomy. *Ophthalmology*. 1999; 106:1490–1497.
41. Hieda O, Kawasaki S, Wakimasu K, et al. Clinical outcomes of phototherapeutic keratectomy in eyes with Thiel-Behnke corneal dystrophy. *Am J Ophthalmol*. 2013;155:66–72.e1.
42. Das S, Langenbucher A, Seitz B. Excimer laser phototherapeutic keratectomy for granular and lattice corneal dystrophy: a comparative study. *J Refract Surg*. 2005;21:727–731.
43. Wiley LA, Joseph MA, Pemberton JD. Microkeratome-assisted anterior lamellar keratoplasty. *Arch Ophthalmol (Chicago, Ill 1960)*. 2008;126: 404–408.
44. Vajpayee RB, Tyagi J, Sharma N, et al. Deep anterior lamellar keratoplasty by big-bubble technique for treatment corneal stromal opacities. *Am J Ophthalmol*. 2007;143:954–957.
45. Mattila JS, Krootila K, Kivelä T, et al. Penetrating keratoplasty for corneal amyloidosis in familial amyloidosis, Finnish type. *Ophthalmology*. 2015;122:457–463.
46. Lewis DR, Price MO, Feng MT, et al. Recurrence of granular corneal dystrophy type 1 after phototherapeutic keratectomy, lamellar keratoplasty, and penetrating keratoplasty in a single population. *Cornea*. 2017; 36:1227–1232.
47. Kim T-I, Roh MI, Grossniklaus HE, et al. Deposits of transforming growth factor-beta-induced protein in granular corneal dystrophy type II after LASIK. *Cornea*. 2008;27:28–32.

48. Kemer Atik B, Yildirim Y, Sonmez O, et al. Phototherapeutic keratectomy in macular and granular dystrophy: two-year results. *Semin Ophthalmol*. 2020;35:182–186.
49. Rouland J-F. [Clinical pilot study to evaluate the efficacy of a preservative-free hypertonic ophthalmic solution for patients with symptomatic corneal edema]. *J Français d'Ophtalmologie*. 2015;38:800–808.
50. Deng SX, Lee WB, Hammersmith KM, et al. Descemet membrane endothelial keratoplasty: safety and outcomes: a report by the American Academy of Ophthalmology. *Ophthalmology*. 2018;125:295–310.
51. Schmid E, Lisch W, Philipp W, et al. A new, X-linked endothelial corneal dystrophy. *Am J Ophthalmol*. 2006;141:478–487.